EFFECTS OF AGGREGATE TYPE, WATER-TO-CEMENTITIOUS MATERIAL RATIO, AND AGE ON MECHANICAL AND FRACTURE PROPERTIES OF CONCRETE

By
Shawn Barham
David Darwin

A Report on Research Sponsored by
THE NATIONAL SCIENCE FOUNDATION
Research Grant No. CMS-9402563

THE U.S. DEPARTMENT OF TRANSPORTATION
FEDERAL HIGHWAY ADMINISTRATION

Structural Engineering and Engineering Materials
SM Report 56

UNIVERSITY OF KANSAS CENTER FOR RESEARCH, INC.
LAWRENCE, KANSAS
August 1999

EFFECTS OF AGGREGATE TYPE, WATER-TO-CEMENTITIOUS MATERIAL RATIO, AND AGE ON MECHANICAL AND FRACTURE PROPERTIES OF CONCRETE

ABSTRACT

The effects of age and aggregate type on the behavior of normal, medium, and high-strength concrete, and the relationships between compressive strength, flexural strength, and fracture properties (fracture energy and characteristic length) are studied. The concrete mixes contain either basalt or crushed limestone aggregate with a maximum size of 19 mm (3/4 in.) and an aggregate volume factor (ACI 211.1-91) of 0.67. Mixes are tested at ages of 7, 28, 56, 90, and 180 days. Water-to-cementitious material (w/cm) ratios range between 0.25 and 0.46.

In the study, compressive strengths range from 20 MPa (2,920 psi) (7 day normal-strength limestone concrete) to 99 MPa (14,320 psi) (180 day high-strength basalt concrete). High-strength concrete containing basalt attains a higher compressive strength than high-strength concrete containing limestone, even at a slightly higher w/cm ratio. Medium-strength concrete containing limestone exhibits slightly higher compressive strength than concrete containing basalt. Compressive strengths for normal-strength concrete are similar for limestone and basalt. The w/cm ratio is the primary controlling factor for determining compressive strength. Higher strength concretes gain a greater portion of their long-term compressive strength at an earlier age than lower strength concretes.

The flexural strengths range from 4 MPa (550 psi) to 14 MPa (1,960 psi). High-strength concrete containing basalt yields significantly higher flexural strengths than high-strength concrete containing limestone at the same age. The limiting factor appears to be the tensile strength of the aggregate. For the normal and medium-strength concretes, aggregate does not significantly affect the flexural strength. The

w/cm ratio and aggregate strength are the primary controlling factors for determining flexural strength. Flexural strength generally increases with increasing age.

The fracture energies range from 27.7 N/m (0.158 lb/in.) to 202 N/m (1.152 lb/in.). Concrete containing basalt yields significantly higher fracture energies than concrete containing limestone at all w/cm ratios and ages. This is due to less aggregate fracture and a more irregular fracture surface in basalt concrete, causing greater energy dissipation. Compressive strength, w/cm ratio, and age seem to have no effect on fracture energy, which is principally governed by coarse aggregate type.

The characteristic length is higher for concrete containing basalt than for concrete containing limestone. Characteristic length decreases with an increase in compressive strength. The peak bending stress in a fracture test is linearly related to flexural strength.

Keywords: age, aggregates; characteristic length; compression; concrete; cracking (fracturing); flexural; fracture energy; fracture mechanics; high-strength concrete; modulus of elasticity; strength; tension; tests; water-to-cementitious materials

ACKNOWLEDGEMENTS

This report is based on a thesis submitted by Shawn Barham in partial fulfillment of the requirements of the M.S.C.E. degree. Support for this research was provided by the National Science Foundation under NSF Grant No. CMS 9402563, the U.S. Department of Transportation – Federal Highway Administration, and the Lester T. Sunderland Foundation. The basalt coarse aggregate was supplied by Geiger Ready-Mix and Iron Mountain Trap Rock Company. Additional Support was provided by Richmond Screw Anchor Company.

TABLE OF CONTENTS

LIST OF TABLES

LIST OF FIGURES

CHAPTER 1
INTRODUCTION

1.1 GENERAL

It is generally accepted that as concrete ages the compressive strength increases, as does the flexural strength (although at a slower rate). Also accepted is the fact that the strength of concrete increases as the water-to-cementitious material (w/cm) ratio decreases. Less understood is the effect that aggregate type has on concrete strength. The relation of fracture properties (in this study, fracture energy and characteristic length; described at the end of this section and in Chapter 3) of concrete to aggregate type, w/cm, and age is even more inconclusive, especially when correlated with strength properties.

Aggregate type plays a role in determining the strength and fracture energy of concrete. Petersson (1980) studied fracture energy as a function of several variables. He found that stronger aggregate produced higher fracture energies. Research by Ezeldin and Aitcin (1991), using four different coarse aggregates with the same concrete mix proportions, demonstrated that the type of coarse aggregate has little effect on the compressive strength of normal-strength concrete. For high-strength concrete, however, higher strength coarse aggregate usually results in a higher compressive strength. In one study comparing the effects of limestone and basalt on the compressive strength of high-strength concrete (Giaccio, Rocco, Violini, Zappitelli, and Zerbino 1992), almost all of the coarse aggregate was fractured in the limestone specimens, while load-induced cracks occurred mostly at the matrix-aggregate interface in concrete containing basalt. Giaccio, Rocco, and Zerbino (1993) investigated the fracture energies for a range of high-strength concretes. They concluded that differences in fracture energy due to aggregate type are mainly related to the resulting variations in concrete strength and that fracture energy depends on aggregate size. Kozul and Darwin (1997) observed that fracture energy is far more

dependent upon coarse aggregate type than on compressive strength.

The effects of w/cm ratio on the strength of concrete are well documented; strength increases as the w/cm ratio decreases. However, the effect of the w/cm ratio on fracture energy is not clear. Some research (Nallathambi, Karihaloo, and Heaton 1984, Xie, Elwi, and MacGregor 1995, Zhou, Barr, and Lydon 1995) shows that fracture energy increases with a decrease in w/cm ratio and an increase in compressive strength. In all cases, the increase in fracture energy occurs at a slower rate than the increase in compressive strength. Other research indicates that fracture energy may even decrease as compressive strength increases (Kozul and Darwin 1997, Lam et al. 1998). In some cases, the increase in fracture energy occurs only for certain types and size combinations of aggregate (Zhou, Barr, and Lydon 1995).

The effect of concrete age on concrete strength is also well recognized (strength increases with increasing age, although at a diminishing rate); yet, the effect of age on fracture energy has not been clearly established. Petersson (1980), who tested specimens at 2, 7, 28, and 91 days, found that fracture energy increases with increasing age. Niwa and Tangtermsirikul (1997), with tests at 1, 3, 7, and 28 days, came to the same conclusion.

This report is aimed at providing a better understanding of the effects of aggregate type, w/cm ratio, and concrete age on the strength and fracture characteristics of concrete, and the correlations between these properties. Two fracture characteristics, fracture energy and characteristic length, are given special consideration in this report. Fracture energy is the work needed to produce a crack of unit area (this energy is absorbed within the fracture process zone). The fracture process zone is the region at the tip of a crack in which failure occurs. Characteristic length is a material property that represents the ratio of fracture energy to strain energy density at the maximum stress. It provides a means to evaluate how sensitive a material is to cracking. The lower the value of characteristic length, the more sensitive the material is to cracking and the more brittle it is.

1.2 PREVIOUS WORK

Kaplan (1959) studied the effects of the properties of 13 coarse aggregates on the compressive and flexural strength of normal-strength and high-strength concrete. Mixes containing basalt always had a higher compressive strength than mixes containing limestone. However, the difference decreased at lower w/cm ratios. The mixes containing basalt also yielded higher flexural strengths than limestone mixes with the same mix proportions. Both the limestone and basalt mixes had flexural strength-to-compressive strength ratios of 9 to 12 percent. In contrast to most results, Kaplan observed that concrete with compressive strengths in excess of 69 MPa (10,000 psi) at 91 days had a higher compressive strength than mortar with the same w/cm ratio, leading him to conclude that coarse aggregate plays an important role in determining the compressive strength of high-strength concrete. In addition, Kaplan found that for concrete with 69 MPa (10,000 psi) and greater strengths, mortar had a higher flexural strength than the concrete, when made with the same w/cm ratio, while the flexural strengths were similar for concrete strengths below 69 MPa (10,000 psi).

Petersson (1980) investigated the fracture energy of concrete as a function of aggregate type and size, w/cm ratio, cement paste-aggregate volume ratio, and age. 8, 12, and 16 mm quartzite, gravel, limestone, and expanded clay coarse aggregates were used. The concrete had w/cm ratios of 0.3, 0.4, 0.5, 0.6, and 0.7 and cement paste-aggregate volume ratios of 0.4, 0.5, and 0.6. The concrete was tested 2, 7, 28, and 91 days after casting. Petersson found that the stronger aggregates produced higher fracture energies and characteristic lengths, caused by the cracks running around the stronger aggregates and through the weaker aggregates, producing different failure surfaces. Fracture energy, tested at 28 days, increased about 34 percent with a decrease in w/cm from 0.70 to 0.40, then remained constant at lower w/cm ratios. Fracture energy also increased about 32 percent with an increase in age from 2 to 91 days with a w/cm ratio of 0.50. Characteristic length, tested at 28 days,

remained constant with an increase in w/cm until 0.5, then increased sharply (almost double at w/cm of 0.70). It also decreased with an increase in age to 28 days, then remained unchanged for a w/cm ratio of 0.50. The author also discovered that fracture energy and characteristic length increase as cement paste-aggregate volume ratios increase and as aggregate size increase, resulting from an increase in crack surface.

Carrasquillo, Slate, and Nilson (1981) studied microcracking in concrete under uniaxial compression. Compressive strengths ranged from 31 to 76 MPa (4,500 to 11,000 psi). Normal-strength concrete [about 31 MPa (4,500 psi)] acted like a highly nonhomogeneous material, with its weakest link at the matrix-aggregate interface; microcracks advanced as mortar cracks coalesced between the nearby bond cracks. Medium-strength concrete [about 55 MPa (8,000 psi)] had microcracks similar to those in normal-strength concrete, but at higher strains. High-strength concrete [about 76 MPa (11,000 psi)] had fewer and shorter microcracks than the lower strength concretes at all strains. Carrasquillo et al. concluded that the differences in behavior were due to the increase in homogeneity as strength increased; in high-strength concrete, the matrix is denser and the matrix and aggregate have greater compatibility between strength and elastic properties. This improved compatibility lowers the stress at the matrix-aggregate interface, which decreases the chance of interfacial failure, causes the cracks to propagate through the aggregate, and reduces the amount of microcracking.

Carrasquillo, Nilson, and Slate (1981) also studied the properties of normal, medium, and high-strength concrete with compressive strengths ranging from 21 to 76 MPa (3,000 to 11,000 psi). At early ages, the higher strength concretes showed a higher rate of strength development than the lower strength concretes. In flexural strength tests, using third-point loading, the amount of aggregate fracture in the plane of failure was significantly higher in high-strength concrete [62 to 76 MPa (9,000 to 11,000 psi)] than in normal-strength concrete [21 to 41 MPa (3,000 to 6,000 psi)]. The authors found higher moduli of elasticity at higher compressive strengths,

resulting from a greater stiffness in the mortar and (they felt) a higher matrix-aggregate tensile bond. Also, higher rates of loading increased the strength of normal-strength concrete more than high-strength concrete.

Nallathambi, Karihaloo, and Heaton (1984) examined the effects of w/cm ratio, specimen dimensions, maximum aggregate size, and notch depth on the fracture energy of normal-strength concrete (compressive strengths below 42 MPa). The w/cm ratio ranged from 0.50 to 0.65. Fracture energy was evaluated by three-point bending on notched beams. As the w/cm ratio decreased 23 percent, the fracture energy increased 38 percent for rounded aggregate and 50 percent for crushed aggregate. Comparatively, with the same decrease in w/cm ratio, modulus of elasticity and compressive strength increased 41 and 38 percent, respectively, for rounded aggregate and 39 and 39 percent, respectively, for crushed aggregate. Fracture energy increased with an increase in beam depth for a given notch-depth ratio and span, decreased with an increase in span at a constant depth, and decreased with an increase in notch-depth ratio for a given depth. The authors concluded that the effect of increased beam depth on fracture toughness is due to the increased probability of voids, microcracks, and bond cracks in the path of the growing crack, as well as, greater coarse aggregate resistance. The effect of beam span on fracture energy results from in-plane shear stresses having more influence in shorter spans and causing a greater damage zone. As the maximum size of the aggregate increased, the fracture energy increased. They concluded that this occurs because microcracking and debonding of the aggregate consumes a large amount of energy, and the larger the aggregate, the larger the crack surface and, thus, the greater amount of energy consumed.

A study of crack propagation was carried out by Bentur and Mindess (1986) using wedge loaded contoured double cantilever beams. Three types of concrete were tested: normal-strength (w/cm ratio of 0.50), high-strength (w/cm ratio of 0.33), and lightweight aggregate (w/cm ratio of 0.68) concrete. All three types were loaded slowly (1 mm/min); normal and high-strength specimens were also loaded rapidly

(250 mm/min). At both rates of loading, the crack path in normal-strength concrete went around the aggregates and was tortuous. When loaded slowly, the crack paths in the high-strength concrete were similar to those in normal-strength concrete, in that, in most cases, the crack propagated around coarse aggregate particles and was frequently discontinuous in the matrix with the discontinuities usually being air voids, which seemed to act as crack arrestors. At the higher load rate, a straighter path was observed in high-strength concrete, with most of the aggregate being fractured. This is explained by the fact that, if energy is introduced into the system over a short time, the cracks are forced to take shorter paths of higher resistance, which are through the aggregates.

Yogendran, Landan, Haque, and Ward (1987) studied the effects of silica fume on the mechanical properties of high-strength concrete with 28-day compressive strengths between 50 and 70 MPa (7,500 and 10,500 psi). Limestone concrete with a maximum aggregate size of 14 mm (0.6 in.) was used with w/cm ratios of 0.28 and 0.34 and silica fume replacements of 0 to 30 percent. For concrete with a w/cm ratio of 0.34, the compressive strength was maximum at 7, 28, 56, and 91 days using 15 percent silica fume replacement. However, at a w/cm ratio of 0.28, the compressive and flexural strengths attained a maximum at 28, 56, and 91 days with no silica fume replacement and at 7 days with a 5 percent silica fume replacement. They concluded that the contribution of silica fume to compressive and flexural strength decreases with decreasing w/cm ratio and increasing cement content.

Aitcin and Mehta (1990) examined the effects of coarse aggregate characteristics on the mechanical properties of high-strength concretes with compressive strengths up to 105 MPa (15,500 psi). They used a w/cm ratio of 0.275 and four coarse aggregate types: granite, diabase, limestone, and gravel, all having a maximum size of 10 mm (0.4 in.), except for granite, which had a maximum size of 14 mm (0.6 in.). The concrete was tested at 1, 28, and 56 days. The concrete containing diabase had the highest compressive strength, while that containing limestone had the highest modulus of elasticity. Concrete containing limestone or

diabase had mostly transgranular fracture, with only a small amount of matrix-aggregate debonding. Concrete containing gravel had the second lowest compressive strength and modulus of elasticity. The authors concluded that this was due to a weak interfacial zone, which caused significant debonding of the aggregate particles. The concrete containing granite had the lowest compressive strength and elastic modulus. Granite was considered to be the weakest aggregate, since all of the aggregate on the failure surfaces fractured.

Gettu, Bazant, and Karr (1990), using three-point bending tests, studied the fracture properties and brittleness of high-strength concrete [28-day compressive strength in excess of 83 MPa (12,000 psi)]. They used 9.5 mm (3/8 in.) crushed limestone coarse aggregate, a w/cm ratio of 0.27, and cement replacements with fly ash and silica fume of 19 and 3 percent by weight, respectively. The authors observed that cracks passed through the crushed limestone, whereas in past studies of normal-strength concrete the cracks had propagated mainly along the matrix-aggregate interface. They concluded that the change for the high-strength concrete was due to a strong matrix-aggregate bond and a matrix strength approaching that of the aggregate. They also found that an increase in compressive strength of 160 percent resulted in an increase in fracture energy of only 12 percent. As compressive strength increased, the characteristic length decreased considerably, indicating a more brittle behavior. The authors concluded that the almost homogeneous behavior of high-strength concrete decreased the width of the fracture process zone and decreased the intensity of the toughening and crack-tip shielding effect of the aggregates, causing the observed brittle behavior.

Ezeldin and Aitcin (1991) studied the effects of coarse aggregate size and type on the strength of normal and high-strength concrete. They concluded that the compressive and flexural strength of normal-strength concrete and the flexural strength of high-strength concrete were not significantly influenced by the size or type of aggregate. In contrast, they found that the compressive strength and failure mode of high-strength concrete was affected by the size and type of coarse aggregate.

For high–strength concretes with a strong coarse aggregate, both transgranular failure and matrix-aggregate debonding occurred, with the cracks passing through the weak part of the aggregate. The use of weaker coarse aggregate in high-strength concrete resulted in virtually all transgranular failure, with the cracks passing through the aggregate.

Three crushed coarse aggregate types (granite, basalt, and limestone) with a maximum size of 19 mm (3/4 in.) were used by Giaccio, Rocco, Violini, Zappitelli, and Zerbino (1992) in a study of high-strength concrete (compressive strengths in excess of 90 MPa). Concrete, mortar, and rock were analyzed for compressive strength, flexural strength, and modulus of elasticity. Concrete was also analyzed for matrix-aggregate bond strength by constructing beams made of half coarse aggregate (one side) and half mortar (the other side) and placing them in flexure. Concrete containing basalt had significantly higher values of compressive and flexural strength and modulus of elasticity than concrete containing granite or limestone. Mortar (concrete passed through a No. 4 sieve) had the highest compressive strength, followed by the basalt, granite, and limestone concretes, in that order. The flexural strengths of the concretes made with the three coarse aggregates were comparable, indicating that aggregate type had little effect on flexural strength. The moduli of elasticity of the three concretes, highest to lowest, were basalt, limestone, and granite, with the granite concrete having a modulus close to that of the mortar (best elastic compatibility between aggregate and matrix). The highest matrix-aggregate bond strength was obtained by limestone, followed by basalt and granite.

Giaccio, Rocco, and Zerbino (1993) studied the fracture energies of a large range of high-strength concretes with w/cm ratios from 0.28 to 0.40. Compressive strengths ranged from 64 to 107 MPa (9,280 to 15,515 psi) for concrete containing basalt, granite, limestone, smooth river gravel, and crushed river gravel as coarse aggregate. High-strength mortar and normal-strength concrete (w/cm of 0.75) made with granite were also included for comparison. They found that concrete containing limestone produced lower compressive strengths than concrete containing river

gravel, although the concretes had similar tensile strengths. The authors also studied the influence of the surface characteristics of coarse aggregate on the properties of concrete by comparing concrete containing smooth river gravel to concrete containing crushed river gravel. The concrete containing crushed river gravel had 7 percent higher compressive strength and 6 percent higher fracture energy than that containing smooth river gravel. In the load-deflection curves from the fracture tests, concrete containing the same aggregate had a greater peak load, followed by a steeper gradient of the softening branch, as strength increased (or w/cm decreased). Final deflections were similar for the different concretes. They found that fracture energy increased as compressive and flexural strength increased, but at a slower rate than either. Giaccio et al. concluded that fracture energy is mostly controlled by aggregate size (mortar had the smallest energy); changes in fracture energy due to aggregate type are mainly related to the resulting variations in concrete strength. Characteristic lengths decreased greatly with an increase in compressive strength (high-strength concrete produced values two to three times smaller than the normal-strength concrete).

Xie, Elwi, and MacGregor (1995) investigated concrete in uniaxial compression, tension (splitting tension and notched beams), and triaxial compression with target 28-day compressive cylinder strengths of 60, 90, and 120 MPa (8,700, 13,050, and 17,400 psi) containing gravel aggregate with a maximum size of 14 mm (0.55 in.). The w/cm ratios were 0.321 (series A), 0.283 (series B), 0.216 (series C). The actual compressive strengths were 60.2, 92.2, and 120 MPa at 29 (series A), 35 (series B), and 39 (series C) days, respectively. Split-cylinder strength increased as uniaxial compressive strength increased, although at a slower rate. The increase in tensile strength from series A to B was 28 percent, compared to a 53 percent increase in compressive strength. The increase in tensile strength from series B to C was 17 percent, compared to a 29 percent increase in compressive strength. The authors found that fracture energy also increases as compressive strength increases, but at an even slower rate than the split-cylinder strength. The increase in fracture energy from series A to B was 13 percent and from series B to C was 11 percent. In the load-

deflection curves of the fracture tests, the post-peak response became steeper as compressive strength increased.

Zhou, Barr, and Lydon (1995) investigated the fracture properties of concrete (w/cm ratios of 0.32 and 0.23) made using 10 mm (0.4 in.) gravel and 10 mm (0.4 in.) and 20 mm (0.8 in.) crushed limestone with compressive strengths of 80 to 115 MPa (11,600 to 16,700 psi). Cement replacements of 10 and 15 percent by weight with silica fume were used. They found that increasing the silica fume content from 10 to 15 percent did not affect compressive strength at a w/cm of 0.23, but did increase compressive strength for concrete containing limestone at a w/cm of 0.32. Unlike most studies, they observed increasing limestone size from 10 mm to 20 mm resulted in an increase in compressive strength. Zhou et al. found that the fracture energy of concrete containing gravel was higher than concrete containing limestone of the same size. They felt that the matrix-aggregate bond was similar, so the difference must be the superior strength of the gravel. They also observed an increase in fracture energy for the gravel and 20 mm limestone concretes as w/cm decreased. However, they found the opposite to be found for 10 mm limestone concretes. The authors hypothesized that due to the improved bond of the 10 mm limestone, the crack propagated through the aggregate, decreasing the fracture energy for this particular combination of aggregate type and size. Characteristic length was reduced with an increase in compressive strength, indicating that the concrete became more brittle, as the w/cm decreased. The characteristic length was greater for the concretes containing stronger and larger aggregates.

Tasdemir, Tasdemir, Lydon, and Barr (1996) studied the effects of silica fume and aggregate size on the brittleness of concrete with compressive strengths ranging from 72 to 88 MPa (10,440 to 12,760 psi). The w/cm ratio remained constant at 0.36, with and without a silica fume replacement of 10 percent. Two sizes of crushed limestone (10 mm and 20 mm) were used. They found virtually no change in compressive strength with an increase in aggregate size, but an increase in compressive strength with the addition of silica fume. The splitting tensile strength

increased with the addition of silica fume and increasing aggregate size. The modulus of elasticity remained largely unaffected by aggregate size and silica fume content. The concrete containing silica fume produced lower fracture energies compared to concrete without silica fume, with a greater drop for concrete containing larger aggregates. Increasing the aggregate size, increased the fracture energy for concrete without silica fume, because of increased mechanical surface interlock (due to crack surface roughness) and crack surface, but had no effect on the fracture energy of concrete containing silica fume. The characteristic length was more than double for concrete without silica fume and 20 mm aggregate compared to the other concretes. Tasdemir et al. observed that load-deflection curves for the silica fume concrete fracture specimens had a greater peak load and a steeper gradient in the softening branch, as well as lower final deflection values in load-deflection curves compared to concrete without silica fume. They also showed that transgranular failure usually occurred in concrete with silica fume and that cracks developed principally around the coarse aggregate, forming a tortuous path, in concrete without silica fume, the former having more brittle behavior. From a microscopic analysis, the authors found that the matrix-aggregate interface had an abundance of calcium hydroxide and much less dense calcium silicate hydrate in concrete without silica fume than in concrete with silica fume, causing cracks to form in this weak boundary. In concrete with silica fume, the interface was more homogeneous and dense, resulting in fracture of the aggregates.

Kozul and Darwin (1997) studied the effects of aggregate type (basalt and limestone), size (19 and 12 mm), and content (rodded volumes of coarse aggregate per unit volume of concrete of 0.67 and 0.75) on the strength and fracture properties of normal and high-strength concrete with strengths ranging from 25 to 97 MPa (3,670 to 13970 psi). The authors found that basalt mixes had slightly higher compressive strengths than limestone mixes for high-strength concrete, while basalt mixes had slightly lower compressive strengths than limestone mixes for normal-strength concrete. Aggregate size had a negligible effect on compressive strength.

Compressive strengths were higher for higher coarse aggregate contents in high-strength concrete containing basalt and normal-strength concrete containing basalt or limestone (high-strength limestone concrete was not affected). They also found that basalt high-strength concrete yielded higher flexural strengths than limestone high-strength concrete, while the flexural strength of normal-strength concrete was not affected by aggregate type. Aggregate size did not affect the flexural strength of normal and high-strength concrete. Basalt normal and high-strength concretes had higher flexural strengths at higher coarse aggregate contents. Fracture energies of normal and high-strength concretes were significantly higher for concretes containing basalt than for concretes containing limestone. Increasing the aggregate size decreased the fracture energy in high-strength concrete and increased the fracture energy in normal-strength concrete. Basalt high-strength concrete and limestone normal-strength concrete yielded higher fracture energies with higher coarse aggregate contents. The fracture energy of basalt normal-strength concrete and limestone high-strength concrete was not affected by coarse aggregate content. In the fracture specimen load-deflection curves, basalt concrete had higher peak loads and final deflections than limestone concrete.

The effects of coarse aggregate on the mechanical properties of concrete were studied by Ozturan and Cecen (1997). 28-day target compressive strengths were 30, 60, and 90 MPa (4,350, 8,700, and 13,050 psi) (normal, medium, and high-strength) with concrete made using basalt, limestone, and gravel coarse aggregate. W/cm ratios of 0.58, 0.40, and 0.30 were used. The high-strength basalt concrete had the highest compressive and flexural strengths, while concrete made with gravel had the lowest. The authors concluded that the low strength attained by the gravel concrete resulted from a lower strength of aggregate and a weaker bond, caused by the round shape and smooth surface of the aggregate. The normal-strength limestone concrete had higher compressive and flexural strengths, while concrete had similar compressive and flexural strengths containing other aggregates. They concluded that the reason for the relative increase in strength for concrete containing limestone might

be due to interfacial chemical reactions which improve bond strength. Also, an experiment was conducted, replacing the cement with that of higher strength, while keeping the other parameters fixed in high-strength gravel concrete. No change occurred in compressive strength, but the flexural and splitting tension increased about 30 percent, suggesting that compressive strength was heavily influenced by the strength and the bonding characteristics of the coarse aggregate, whereas tensile strength was mostly controlled by the matrix strength in high-strength concretes.

Niwa and Tangtermsirikul (1997) completed a comparative study of the fracture properties of normal-strength concrete, high-strength, and "high performance" concrete with 19 mm limestone coarse aggregate and w/cm ratios of 0.65, 0.40, and 0.30. A 30 percent fly ash replacement for cement by weight was used in the high performance concrete, as well as, a significantly lower coarse aggregate content than the normal or high-strength concretes (a little over half). Compressive and tensile strengths and fracture energies were obtained at 1, 3, 7, and 28 days. At all ages, the high-strength concrete had the highest fracture energy and the high performance concrete had the highest compressive and tensile strengths. From 1 to 3 days, the normal-strength concrete had a significantly higher percent increase in compressive strength, tensile strength, and fracture energy than the high-strength and high performance concretes; however, it had the lowest values in all three categories at all ages. From 7 to 28 days, normal and high-strength concrete exhibited a 21 percent increase in compressive strength compared to a 9 percent increase in fracture energy, while the high performance concrete had a 25 percent increase in compressive strength and only a 2 percent increase in fracture energy. The authors concluded the reason for the difference was the reduced coarse aggregate content in the high performance concrete, which resulted in easier crack propagation. They also concluded that fracture energy decreased with an increase in cementitious material content and a decrease in aggregate content.

Lam, Wong, and Poon (1998) studied the effects of fly ash and silica fume on the mechanical and fracture behavior of concrete (compressive strengths up to 108

MPa). W/cm ratios of 0.3, 0.4, and 0.5 were used. The concrete contained cement replacements of between 0 and 55 percent by weight with fly ash and, in some mixes, a cement replacement of 5 percent by weight with silica fume. Test ages were 3, 7, 28, 56, 90, and 180 days. Granite coarse aggregate was used with a maximum size of 10 mm for mixes with a w/cm ratio of 0.3 and 20 mm for mixes with a w/cm ratio of 0.4 and 0.5. Concrete with a w/cm ratio of 0.30, containing 25 percent fly ash and no silica fume, produced the highest compressive strength at 180 days (concrete containing silica fume and no fly ash had a higher compressive strength at earlier ages, though). The authors confirmed that fly ash contributed little to compressive strength at early ages, observing larger reductions in early compressive strength as the volume of fly ash increased. At later ages and lower w/cm ratios, the contribution of the fly ash to compressive strength increased. Fly ash also improved the post-peak compressive behavior, resulting in a lower gradient in the descending branch of the stress-strain curve. The authors concluded that silica fume and fly ash contents of 15 to 25 percent may have improved the interfacial bond between the paste and the aggregate, creating higher tensile strengths, with the trend becoming more evident as compressive strength increased. Fracture energy was the highest for high volume fly ash replacement and lowest for silica fume replacement. The authors felt that the higher fracture energy of the high volume fly ash concrete resulted from the unreacted fly ash particles acting as micro-aggregates, with a higher modulus of elasticity, which increased the resistance to crack propagation. Cracking around the unreacted particles caused more energy dissipation. They felt that the low fracture energy of the silica fume concrete was due to the enhanced matrix-aggregate bond, which caused more brittle and homogeneous behavior, leading to rapid crack propagation after the peak load. In concrete without silica fume, the fracture energy increased as compressive strength increased, especially in concrete without fly ash. Concrete with silica fume actually decreased in fracture energy with an increase in compressive strength.

Maher and Darwin (1976, 1977) concluded that the tensile bond strength of

the matrix-aggregate interface has less effect on compressive strength than usually thought. Using finite element analysis, the authors observed a decrease of only 11 percent in compressive strength, as the bond strength decreased from normal values to zero. Perfect bond (no failure at the interfacial region) increased the compressive strength just 4 percent. These findings, along with previous tests on matrix-aggregate bond, which showed little variation in bond strength with a decrease in w/cm ratio (Hsu and Slate 1963, Taylor and Broms 1964), lead to the conclusion that matrix strength is the main factor controlling compressive strength.

1.3 SUMMARY

The following information summarizes the findings of previous studies on the effects of aggregate type, water-cementitious material ratio, and concrete age on normal, medium, and high-strength concretes.

Aggregate Type

1. The type of coarse aggregate has little effect on the strength of normal-strength concrete. Stronger aggregates in high-strength concrete produce greater strengths. The fracture energy and modulus of elasticity of normal and high-strength concrete are also increased by stronger aggregates.
2. Most research concludes there is a marginal effect of aggregate type on flexural strength. However, some research indicates higher strengths with higher strength coarse aggregate.

Water-Cementitious Material Ratio

1. Decreasing the w/cm ratio, increases the strength on concrete, with a more profound effect on compressive strength than on tensile strength. It also increases the modulus of elasticity.

2. Most studies report an increase in fracture energy with a decrease in w/cm ratio, although the rate of increase diminishes as the w/cm ratio decreases and is lower than that exhibited by flexural strength. Some researchers have reported a decrease in fracture energy with a decrease in w/cm ratio for certain combinations of aggregate and cementitious materials.

Concrete Age

1. The strength of concrete increases with increasing age, again with flexural strength and modulus of elasticity gaining at a reduced rate as compared to compressive strength.
2. It is generally agreed that fracture energy increases with increasing age, although the percent increase varies widely.

1.4 OBJECT AND SCOPE

The purpose of this research is to compare the compressive strength, flexural strength, and fracture energy of concrete as a function of aggregate type (limestone and basalt), w/cm ratio (0.25, 0.35, and 0.46), age (7, 28, 56, 90, and 180 days), cementitious material (Type I portland cement, fly ash, and silica fume), and chemical admixture (normal and high-range water reducer).

Compressive strengths range from 20 to 99 MPa (2,920 to 14,320 psi). Thirteen batches (5 normal-strength, 4 medium-strength, and 4 high-strength) of 15 specimens each and 2 batches (1 normal-strength and 1 high-strength) of 10 specimens each were tested. The results of 69 compressive strength, 69 flexural strength, and 77 fracture energy tests are reported.

CHAPTER 2
EXPERIMENTAL WORK

2.1 GENERAL

Concrete specimens were tested to determine the relationships between compressive strength, flexural strength, and fracture energy as a function of age. Center-point loading was used for both the flexure and fracture tests. The concrete contained 19 mm (3/4 in.) maximum size basalt or limestone aggregate with an ACI aggregate volume factor (ACI 211.1-91) of 0.67. Three concrete strengths were produced (termed normal, medium, and high-strength), using water-cementitious material ratios ranging from 0.26 to 0.46. Concrete was tested at ages of 7, 28, 56, 90, and 180 days.

2.2 MATERIALS

Normal-strength concrete contained Type I portland cement. Medium-strength concrete contained Type I portland cement and fly ash. High-strength concrete contained Type I portland cement, fly ash, and silica fume.

The type I portland cement contained 64 percent CaO, 22 percent SiO_2, 5 percent Al_2O_3, 4 percent Fe_2O_3, 2.3 percent SO_3, 2 percent MgO, 0.45 percent K_2O, 0.22 percent TiO_2, 0.18 percent SrO, 0.12 percent Na_2O, 0.11 percent P_2O_5, 0.10 percent Mn_2O_3, and 0.83 percent loss on ignition (53 percent C_3S, 22 percent C_2S, 11 percent C_4AF, and 6 percent C_3A by Bogue analysis). Class C fly ash was provided by Flinthills Fly Ash. It had a specific gravity of 2.25 and contained 34 percent SiO_2, 29 percent CaO, 20 percent Al_2O_3, 7 percent MgO, 4 percent Fe_2O_3, and 3 percent SO_3. The dry, compacted silica fume was Master Builders MB-SF. It had a specific gravity of 2.65 and contained 92 percent SiO_2, 0.45 percent Na_2O, 0.36 percent SO_3, 0.10 percent Cl, and 0.52 percent loss on ignition.

The coarse aggregates were basalt, supplied by Iron Mountain Trap Rock, and limestone, supplied by Fogle Quarry. The basalt had a bulk specific gravity (SSD) of 2.64, an absorption (dry) of 0.37 percent, and a unit weight of 1573 kg/m^3 (98.2 lb/ft^3). The limestone had a bulk specific gravity (SSD) of 2.54, an absorption (dry) of 3.9 percent, and a unit weight of 1480 kg/m^3 (92.4 lb/ft^3).

The fine aggregate used in the study was Kansas river sand with a specific gravity (SSD) of 2.60, an absorption (dry) of 0.43 percent, and a fineness modulus of 2.58.

The water reducers used in the study included a Type A normal-range water reducer (NRWR-Master Builders Polyheed 997) and a Type F high-range water reducer (HRWR-Master Builders Rheobuild 1000), which is a calcium naphthalene sulfonate condensate-based material. The Type A admixture had a specific gravity of 1.27 and contained 47 percent solids by weight. The Type F admixture had a specific gravity of 1.20 and contained 40 percent solids by weight. NRWR was added at a rate of 460 ml per 100 kg of cementitious material (7 oz/cwt) to the high-strength concrete and as needed to the medium-strength concrete to achieve the desired slump. The HRWR was added to the high-strength concrete in the quantity needed to achieve workability and formability.

Fly ash was used as 15 percent of the cementitious material in the medium-strength concrete and 5 percent in the high-strength concrete. Silica fume was used as 10 percent of the cementitious material in the high-strength concrete. The concrete was mixed in 0.061 m^3 (2.15 ft^3) batches. Mix designs in SI and customary units, respectively, are presented in Tables 2.1 and 2.2.

2.3 APPARATUS AND PROCEDURE

The aggregates were evaluated for bulk specific gravity, absorption (dry), unit weight, material finer than 75 μm (No. 200 sieve), organic impurities (fine aggregate

only), and gradation (ASTM C 127, ASTM C 29, ASTM C 117, ASTM C 40 and ASTM C 136, respectively).

The concrete mixes were proportioned based on absolute volume. Prior to mixing, the aggregates were dried for about 24 hours at a temperature of 105-115° C (221-239° F) and allowed to cool to room temperature. Mix water was adjusted to account for absorption.

The concrete was mixed in a Lancaster counter-current mixer with a nominal capacity of 0.057 m^3 (2.0 ft^3). The mixer pan was wiped with a wet sponge prior to batching. Because the batch volume, 0.061 m^3 (2.15 ft^3), exceeded the nominal mixer capacity, care was needed to properly mix the concrete. The coarse aggregate was added, then the fine aggregate. Approximately 75 percent of the mix water was then added. This helped prevent the aggregates from spilling out of the mixer. After mixing the aggregates and water, the cementitious material was added, followed by the rest of the water. For high-strength concrete, the NRWR was added with the remaining portion of the water. The HRWR was added until the desired slump (ASTM C 143) of 190 to 230 mm (7.5 to 9 in.) had been achieved. For medium-strength concrete, after an initial slump was taken, NRWR was added, if needed, until the desired slump of 125 to 165 mm (5 to 6.5 in.) was met. After all of the ingredients had been added, the concrete was mixed until uniform, which required 3 to 5 minutes, depending on the batch. After mixing the final slump and unit weight (ASTM C 138) were measured.

The concrete was placed in prismatic steel forms with the dimensions 100 x 100 x 350 mm (4 x 4 x 14 in.). The forms were oriented vertically and the concrete was consolidated in three equal layers. Each layer was rodded 25 times with a 16 mm (5/8 in.) steel tamping rod. After rodding each layer, the forms were struck smartly 10-15 times with a rubber mallet. Following consolidation, the forms were sealed and stored in a horizontal position at 23-24° C (74-76° F) for 48 hours. Forty-eight hours was needed to limit the potential for cracking. After the 48 hours, the molds were removed and the specimens placed in lime saturated water at 21-24° C (70-

76° F). At least 24 hours before the compressive specimens were tested, 25 mm (1 in.) was sawed off each end using a high-speed masonry saw, to achieve a 3 to 1 length-to-width ratio, and capped with a 1.6 mm (1/16 in.) thick layer of Forney Hi-Cap capping compound. The fracture energy specimens were prepared by cutting a 25 mm (1 in.) deep by 5 mm (0.2 in.) wide notch on one side at the midpoint, perpendicular to the long direction. The specimens were then placed back in the lime-saturated water until the time of the test. The specimens were wrapped in plastic wrap after removal from the water to minimize moisture loss during the test.

Thirteen batches (5 normal-strength, 4 medium-strength, and 4 high-strength) of 15 specimens each (equal numbers and tested at 7, 28, 56, 90, and 180 days) and 2 batches (1 normal-strength and 1 high-strength) of 10 specimens each (equal numbers and tested at 7 and 28 days) were cast. Sixty-nine compressive strength, 69 flexural strength, and 77 fracture energy specimens were tested

Compression tests were performed in accordance with ASTM C 39 in a Forney 1,800 kN (400 kip) capacity hydraulic testing machine. Specimens were loaded at rate of 0.14 to 0.34 MPa/s (20 to 50 psi/s) until failure.

Flexure specimens were loaded to failure at an extreme fiber stress rate between 0.86 and 1.21 MPa/min (125 to 175 psi/min) in accordance with ASTM C 293, using center-point loading in a 150 kN (35 kip) MTS closed-loop servo-hydraulic testing system under load control. The load cell had a capacity of 45 kN (10 kip).

The fracture energy test followed the guidelines established by RILEM (1985), using the MTS test machine under crack mouth opening displacement (CMOD) control and instrumentation developed by Kozul and Darwin (1997) (Figure 2.1). Prior to the test, the bottom surface of the concrete on either side of the notch matching the dimensions of two small steel plates was dried using a hair dryer on low heat. The two steel plates, with dimensions of 25 x 76 mm (1 x 3 in.) and lips to fit into the sawed notch, were attached on both sides of the notch using Duro Quick Gel cement. The clip gage used to measure CMOD was then placed between knife edges

attached to the steel plates. Two nails were then glued on both sides at the top of the specimen at mid-span to hold the ferro-magnetic cores of two linear variable differential transformers (LVDTs) used to measure deflection. The cores were supported by washers suspended by the nails. The coil housings of the LVDTs were held by aluminum bars screwed into the concrete at the mid-depth of the beam over the supports. A data acquisition system was used to record the load cell, clip gage, and LVDT readings. The data acquisition system was interfaced with an IBM compatible personal computer. A constant CMOD rate of 0.08 mm/min (0.003 in./min) was set so that the peak load would be attained in about 30 seconds. Tests lasted between 15 to 50 minutes, depending on aggregate type, specimen age, and water-cementitious material ratio.

CHAPTER 3
RESULTS AND EVALUATION

The results and evaluation of compression, flexure, and fracture energy tests on normal, medium, and high-strength concrete are reported and compared to past studies. The tests were conducted to determine the effects of aggregate type, water-cementitious materials (w/cm) ratio, and concrete age on the compressive, flexural, and fracture properties of concrete and to determine how these properties relate to each other; special emphasis is placed on fracture properties.

3.1 DATA ANALYSIS

The following explains how fracture energy, modulus of elasticity, and characteristic length are determined.

3.1.1 Fracture Energy

Fracture energy is the energy dissipated per unit area during the formation of a crack. The energy is dissipated within the fracture process zone, the region in front of a crack tip where the stress decreases as the crack opens. The area of fracture is the projected area on a plane perpendicular to the direction of stress. A schematic is presented in Figure 3.1 for further clarification.

As discussed in Chapter 2, in the current study, fracture energy is determined using a notched beam in three-point bending. The average deflection is measured at the centerline of the beam. Load-deflection curves are plotted, with the energy, W_o, representing the area under the curve.

RILEM (1985) and Hillerborg (1985) suggest that fracture energy be calculated using the following expression:

$$G_f = (W_o + mg\delta_f)/A \qquad (3.1)$$

where: G_f = fracture energy (N/m or lb/in.)

W_o = area under the load-deflection curve (N-m or lb.-in.)

$m = m_1 + 2m_2$ (kg or slug)

m_1 = mass of the beam between the supports

m_2 = mass of the loading frame not attached to the loading machine that follows the specimen until failure

g = acceleration due to gravity

δ_f = final deflection of the beam (m or in.)

A = cross-sectional area of the beam above the notch (m or in.)

The need for the term, $mg\delta_f$, results from the fact that the imposed load from the machine is not the only load acting on the specimen during the test; the weight of the specimen between the supports and the weight of the testing equipment supported by the specimen also play a role. Therefore, the measured load-deflection curve does not account for the full load on the beam and, thus, does not reflect the total energy necessary to cause fracture.

A hypothetically complete load-deflection curve is shown in Figure 3.1. F_1 is the additional load caused from the weight of the specimen ($1/2\ m_1g$) and the weight of the loading arrangement (m_2g).

The total energy required to fully fracture the specimen is:

$$W = W_o + W_1 + W_2 \qquad (3.2)$$

where: $W_1 = F_1\delta_f = (1/2m_1 + m_2)g\delta_f = 1/2mg\delta_f$

Hillerborg (1985) demonstrated that W_2 is approximately equal to W_1, making the

total energy:

$$W = W_o + 2F_1\delta_f = W_o + mg\delta_f \qquad (3.3)$$

This total amount of energy is divided by the projected area of fracture to give the fracture energy, G_f.

3.1.2 Modulus Of Elasticity

The modulus of elasticity is defined as the slope of the stress-strain curve or the stress divided by the strain in the linear region. It measures the elastic stiffness of a material.

RILEM (1991) recommends a method for determining the modulus of elasticity of a material based on the load-crack mouth opening displacement (CMOD) curve for a fracture specimen. It is determined using the following equation:

$$E = 6Sa_oV_1(\alpha)/(C_id^2b) \qquad (3.4)$$

where:

E = modulus of elasticity (MPa or psi)

S = span of the beam (m or in.)

a_o = initial notch length of the beam (m or in.)

$V_1(\alpha) = 0.76 - 2.28\alpha + 3.87\alpha^2 - 2.04\alpha^3 + 0.66/(1-\alpha)^2$

$\alpha = (a_o + HO)/(d + HO)$

C_i = initial compliance from load-CMOD curve (m/N or in./lb)

d = depth of the beam (m or in.)

b = width of the beam (m or in.)

HO = thickness of steel plates that hold clip gauge (m or in.)

3.1.3 Characteristic Length

When a crack propagates, energy is consumed within the fracture process zone (damage zone). This energy, the fracture energy or strain-energy release rate, resists crack growth. There is also elastic energy that is released in the region neighboring the fracture process zone as the crack propagates. This elastic energy, expressed as the strain-energy density, serves to drive crack propagation. The characteristic length, defined by Hillerborg (1976, 1983, 1985), is the ratio of the fracture energy to the strain-energy density at the peak stress. Since the ratio is of energy per unit area to energy per unit volume, it has units of length. The characteristic length is a measure of how sensitive a material is to crack propagation (the lower the characteristic length, the more brittle the material). Characteristic length is a pure material property that is approximately proportional to the length of the fracture process zone (Hillerborg 1983).

The characteristic length of a material is:

$$l_{ch} = G_f E/(f'_t)^2 \qquad (3.5)$$

where:

l_{ch} = characteristic length (m or in.)

G_f = fracture energy or strain-energy release rate (N/m or lb./in.)

E = modulus of elasticity (MPa or psi)

f'_t = uniaxial tensile strength (MPa or psi)

$(f'_t)^2/E$ = strain-energy density on both sides of a crack (N/m^2 or psi)

3.1.4 Uniaxial Tensile Strength

Uniaxial tensile strength is needed for the calculation of characteristic length.

However, in the current study, only the modulus of rupture was measured. Bazant and Planas (1997) recommend the following expression to determine the uniaxial tensile strength based on the modulus of rupture using a 3 or 4-point bending test.

$$f'_t = R(1 - 0.1773D/S) \qquad (3.6)$$

where: f'_t = uniaxial tensile strength (MPa or psi)
R = modulus of rupture (MPa or psi)
D = depth of the beam (m or in.)
S = total span of the beam (m or in.)

For current tests, $f'_t = 0.941$ to 0.955 R.

3.2 COMPRESSION TEST RESULTS

The results of the compression tests are presented in Table 3.1 for tests at 7, 28, 56, 90, and 180 days. As stated in Chapter 2, the tests were performed on 69 specimens with a 3 to 1 aspect ratio. Compressive strengths range from 20 to 99 MPa (2,920 to 14,320 psi).

3.2.1 Effects of Aggregate Type

The effects of aggregate type on compressive strength show scatter. Comparing basalt and limestone high-strength concrete, basalt concrete generally yields higher compressive strength (Figure 3.2). For example, at 7 days, the basalt high-strength specimens averaged 19 percent higher compressive strength than the limestone specimens. At 180 days, the basalt high-strength specimens averaged 25 percent higher compressive strength than the limestone specimens. These observations are supported by other researchers (Kaplan 1959, Giaccio et al. 1992,

Kozul and Darwin 1997, Ozturan and Cecen 1997) who found that higher strength aggregates, such as basalt in this study, provide higher compressive strengths than weaker aggregates, such as limestone, in high-strength concrete. The matrix is denser and the voids are considerably reduced in high-strength concrete, giving a greater compatibility between matrix and aggregate strength and stiffness, which lowers the stress concentrations at the matrix-aggregate interface. The tensile strength of the aggregate, instead of the interfacial strength (as in normal-strength concrete), becomes the weak link. Because of this, the compressive strength of high-strength concrete can be limited by aggregate strength.

The medium-strength limestone concrete usually had slightly higher compressive strengths than that containing basalt (Figure 3.3). At 7 days, the limestone medium-strength specimens averaged 5 percent higher compressive strength than the basalt specimens. At 180 days, the limestone medium-strength specimens averaged 8 percent higher compressive strength than the basalt specimens. These differences probably result from the basalt concrete having higher stress concentrations in the matrix around the aggregate, caused by the basalt aggregate having a higher relative stiffness than the limestone aggregate. These higher stress concentrations in basalt concrete cause lower compressive strengths.

In normal-strength concrete, the results were somewhat inconsistent, since the second batch of limestone concrete, NL2, yielded slightly higher compressive strengths and the first batch of limestone concrete, NL1, yielded lower compressive strengths than either basalt batch at all ages (Figure 3.4). At 7 days, limestone specimen NL2-7C had 8 percent higher compressive strength than basalt specimen NB2-7C, but limestone specimen NL1-7C had 38 percent lower compressive strength. At 180 days, limestone specimen NL2-180C had 2.5 percent higher compressive strength than basalt specimen NB2-180C, but limestone specimen NL1-180C had 22 percent lower compressive strength. No definite conclusion can be drawn about the effect of aggregate type on normal-strength concrete. This kind of inconclusive behavior is not unexpected, because most past studies have

demonstrated that aggregate type does not play a significant role in determining the compressive strength of normal- strength concrete.

The type of aggregate determines the failure surface of the specimens in compression. In normal-strength concrete with both types of aggregate, the fracture surface was tortuous, with significant crack branching. The basalt concrete had virtually no fractures through the coarse aggregate. In the limestone concrete, there was evidence of some transgranular fracture, which left the fracture surface less rough than in the basalt concrete. In high-strength concrete, the branching was similar, although less severe than in normal-strength concrete. However, there was a large increase in the fracture of coarse aggregate particles. In the basalt concrete, most, but not all, of the coarse aggregate fractured. The limestone concrete had complete transgranular fracture, leaving the crack surface less tortuous than in basalt concrete and the smoothest overall. The medium-strength concrete had fracture surfaces that were a composite of those observed in normal-strength and high-strength concrete.

3.2.2 Effects of Water-to-Cementitious Material Ratio

Figure 3.5 shows the relation between average compressive strength and average w/cm ratio for limestone concrete. In this case, the medium-strength concrete always surpassed the normal-strength concrete in compressive strength at the same age. For example, at 7 days, the medium-strength specimens averaged 55 percent greater strength than the normal-strength specimens. At 180 days, the medium-strength specimens averaged 33 percent greater compressive strength than the normal-strength specimens. The decrease in w/cm ratio from normal-strength concrete to medium-strength was 24 percent. The high-strength concrete always exceeded the medium-strength concrete in compressive strength at the same age. At 7 days, the high-strength specimens averaged 37 percent greater compressive strength than the medium-strength specimens. At 180 days, the high-strength specimens

averaged 28 percent higher compressive strength than the medium-strength specimens. The decrease in w/cm ratio from medium-strength concrete to high-strength was 26 percent.

Figure 3.6 shows the relation between average compressive strength and average w/cm ratio for basalt concrete. Like the limestone concrete, a reduction in w/cm ratio resulted in an increase in compressive strength. At 7 days, the medium-strength specimens averaged 20 percent greater compressive strength than the normal-strength specimens and the high-strength specimens averaged 72 percent greater compressive strength than the medium-strength specimens. At 180 days, the respective values were 9 and 72 percent. The w/cm ratio decreased 24 percent from normal-strength concrete to medium-strength concrete and by another 17 percent from medium-strength concrete to high-strength concrete.

The w/cm ratio is usually accepted as the primary controlling factor in the compressive strength of concrete. The compressive strength increases as the w/cm ratio decreases. Limestone concrete had almost twice the percent increase in compressive strength from normal to medium-strength as basalt concrete (probably resulted from better bonding characteristics and elastic compatibility of limestone and the matrix at those w/cm ratios). On the other hand, basalt concrete had almost twice the percent increase in compressive strength from medium to high-strength as limestone concrete. The higher increase in strength for the basalt concrete might be caused by the matrix-aggregate bond strength [the weak link in basalt concrete that is improved by the addition of silica fume (Tasdemir et al. 1996)] increasing close to the tensile strength of basalt, as well as, limestone concrete being limited by the strength of its aggregate.

The w/cm ratio had an effect on the nature of concrete fracture in compression. The normal-strength concrete was observed to fracture with a large number of diagonal cracks, generally sloping towards the middle third of the specimen. The cracks rarely affected the extreme ends of the specimen, which were confined by friction from the loading platens. Ultimate fracture of the specimens

occurred within seconds of strain-softening. In the high-strength concrete, the failure after peak load was violent and explosive, with the cracks in the specimen running mostly parallel to the axis of loading. This type of failure is caused by the testing machine being somewhat flexible, resulting in a great amount of stored energy within both the specimen and the machine right before failure. The release of energy at failure shatters the specimen.

3.2.3 Effects of Concrete Age

Figure 3.7 shows the relation between average compressive strength and age. In limestone concrete, all mixes yielded a higher compressive strength with an increase in age. The medium-strength concrete seemed to gain more of its 180 day strength earlier than the normal-strength concrete. A similar effect occurs when comparing high-strength and medium-strength concrete (the higher the strength, the higher the rate of early strength development). Figure 3.8 shows the relation between the average percentage of compressive strength at 180 days and age.

In basalt concrete, all strengths yielded a higher compressive strength with an increase in age (with the exception of 56 to 90 day high-strength concrete, which actually decreased slightly in strength). Similar to limestone concrete, the medium-strength concrete attained a higher percentage of its 180 day strength at earlier ages than the normal-strength concrete. Unexpectedly, high-strength concrete attained a lower percentage of its 180 day strength at 7, 28, 56, and 90 days than did the medium-strength concrete. This may be due to the silica fume not contributing as much to the early strength of the high-strength concrete as fly ash contributes to the later strength (Lam et al. 1998). Also, the small number of specimens at each age may have skewed the results.

Compressive strength is recognized to increase with an increase in age, with the effect more evident at earlier ages. The results of this study revealed similar findings. Both limestone and basalt concrete had similar rate developments of

compressive strength with age for normal and medium-strength concrete. For the normal-strength concretes, the two aggregates produced similar compressive strengths with age. For the medium-strength concretes, concrete containing limestone yielded slightly higher compressive strengths compared to concrete containing basalt. In high-strength concrete, concrete containing basalt exhibited higher compressive strength, but lower early percentage gains with age compared to concrete containing limestone.

Concrete age had little effect on the appearance of failure surfaces for the compression specimens.

3.3 FLEXURAL TEST RESULTS

Flexural test results are shown in Table 3.2. As stated in Chapter 2, the flexural strengths were obtained using beams in three-point bending. The 64 flexural tests were performed on the same days as the compressive strength tests for concrete in the same batch, at 7, 28, 56, 90, and 180 days. Flexural strengths range from 4 to 14 MPa (550 to 1,960 psi).

3.3.1 Effects of Aggregate Type

In high-strength concrete, basalt concrete always yielded significantly higher moduli of rupture than limestone concrete at the same ages (basalt concrete had up to almost twice the strength) (Figure 3.9). For example, at 7 days, the basalt high-strength specimens averaged 61 percent higher flexural strength than the limestone specimens, and at 180 days, the basalt high-strength specimens averaged 92 percent greater flexural strength than the limestone specimens. These results match those of Kozul and Darwin (1997) for concrete containing the same aggregates. Other studies (Kaplan 1959, Ozturan and Cecen 1997) have also shown comparable results. Ezeldin and Aitcin (1991) and Giaccio et al. (1992, 1993), however, found that

aggregate type does not affect flexural strength. This contradiction in results is puzzling, considering that in the current study, the strength of the aggregate played a major role in determining the flexural strength. All the coarse aggregate particles on the failure surface fractured for the limestone specimens, while only partial transgranular fracture was observed for the basalt specimens.

For medium-strength concretes, concrete containing basalt yielded similar moduli of rupture to concrete containing limestone at the same age (Figure 3.10). The average values of flexural strength deviated by a maximum of 8 percent (28 days) at any age.

The normal-strength concrete made with either aggregate produced similar moduli of rupture at early ages (Figure 3.11). At 7, 28, and 56 days, the basalt normal-strength specimens averaged 3, 22, and 4 percent, respectively, greater flexural strength than the limestone specimens. However, at 90 and 180 days, the limestone specimens produced higher flexural strengths averaging 14 and 27 percent, respectively, greater than the basalt specimens. Overall, aggregate type seems to have little effect on flexural strength in normal and medium-strength concrete. Some research has demonstrated that aggregate type does not play a significant role in the flexural strength (Ezeldin and Actin 1991, Kozul and Darwin 1997). Ozturan and Cecen (1997) concluded that limestone concrete had higher flexural strengths than basalt or gravel concrete at lower compressive strengths, due to its superior bond.

The fracture surfaces in the flexural specimens were similar to those in compression, although there was slightly more transgranular fracture in the flexural specimens.

3.3.2 Effects of Water-to-Cementitious Material Ratio

Figure 3.12 shows the average modulus of rupture as a function of average w/cm ratio for limestone concrete. The results indicate relatively little change in flexural strength with a decrease in w/cm ratio. At 7 days, the medium-strength

specimens averaged 27 percent greater flexural strength than the normal-strength specimens and the high-strength specimens averaged 4 percent greater flexural strength than the medium-strength specimens. At 180 days, the corresponding values are 0 and 9 percent. It seems clear that the weak tensile strength of the limestone limited the flexural strength of the concrete.

Figure 3.13 shows the average modulus of rupture as a function of average w/cm ratio for basalt concrete. Unlike limestone concrete, basalt concrete increases in flexural strength significantly with a decrease in w/cm ratio (especially at lower w/cm ratios). At 7 days, the medium-strength specimens averaged 21 percent greater flexural strength than the normal-strength specimens and the high-strength specimens averaged 61 percent greater flexural strength than the medium-strength specimens. At 180 days, the respective values are 21 and 92 percent. The strong tensile strength of the basalt enhanced the flexural strength of the concrete as the strength of the cement matrix increased.

Basalt, the stronger aggregate, produced concrete with a significant increase in flexural strength with a decrease in w/cm ratio. The transition from medium to high-strength yielded the highest average increase in flexural strength (high-strength concrete was almost double medium-strength concrete), which may be due to the use of silica fume in high-strength concrete, which is known to increase matrix-aggregate bond strength.

3.3.3 Effects of Concrete Age

Figure 3.14 shows the average modulus of rupture as a function of age for both concretes. The basalt high-strength concrete had higher moduli of rupture than limestone high-strength concrete. The normal and medium-strength concretes had similar moduli of rupture.

For limestone concrete, all three mixes yielded higher flexural strengths with an increase in age. Both high-strength and medium-strength concretes attained higher

early strengths than normal-strength concrete. Figure 3.15 shows the average percentage of modulus of rupture at 180 days versus age.

For basalt normal and medium-strength concrete, flexural strength increased from 7 to 28 days, and then slowly dropped out to 180 days. Basalt high-strength concrete yielded higher flexural strengths with age.

Like compressive strength, flexural strength is generally understood to increase with age, although at a substantially slower rate than compressive strength. In the current study, compressive strength increased on average, by 51 percent from 7 to 180 days, while flexural strength increased by 26 percent. Conversely, concrete gains a greater percentage of its long-term flexural strength at an early age. In this study, the greatest increase in flexural strength usually occurred from 7 to 28 days (about 20 to 25 percent).

Age had little effect on the appearance of the failure surface.

3.4 FRACTURE ENERGY TEST RESULTS

The fracture test results are shown in Table 3.3. Detailed results are presented in Tables A.1 (SI units) and A.2 (customary units). As described in Chapter 2, the 77 fracture energy tests were performed on notched beams in three-point bending. The tests were performed on the same days as compressive and flexural strength tests for concrete in the same batch at 7, 28, 56, 90, and 180 days.

3.4.1 Effects of Aggregate Type

The basalt concrete had significantly higher fracture energies than the limestone concrete at all w/cm ratios and ages, matching the results in Kozul and Darwin (1997). Petersson (1980) also found concretes with stronger aggregates produced higher fracture energies.

For high-strength concrete at 7 days, basalt specimen HB2-7E had 207

percent higher fracture energy than limestone specimen HL2-7E even though their compressive strengths were similar (the basalt concrete had only a 3 percent higher compressive strength than the limestone concrete). At 90 days, comparable compressive strengths (limestone concrete was 4 percent higher) were achieved by specimens, HL2-90C and HB2-90C. However, the basalt specimen had 176 percent higher fracture energy.

For medium-strength concrete at 7 days, basalt specimen MB1-7E exhibited 224 percent higher fracture energy than limestone specimen ML1-7E, although the basalt concrete only had 3 percent higher compressive strength than the limestone concrete. At 90 days, the limestone concrete yielded 1 percent higher compressive strength, while basalt specimen MB2-90E had 174 percent higher fracture energy than limestone specimen ML1-90E.

For normal-strength concrete at 7 days, basalt specimen NB1-7E produced 138 percent higher fracture energy than limestone specimen NL2-7E. The limestone concrete had 1 percent higher compressive strength. Comparing 90 day test specimens NL2-90E and NB2-90E, the basalt specimen yielded a 321 percent greater fracture energy, while the limestone concrete produced 5 percent higher compressive strength. At 180 days, basalt specimen NB2-180E had 177 percent higher fracture energy than limestone specimen NL2-180E, although the limestone concrete had 3 percent higher compressive strength. These differences are due to the greater tendency of the limestone to fracture, while the stronger basalt produces less aggregate fracture and a more tortuous and meandering crack surface. As a result, the basalt concrete has a larger fracture surface area, more mechanical interlock in the fracture region, and, therefore, more fracture energy.

Looking at the load-deflection curves, basalt high-strength concrete yielded an average of 39 percent higher peak load (significantly larger than the increase for medium or normal-strength concrete) and a 58 percent greater final deflection than limestone high-strength concrete at all ages. In a similar fashion, medium-strength concrete containing basalt averaged 15 percent higher peak load and 68 percent

greater final deflection than medium-strength concrete containing limestone at all ages, and normal-strength concrete containing basalt averaged of 17 percent higher peak load and 61 percent greater final deflection than limestone normal-strength concrete at all ages. In addition to limestone concrete having lower peak loads and final deflections than basalt concrete, it also exhibits a steeper softening branch (curve after peak load), as shown in Figures 3.16–3.18. All three of these factors result in less area under the load-deflection curve and thus, lower fracture energy. Kozul and Darwin (1997) obtained similar results.

A profile view of the failure surfaces of fracture specimens are shown in Figure 3.19. For normal-strength concrete, the fracture surface of basalt concrete was the most tortuous overall (as it was in compression and flexural specimens) and was somewhat rougher than on the limestone concrete specimens, because of lower trangranular fracture (less than half of the aggregate fractured) than the limestone concrete, in which most of the aggregate fractured on the failure surface. The high-strength concrete containing limestone had the smoothest surface, overall, with complete transgranular fracture, while high-strength concrete containing basalt had a surface comparable to normal-strength limestone concrete.

3.4.2 Effects of Water-to-Cementitious Material Ratio

Figure 3.20 shows average fracture energy as a function of average w/cm ratio for limestone concrete. Fracture energy is nearly constant at all ages

Figure 3.21 shows average fracture energy as a function of average w/cm ratio for basalt concrete. Except for the 90 day specimens, fracture energy remains nearly constant with w/cm ratio and independent of age. For the 90 day specimens, fracture energy *increases* with increasing w/cm ratio.

Overall, fracture energy appears to depend principally on aggregate type.

Load-deflection curves, comparing concretes containing limestone, show an average increase of 15 percent in peak load from normal to medium-strength (Figure

3.22), while final deflections are similar. From medium to high-strength, concretes containing limestone have similar peak loads and an average decrease in final deflections of 28 percent (Figure 3.23).

The peak loads for basalt concrete increase an average of 13 percent from normal to medium-strength concrete (Figure 3.24), while final deflections are similar. Peak loads increase an average of 29 percent from medium to high-strength basalt concrete. Final deflections decrease an average of 47 percent (Figure 3.25).

Petersson (1980) found that fracture energy increases with decreasing w/cm ratio, for w/cm ratios above 0.4. Below a w/cm ratio of 0.4, he observed that fracture energy remains constant. Nallathambi et al. (1984) found that normal-strength concrete increases in fracture energy with a decrease in w/cm ratio. The current study demonstrates no change in fracture energy for the same percent decrease in w/cm ratio (although this study's w/cm ratios are lower). Zhou et al. (1995) found an increase in fracture energy with a decrease in w/cm ratio for concrete containing gravel and 20 mm limestone. However, they discovered a decrease in fracture energy with a decrease in w/cm ratio for concrete containing 10 mm limestone. They concluded that the 10 mm limestone provided a better matrix-aggregate bond, causing more aggregate to fracture, resulting in less surface area, and, hence, less fracture energy.

Failure surfaces for the fracture specimens reveal that the surfaces of normal-strength concretes were rougher and more tortuous than medium-strength and, especially, high-strength concrete. Again, basalt normal-strength concrete had the most tortuous surface, while limestone high-strength had the least tortuous surface.

3.4.3 Effects of Concrete Age

Figure 3.26 shows average fracture energy as a function of age. The figure illustrates again that fracture energy is more dependent on aggregate type than on w/cm ratio or age.

Medium-strength limestone concrete generally exhibits a slight increase in fracture energy with an increase in age. The other concretes show no variation in fracture energy.

Petersson (1980) found that fracture energy increased with an increase in age up to 28 days, then remained constant. Niwa et al. (1997) also found that fracture energy increases at early ages. However, both authors agreed that there is only a slight increase in fracture energy due to age and that the rate of this increase slowly diminishes over time.

3.5 FLEXURAL STRENGTH VERSUS COMPRESSIVE STRENGTH

The relationship between flexural strength (modulus of rupture) and compressive strength has been well researched. ACI Committee 363 (ACI 363R-92) developed the following equation to describe the relationship:

$$R = 0.94(f'_c)^{0.5} \quad \text{MPa}$$
$$(21 \text{ MPa} < f'_c < 83 \text{ MPa}); \text{ or} \qquad (3.7)$$
$$R = 11.7(f'_c)^{0.5} \quad \text{psi}$$
$$(3{,}000 \text{ psi} < f'_c < 12{,}000 \text{ psi})$$

where: R = flexural strength (MPa or psi)
f'_c = compressive strength (MPa or psi)

The results of this study are plotted along with Eq. 3.7 in Figure 3.27. [Note: Eq. 3.7 is based on compression specimens with height to width ratios of 2 to 1, which typically yield slightly higher compressive strengths than the 3 to 1 ratio specimens used in this study and on flexural specimens under third-point loading, which give slightly lower flexural strengths than the center-point loading used in this study]. The

modulus of rupture increases almost linearly with compressive strength for the basalt concrete, while the data points for the limestone concrete seem to follow the ACI equation.

For normal-strength concrete, the basalt and limestone mixes yield flexural strengths from 17 percent below to 10 percent above the flexural strengths determined by Eq. 3.7. The limestone mixes tend to be a little higher in the range and basalt mixes tend to be somewhat lower.

For medium-strength concrete, the limestone mixes give flexural strengths that are slightly higher than Eq. 3.7, with greatest difference equal to 5 percent. The basalt mixes give flexural strengths above those predicted by Eq. 3.7, by values as high as 12 percent.

For high-strength concrete, mixes containing limestone have flexural strengths from 4 to 12 percent below those predicted by Eq. 3.7. In contrast, the basalt mixes have strengths from 19 to 31 percent greater than predicted by Eq. 3.7. Overall, the limestone concretes have flexural-to-compressive strength ratios between 11 and 16 percent, independent of w/cm ratio or age.

For the basalt concretes, the flexural-to-compressive strength ratios varied in somewhat narrower ranges that depended on the w/cm ratio. Normal-strength concrete has ratios between 11 and 16 percent, medium-strength concrete has ratios between 12 to 16 percent, and high-strength concrete has ratios between 14 to 15 percent.

The flexural-to-compressive strength ratios for normal and medium-strength basalt concrete seem to agree reasonably well with those derived from Eq. 3.7, while the flexural-to-compressive strength ratios of the high-strength basalt concrete are high in comparison. The ratios for the limestone concretes are slightly low for normal-strength concrete, similar for medium-strength concrete, and slightly high for high-strength concrete compared to Eq. 3.7. Based on Eq. 3.7, flexural-to-compressive strength ratios of 14 to 19 percent for normal-strength concrete, 11 to 14 percent for medium-strength concrete, and 9 to 11 percent for high-strength concrete

are calculated.

The normal-strength basalt concrete and all limestone concretes have slightly higher flexural-to-compressive strength ratios, while basalt high-strength concrete have noticeably higher flexural-to-compressive strength ratios compared to past studies. Kaplan (1959) had ratios of 8 to 11 percent for basalt and limestone high-strength concrete. Cook (1989) found that flexural-to-compressive strength ratios stay almost constant at 12 percent for high-strength concrete. Walker (1960) discovered the same flexural-to-compressive strength ratio (12 percent) for normal-strength concrete.

3.6 MODULUS OF ELASTICITY VERSUS COMPRESSIVE STRENGTH

There has been a considerable amount of research on the relationship between modulus of elasticity and compressive strength. An equation commonly used to relate the two is (ACI 318-95):

$$E = 0.043 w^{1.5} (f'_c)^{0.5} \quad \text{MPa}$$
$$(5.6\ \text{kg/m}^3 < w < 9.7\ \text{kg/m}^3); \text{ or} \qquad (3.8)$$
$$E = 33 w^{1.5} (f'_c)^{0.5} \quad \text{psi}$$
$$(90\ \text{lb/ft}^3 < w < 155\ \text{lb/ft}^3)$$

where: E = modulus of elasticity (MPa or psi)
w = unit weight of concrete (kg/m^3 or lb/ft^3)
f'_c = compressive strength (MPa or psi)

This equation, along with the results of this research, are plotted in Figure 3.28. Table 3.4 gives the values of moduli of elasticity obtained from the fracture energy tests. [Note: Eq. 3.8 is based on moduli of elasticity obtained from compression tests,

while this study used data from the fracture tests (see section 3.1.2).]

Overall, the data matches Eq. 3.8 quite well, with the stronger, stiffer basalt producing points that are generally above the curve and the limestone producing points that are generally below the curve. The values of experimental modulus of elasticity are within a range of + 26.5 percent (basalt medium-strength concrete) to – 20.4 percent (limestone medium-strength concrete) of the values predicted by Eq. 3.8.

3.7 FRACTURE ENERGY VERSUS COMPRESSIVE STRENGTH

Figure 3.29 compares fracture energy with compressive strength for the specimens tested in this study. Unlike flexural strength and modulus of elasticity, fracture energy appears to have no relationship to compressive strength. Rather, fracture energy appears to depend primarily on aggregate type. Concrete containing basalt yielded significantly higher fracture energy and greater scatter in the values of fracture energy than concrete containing limestone for all mixes. For concretes with ages between 7 and 180 days, w/cm ratio and age do not appear to affect fracture energy. Gettu, Bazant, and Karr (1990) found an increase in compressive strength of 160 percent resulted in an increase in fracture energy of only 12 percent. Giaccio et al. (1993) observed that fracture energy increased as compressive strength increased, but at only a fraction of the rate. Xie, Elwi, and MacGregor (1995) found increases in compressive strength of 53 and 29 percent resulted in fracture energy increases of only 13 and 11 percent, respectively. Zhou, Barr, and Lydon (1995) found fracture energy increased or decreased with an increase in compressive strength, depending on the aggregate. Kozul and Darwin (1997) found no discernible relation between fracture energy and compressive strength.

3.8 FRACTURE ENERGY VERSUS FLEXURAL STRENGTH

As shown in Figure 3.30, fracture energy appears to be unrelated to flexural strength. Fracture energy may even decrease slightly with increased flexural strength for basalt concrete, but remains constant for limestone concrete.

3.9 CHARACTERISTIC LENGTH VERSUS COMPRESSIVE STRENGTH

The calculated values for characteristic length are given in Table 3.5. Since characteristic length is a function of fracture energy, it is not unexpected that the relation between characteristic length and compressive strength varies with aggregate type. For all compressive strengths, the limestone concrete has lower characteristic lengths than the basalt concrete, as shown in Figure 3.31. The difference is most obvious for lower strengths.

As shown in Figure 3.31, characteristic length varies greatly for basalt concrete as compressive strength increases from about 50 to 80 MPa, with values dropping from 209 mm at 50.8 MPa (NB2-180) to 44 mm at 81.7 MPa (HB2-90). For limestone concrete, characteristic lengths vary little, the values decreasing from 36 mm at 49.0 MPa (NL2-90) to 32 mm at 76.5 MPa (HL2-56). The rate of decrease in characteristic length with increasing compressive strength decreases with increasing compressive strength.

At lower compressive strengths, basalt concrete has significantly higher characteristic lengths than limestone concrete. The difference decreases sharply at high strengths. Overall, the brittleness of basalt concrete is more sensitive to compressive strength than the brittleness of limestone concrete, which is low at all compressive strengths.

Petersson (1980) found a decrease in characteristic length with w/cm ratio below 0.5. He also found that characteristic length decreases at early ages, then remains unchanged. Gettu et al. (1990) observed that characteristic length decreases

sharply with an increase in compressive strength for high-strength concrete. Giaccio et al. (1993) observed that high-strength concrete has characteristic lengths two to three times smaller than normal-strength concrete. Zhou et al. (1995) concluded that characteristic length decreases with an increase in compressive strength (brittleness increases with a decrease in w/cm ratio). They also found larger characteristic lengths for stronger aggregate.

3.10 PEAK BENDING STRESSES IN FRACTURE TESTS VERSUS FLEXURAL STRENGTH

The peak stresses in the fracture tests are compared to flexural strength in Figure 3.32. The peak stresses in the fracture tests are calculated using the peak load and net section at the plane of the notch. Values are given in Table 3.6. As shown in Figure 3.32, the two values of stress are nearly linearly related, as given by the linear best fit equation:

$$f'_f = 0.667R + 1.20 \quad \text{(MPa)} \qquad (3.9)$$

where: f'_f = fracture stress (MPa)

R = flexural stress (MPa)

This relationship is useful, because flexural stress and compressive stress have a close relationship and, thus, peak fracture stress and compressive stress do as well. Eq. 3.9 shows that the peak fracture stress was about two-thirds of the flexural stress. Kozul and Darwin (1997) found similar results on similar specimens, with $f'_f = 0.666R + 0.71$ (MPa).

The relation between f'_f and R is due to the stress concentration at the notch, strain-softening effects in the concrete, and differences in the rate of loading. According to a finite element analysis using ANSYS, the stress concentration factor

is 2.0 for a linear elastic material with the same dimensions as the fracture specimen. This should result in a peak fracture stress equal to about one-half of the flexural stress. Strain-softening in the concrete reduces the effect of the stress concentration (redistributes the stress over a larger area) and increases the nominal flexural stress the beam can withstand. Also, the fracture tests reach their peak load in about 30 seconds, while the flexural tests take 4 to 13 minutes (240 to 780 seconds) to reach peak load. Since a higher loading rate usually results in slightly higher strength, the fracture specimens may have a higher strength.

Figure 3.32 and Eq. 3.9 are useful in understanding potential problems related to the fracture properties of high-strength concrete. As shown in Figure 3.29, high-strength and normal-strength concrete have similar fracture energies. Since high-strength concrete has dissipated more of its fracture energy by the time it has reached the peak load than has normal-strength concrete, high-strength concrete has less energy available once the load begins to drop (softening portion of the curve - see, for example, Figure 3.25). This, coupled with the fact that high-strength concrete has a higher driving force, (strain-energy stored at peak load), results in more rapid crack growth and more brittle failure than in normal-strength concrete. Quantitatively, this is explained by characteristic length.

CHAPTER 4
SUMMARY and CONCLUSIONS

4.1 SUMMARY

The effects of aggregate type, water-to-cementitious material ratio, and age on compressive strength, flexural strength, and fracture properties of concrete were examined. Concrete mixes contained either basalt or limestone, water-to-cementitious material ratios ranged from 0.25 to 0.46, and tests were performed at 7, 28, 56, 90, and 180 days. The maximum aggregate volume factor (ACI 211.1-91) and maximum aggregate size were constant at 0.67 and 19 mm (3/4 in.), respectively. Two-hundred fifteen total specimens were tested (69 compressive specimens, 69 flexural specimens, and 77 fracture specimens). Compressive strengths ranged from 20 to 99 MPa (2,920 to 14,320 psi).

4.2 CONCLUSIONS

The following conclusions are based on the tests and evaluations presented in this report.

1. High-strength concrete containing basalt has a higher compressive strength than concrete containing limestone, even at a higher w/cm ratio. Medium-strength concrete containing limestone has a slightly higher compressive strength than concrete containing basalt. The compressive strength of normal-strength concrete is not affected by aggregate type.
2. Water-to-cementitious material (w/cm) ratio is the main controlling factor of compressive strength.

3. The compressive strength of concrete increases with age. The greatest percentage of the long-term compressive strength is attained at early ages, especially in higher strength concrete.
4. High-strength concrete containing basalt has significantly higher flexural strength than concrete containing limestone. Medium and normal-strength concrete have similar flexural strengths for the two aggregates.
5. Aggregate strength and water-to-cementitious material (w/cm) ratio are the main controlling factors for flexural strength.
6. Flexural strength increases with age, but at a slower rate than observed for compressive strength.
7. Concrete containing basalt has significantly higher fracture energy than concrete containing limestone for all compressive strengths.
8. Fracture energy appears to be independent of compressive strength, w/cm ratio, and age and is primarily controlled by aggregate type.
9. High and medium-strength concrete containing basalt has a higher modulus of elasticity than concrete containing limestone. At lower strengths, the modulus of elasticity is not affected by aggregate type. The modulus of elasticity increases as compressive strength increases.
10. Characteristic length is greater for concrete containing stronger aggregate (basalt). Characteristic length decreases with an increase in compressive strength.
11. There is a close relation between peak bending stresses in fracture and flexural tests.

4.3 FUTURE WORK

The current study provides information on the effects of aggregate type, water-to-cementitious material ratio, and age on the compression, flexural, and fracture behavior of concrete. The fact that fracture energy remains constant with increasing

compressive strength is the most important observation of the study, because of the rising use of high-strength concretes. Since higher strength concretes obviously take higher loads in service for a given volume of concrete, the probability of catastrophic tension failures is higher than for lower strength concretes. This shortcoming emphasizes the need to increase the ductility and fracture energy of high-strength concrete (systems). The mechanical and fracture properties of the concrete constituents themselves (mortar and aggregates) may need to be examined to gain a better understanding of concrete as a whole. Also, the fracture energy test used in this study was a three-point bending test on notched beams of one size and aspect ratio. Other test procedures or versions of the current test may provide better results. Lastly, consideration should be given to the application of nonlinear finite element analysis to better understand the fracture behavior of concrete.

REFERENCES

ACI Committee 211. (1991) "Standard Practice for Selecting Proportions for Normal, Heavyweight, and Mass Concrete (ACI 211.1-1-91)," *ACI Manual of Concrete Practice*, 1997 Edition, Part 1, American Concrete Institute, Farmington Hills, MI.

ACI Committee 363. (1992) "State-of-the-Art Report on High-Strength Concrete (ACI 363R-92)," *ACI Manual of Concrete Practice*, 1997 Edition, Part 1, American Concrete Institute, Farmington Hills, MI.

Aitcin, P.-C. and Mehta, P. K. (1990) "Effect of Coarse-Aggregate Characteristics on Mechanical Properties of High-Strength Concrete," *ACI Materials Journal*, V. 87, No. 2, Mar.-Apr., pp. 103-107.

Bazant, Z. P. and Planas, J. (1997) "Size Effect on the Modulus of Rupture of Concrete," *Fracture and Size Effect in Concrete and Other Quasibrittle Materials*, pp. 280-281.

Bentur, A. and Mindess, S. (1986) "The Effect of Concrete Strength on Crack Patterns," *Cement and Concrete Research*, V. 16, No. 1, Jan., pp. 59-66.

Carrasquillo, R. L., Nilson, A. H., and Slate, F. O. (1981) "Properties of High Strength Concrete Subject to Short-Term Loads," ACI Journal, *Proceedings* V. 78, No. 3, May-June, pp. 171-178.

Carrasquillo, R. L., Nilson, A. H., and Slate, F. O. (1981) "Microcracking and Behavior of High Strength Concrete Subject to Short-Term Loading," ACI Journal, *Proceedings* V. 78, No. 3, May-June, pp. 179-186.

Cook, J. E. (1989) "10,000 psi Concrete," *Concrete International*, Oct., pp. 67-75.

Ezeldin, A. S. and Aitcin, P.-C. (1991) "Effect of Coarse Aggregates on the Behavior of Normal and High-Strength Concretes," *Cement, Concrete, and Aggregates*, V. 13, No. 2, pp. 121-124.

Gettu, R., Bazant, Z. P., and Karr, M. E. (1990) "Fracture Properties and Brittleness of High-Strength Concrete," *ACI Materials Journal*, V. 87, No. 6, Nov.-Dec., pp. 608-617.

Giaccio, G., Rocco, C., Violini, D., Zappitelli, J., and Zerbino, R. (1992) "High-Strength Concretes Incorporating Different Coarse Aggregates," *ACI Materials Journal*, V. 89, No. 3, May-June, pp. 242-246.

Giaccio, G., Rocco, C., and Zerbino, R. (1993) " The Fracture Energy (G_F) of High-Strength Concretes," *Materials and Structures*, V. 26, No. 161, Aug.-Sept., pp. 381-386.

Hillerborg, A., Modeer, M., and Petersson, P. E. (1976) "Analysis of Crack Formation and Crack Growth in Concrete by Means of Fracture Mechanics and Finite Elements," *Cement and Concrete Research*, V. 6, No. 6, June, pp. 773-782.

Hillerborg, A. (1983) "Analysis of One Single Crack," *Fracture Mechanics of Concrete*, Ed. F. H. Whittmann, Elsevier, Amsterdam, pp. 223-249.

Hillerborg, A. (1985) "The Theoretical Basis of a Method to Determine the Fracture Energy G_f of Concrete," *Materials and Structures*, V. 18, No. 106, pp. 291-296.

Hsu, T. T. C. and Slate, F. O. (1963) "Tensile Bond Strength Between Aggregate and Cement Paste or Mortar," ACI Journal, *Proceedings* V. 60, No. 4, pp. 465-486.

Kaplan, M. F. (1959) " Flexural and Compressive Strength of Concrete as Affected by the Properties of Coarse Aggregate," ACI Journal, *Proceedings* V. 30, No. 11, pp. 1193-1208.

Kozul, R. and Darwin D. (1997) "Effects of Aggregate Type, Size, and Content on Concrete," *SM Report* No. 43, University of Kansas, Center for Research, Lawrence, June, 85 pp.

Lam, L., Wong, Y. L., and Poon, C. S. (1998) " Effect of Fly Ash and Silica Fume on Compressive and Fracture Behaviors of Concrete," *Cement and Concrete Research*, V. 28, No. 2, pp. 271-283.

Maher, A. and Darwin, D. (1976) "A Finite Element Model to Study the Microscopic Behavior of Plain Concrete," *SL Report* No. 76-02, University of Kansas, Center for Research, Lawrence, Nov.

Maher, A. and Darwin, D. (1977) "Microsopic Finite Element Model of Concrete," *Proceedings, First International Conference on Mathematical Modeling*, St. Louis, Vol. III, pp. 1705-1714.

Nallathambi, P., Karihaloo, B. L., and Heaton, B. S. (1984) "Effect of Specimen and Crack Sizes, Water/cement Ratio and Coarse Aggregate Texture Upon Fracture Toughness of Concrete," *Magazine of Concrete Research*, V. 36, No. 129, Dec., pp. 227-236.

Niwa, J. and Tangtermsirikul, S. (1997) " Fracture Properties of High-Strength and Self-Compacting High Performance Concretes," *Transactions of the Japan Concrete Institute*, V. 19, pp. 73-80.

Ozturan, T. and Cecen, C. (1997) "Effects of Coarse Aggregate Type on Mechanical Properties of Concretes with Different Strengths," *Cement and Concrete Research*, V. 27, No. 2, Jan., pp. 165-170.

Petersson, P. E. (1980) "Fracture Energy of Concrete: Practical Performance and Experimental Results," *Cement and Concrete Research*, V. 10, No. 1, Jan., pp. 91-101.

RILEM, 1985-TC 50-FMC, Fracture Mechanics of Concrete, "Determination of the Fracture Energy of Mortar and Concrete by Means of Three-Point Bend Tests on Notched Beams," RILEM Recommendation, *Materials and Structures*, V. 18, No. 16, pp. 287-290.

RILEM, 1990-TC 89-FMT, Fracture Mechanics of Concrete, "Determination of Fracture Parameters (K_{IC} and CTOD) of Plain Concrete Using Three-Point Bend Tests," RILEM Recommendation, *Materials and Structures*, V. 23, No. 138, pp. 457-460.

Tasdemir, C., Tasdemir, M. A., Lydon, F. D., and Barr, B. I. G. (1996) " Effects of Silica Fume and Aggregate Size on the Brittleness of Concrete," *Cement and Concrete Research*, V. 26, No. 1, Jan., pp. 63-68.

Xie, J., Elwi, A. E., and MacGregor, J. G. (1995) "Mechanical Properties of Three High-Strength Concretes Containing Silica Fume," *ACI Materials Journal*, V. 92, No. 2, Mar.-Apr., pp. 135-145.

Yogendran, V., Landan, B. W., Hague, M. N., and Ward, M. A. (1987) "Silica Fume in High-Strength Concrete," *ACI Materials Journal*, V. 84, No. 2, Mar.-Apr., pp. 124-129.

Zhou, F. P., Barr, B. I. G., and Lydon, F. D. (1995) "Fracture Properties of High-Strength Concrete with Varying Silica Fume Content and Aggregates," *Cement and Concrete Research*, V. 25, No. 3, pp. 543-552.

TABLE 2.1

Concrete Proportions-cubic meter batch

Batch *	w/cm	water(kg)	cement(kg)	f. a. (kg)	s. f. (kg)	FA (SSD)(kg)	CA (SSD)(kg)	TA (mL)	TF (mL)	slump(mm)	γ (kg/m3)
NB1	0.460	164	356	0	0	790	1054	0	0	83	2412
NB2	0.460	164	356	0	0	790	1054	0	0	95	2380
NB1-2	0.460	164	356	0	0	790	1054	0	0		
NB3	0.460	164	356	0	0	790	1054	0	0	70	2396
NL1	0.460	164	356	0	0	813	991	0	0	108	2339
NL2	0.460	164	356	0	0	813	991	0	0	114	2355
MB1	0.352	148	360	63	0	764	1054	411	0	108	2398
MB2	0.352	148	360	63	0	764	1054	411	0	121	2364
ML1	0.350	148	360	63	0	787	991	0	0	133	2435
ML2	0.350	148	360	63	0	787	991	0	0	102	2401
HB1	0.281	133	470	28	55	683	1054	1643	18068	165	2443
HB2	0.305	133	470	28	55	683	1054	1643	29566	159	2491
HB3	0.274	133	470	28	55	683	1054	1643	14783	165	2467
HL1	0.256	133	470	28	55	707	991	1643	5749	184	2467
HL2	0.263	133	470	28	55	707	991	1643	9034	241	2419

* N = normal strength concrete
M = medium strength concrete
H = high strength concrete
B = basalt aggregate
L = limestone aggregate
# = batch number

w/cm = water-to-cementitous material ratio
f. a. = fly ash
s. f. = silica fume
FA = fine aggregate
CA = coarse aggregate
TA = type A normal range water reducer
TF = type F high range water reducer
γ = unit weight of concrete

TABLE 2.2

Concrete Proportions-cubic yard batch

Batch *	w/cm	water(lb)	cement(lb)	f. a. (lb)	s. f. (lb)	FA (SSD)(lb)	CA (SSD)(lb)	TA (fl.oz.)	TF (fl.oz.)	slump(in)	γ (pcf)
NB1	0.460	276	600	0	0	1332	1776	0	0	3.25	150.6
NB2	0.460	276	600	0	0	1332	1776	0	0	3.75	148.6
NB1-2	0.460	276	600	0	0	1332	1776	0	0		
NB3	0.460	276	600	0	0	1332	1776	0	0	2.75	149.6
NL1	0.460	276	600	0	0	1371	1671	0	0	4.25	146.0
NL2	0.460	276	600	0	0	1371	1671	0	0	4.50	147.0
MB1	0.352	250	607	107	0	1288	1776	11	0	4.25	149.7
MB2	0.352	250	607	107	0	1288	1776	11	0	4.75	147.6
ML1	0.350	250	607	107	0	1327	1671	0	0	5.25	152.0
ML2	0.350	250	607	107	0	1327	1671	0	0	4.00	149.9
HB1	0.281	224	793	47	93	1152	1776	42	467	6.50	152.5
HB2	0.305	224	793	47	93	1152	1776	42	764	6.25	155.5
HB3	0.274	224	793	47	93	1152	1776	42	382	6.50	154.0
HL1	0.256	224	793	47	93	1191	1671	42	149	7.25	154.0
HL2	0.263	224	793	47	93	1191	1671	42	234	9.50	151.0

* N = normal strength concrete
M = medium strength concrete
H = high strength concrete
B = basalt aggregate
L = limestone aggregate
# = batch number

w/cm = water-to-cementitous material ratio
f. a. = fly ash
s. f. = silica fume
FA = fine aggregate
CA = coarse aggregate
TA = type A normal range water reducer
TF = type F high range water reducer
γ = unit weight of concrete

TABLE 3.1
COMPRESSIVE STRENGTH

Group*	7 days (MPa)	28 days (MPa)	56 days (MPa)	90 days (MPa)	180 days (MPa)
NB1	33.8	38.0	42.3	44.3	49.7
NB2	30.1	41.9	39.0	46.9	50.8
NB1-2	35.7	42.7	44.9	51.0	55.2
NB3	35.4	42.8	X	X	X
NL1	20.1	26.0	30.5	33.4	39.9
NL2	34.0	45.4	47.2	49.0	52.1
MB1	40.0	50.4	51.6	52.9	55.4
MB2	39.6	42.6	49.1	52.8	58.1
ML1	38.8	47.0	50.2	53.3	56.0
ML2	45.1	56.5	58.9	63.5	66.6
HB1	71.5	78.2	87.2	76.5	96.6
HB2	65.3	81.9	78.6	81.7	98.7
HB3	65.6	85.4	X	X	X
HL1	51.2	66.6	67.5	70.9	71.3
HL2	63.7	66.9	76.5	84.7	85.7
	(psi)	**(psi)**	**(psi)**	**(psi)**	**(psi)**
NB1	4900	5510	6130	6430	7210
NB2	4360	6070	5660	6810	7380
NB1-2	5170	6190	6510	7390	8010
NB3	5130	6210	X	X	X
NL1	2920	3770	4420	4840	5780
NL2	4940	6580	6850	7110	7560
MB1	5800	7310	7480	7670	8030
MB2	5740	6180	7130	7650	8430
ML1	5630	6810	7280	7740	8130
ML2	6540	8190	8540	9200	9650
HB1	10370	11340	12650	11100	14010
HB2	9470	11870	11400	11850	14320
HB3	9510	12380	X	X	X
HL1	7430	9660	9780	10280	10350
HL2	9240	9700	11100	12290	12430

*H = high-strength concrete N = normal-strength concrete L = limestone
M = medium-strength concrete B = basalt # = batch number

TABLE 3.2
FLEXURAL STRENGTH

Group*	7 days (MPa)	28 days (MPa)	56 days (MPa)	90 days (MPa)	180 days (MPa)
NB1	4.8	6.4	5.7	6.0	5.7
NB2	4.6	6.3	5.8	5.5	5.3
NB1-2	5.2	6.7	5.6	5.7	5.8
NB3	5.7	6.4	X	X	X
NL1	3.8	4.6	4.5	6.1	6.7
NL2	5.7	6.0	6.5	7.0	7.5
MB1	6.2	7.3	7.3	7.1	6.9
MB2	5.7	7.2	7.0	6.7	6.7
ML1	5.7	6.3	6.3	6.4	6.6
ML2	6.4	7.1	7.3	7.3	7.5
HB1	8.9	11.7	11.9	12.1	12.6
HB2	10.2	11.2	10.7	12.2	13.5
HB3	8.3	10.9	X	X	X
HL1	5.7	7.1	7.3	7.5	7.6
HL2	6.9	7.6	7.7	7.7	7.8
	(psi)	**(psi)**	**(psi)**	**(psi)**	**(psi)**
NB1	700	930	830	870	830
NB2	670	910	840	790	770
NB1-2	760	970	820	830	840
NB3	830	920	X	X	X
NL1	550	670	650	880	970
NL2	830	860	940	1020	1080
MB1	890	1060	1070	1030	1010
MB2	820	1040	1010	970	980
ML1	830	910	920	930	960
ML2	930	1020	1050	1060	1090
HB1	1300	1690	1720	1750	1830
HB2	1490	1620	1560	1780	1960
HB3	1200	1580	X	X	X
HL1	820	1030	1050	1090	1110
HL2	1000	1100	1120	1120	1140

*H = high-strength concrete N = normal-strength concrete L = limestone
M = medium-strength concrete B = basalt # = batch number

TABLE 3.3
FRACTURE ENERGY

Group*	7 days (N/m)	28 days (N/m)	56 days (N/m)	90 days (N/m)	80 days (N/m)
NB1	100	106	133	133	136
NB2	143	127	140	202	133
NB1-2	131	106	131	161	138
NB3	131, 110	106, 128, 120	X	X	X
NL1	44	42	52	45	49
NL2	42	45	44	48	48
MB1	146	141	118	162	160
MB2	139	112	145	167	117
ML1	45	45	56	61	63
ML2	55	63	57	66	65
HB1	116	106	127	119	117
HB2	132	104	140	113	128
HB3	127, 137	103, 109, 142	X	X	X
HL1	28	50	39	40	45
HL2	43	42	43	41	36
	(lb/in)	**(lb/in)**	**(lb/in)**	**(lb/in)**	**(lb/in)**
NB1	0.57	0.60	0.76	0.76	0.77
NB2	0.82	0.72	0.80	1.15	0.76
NB1-2	0.75	0.61	0.75	0.92	0.79
NB3	0.75, 0.63	0.73, 0.69, 0.58	X	X	X
NL1	0.25	0.24	0.30	0.26	0.28
NL2	0.24	0.26	0.25	0.27	0.27
MB1	0.84	0.81	0.67	0.92	0.91
MB2	0.79	0.64	0.83	0.95	0.67
ML1	0.26	0.26	0.32	0.35	0.36
ML2	0.31	0.36	0.33	0.38	0.37
HB1	0.66	0.60	0.73	0.68	0.67
HB2	0.75	0.59	0.80	0.65	0.73
HB3	0.72, 0.78	0. 59, 0.62, 0.81	X	X	X
HL1	0.16	0.29	0.22	0.23	0.26
HL2	0.25	0.24	0.25	0.23	0.21

*H = high-strength concrete N = normal-strength concrete L = limestone
M = medium-strength concrete B = basalt # = batch number

TABLE 3.4
MODULI of ELASTICITY**

Group*	7 days (MPa)	28 days (MPa)	56 days (MPa)	90 days (MPa)	180 days (MPa)
NB1	30248	37223	40442	36191	42358
NB2	28441	36460	34304	34740	39786
NB1-2	33448	38702	39447	43354	41846
NB3	30105, 30416	35568, 32391, 34001	X	X	X
NL1	25057	28453	27864	32355	35667
NL2	29401	30387	29809	34079	36140
MB1	35867	39812	40498	40036	42320
MB2	38375	43640	41787	42292	44964
ML1	31150	31923	32106	32927	35672
ML2	31352	32724	32553	33435	35416
HB1	45790	42897	45238	54274	52918
HB2	41763	43425	46464	52046	52442
HB3	39589, 43142	46866, 43053, 48952	X	X	X
HL1	33221	35874	36395	38303	39298
HL2	34747	36836	41034	38514	39106
	(psi)	(psi)	(psi)	(psi)	(psi)
NB1	4387168	5398725	5865618	5248993	6143483
NB2	4124957	5288083	4975422	5038612	5770508
NB1-2	4851249	5613198	5721330	6287956	6069306
NB3	4369369, 4411513	5158702, 4697941, 4931469	X	X	X
NL1	3634213	4126726	4041397	4692696	5173053
NL2	4264317	4407234	4323428	4942787	5241715
MB1	5202081	5774222	5873734	5806672	6138003
MB2	5565886	6329503	6060723	6133992	6521534
ML1	4517855	4630017	4656534	4775712	5173737
ML2	4547284	4746275	4721416	4849320	5136688
HB1	6641284	6221626	6561277	7871795	7675100
HB2	6057159	6298221	6738986	7548594	7606136
HB3	5741884, 6257184	6797362, 6244367, 7099864	X	X	X
HL1	4818367	5203047	5278594	5555435	5699670
HL2	5039650	5342647	5951420	5586036	5671907

*H = high-strength concrete N = normal-strength concrete # = batch number
M = medium-strength concrete B = basalt, L=limestone ** based on fracture tests

TABLE 3.5
CHARACTERISTIC LENGTHS

Group*	7 days (mm)	28 days (mm)	56 days (mm)	90 days (mm)	180 days (mm)
NB1	145	107	176	150	197
NB2	220	124	159	265	209
NB1-2	186	105	182	242	196
NB3	136, 116	128, 109, 97	X	X	X
NL1	89	63	81	45	46
NL2	42	44	34	36	35
MB1	170	115	103	133	160
MB2	174	109	137	181	128
ML1	48	41	49	54	57
ML2	46	47	39	46	45
HB1	74	38	44	49	42
HB2	57	41	62	44	40
HB3	83, 98	46, 45, 67	X	X	X
HL1	32	41	28	29	33
HL2	36	29	32	28	26
	(in)	(in)	(in)	(in)	(in)
NB1	5.70	4.21	6.92	5.90	7.77
NB2	8.66	4.86	6.24	10.42	8.25
NB1-2	7.31	4.13	7.18	9.52	7.72
NB3	5.37, 4.57	5.02, 4.29, 3.83	X	X	X
NL1	3.51	2.47	3.20	1.78	1.79
NL2	1.64	1.72	1.35	1.43	1.37
MB1	6.71	4.53	4.05	5.24	6.29
MB2	6.85	4.28	5.39	7.11	5.03
ML1	1.89	1.61	1.94	2.12	2.23
ML2	1.80	1.85	1.53	1.81	1.76
HB1	2.92	1.49	1.74	1.91	1.67
HB2	2.23	1.60	2.44	1.75	1.59
HB3	3.25, 3.84	1.82, 1.76, 2.62	X	X	X
HL1	1.27	1.60	1.11	1.15	1.29
HL2	1.40	1.14	1.25	1.12	1.01

*H = high-strength concrete N = normal-strength concrete L = limestone
M = medium-strength concrete B = basalt # = batch number

TABLE 3.6
PEAK BENDING STRESS in FRACTURE TESTS

Group*	7 days (MPa)	28 days (MPa)	56 days (MPa)	90 days (MPa)	180 days (MPa)
NB1	5.0	5.6	5.7	5.7	5.2
NB2	4.9	5.8	5.0	6.3	5.5
NB1-2	6.0	5.7	5.3	5.8	5.2
NB3	5.1, 4.1	5.4, 5.2, 4.6	X	X	X
NL1	3.7	3.6	4.1	4.3	4.6
NL2	4.3	5.1	5.0	5.2	5.5
MB1	5.9	5.9	6.8	6.2	6.8
MB2	5.6	5.6	6.5	6.5	6.1
ML1	4.3	4.6	5.0	5.5	5.9
ML2	5.0	5.5	5.6	6.0	6.0
HB1	7.2	9.4	9.0	10.1	8.6
HB2	7.3	8.1	9.3	8.9	9.8
HB3	8.9, 8.3	9.6, 9.0, 9.2	X	X	X
HL1	4.6	5.3	5.5	5.5	5.5
HL2	4.7	5.5	6.2	6.1	5.9
	(psi)	(psi)	(psi)	(psi)	(psi)
NB1	720	810	830	830	750
NB2	710	840	730	920	800
NB1-2	880	830	770	850	760
NB3	740, 600	790, 760, 660	X	X	X
NL1	530	530	590	630	670
NL2	620	740	730	760	800
MB1	860	850	980	900	990
MB2	820	810	940	950	880
ML1	620	670	730	800	850
ML2	720	790	820	860	860
HB1	1040	1370	1310	1470	1250
HB2	1060	1180	1350	1230	1420
HB3	1290, 1200	1390, 1300, 1330	X	X	X
HL1	670	770	800	780	790
HL2	690	810	890	890	850

*H = high-strength concrete N = normal-strength concrete L = limestone
M = medium-strength concrete B = basalt # = batch number

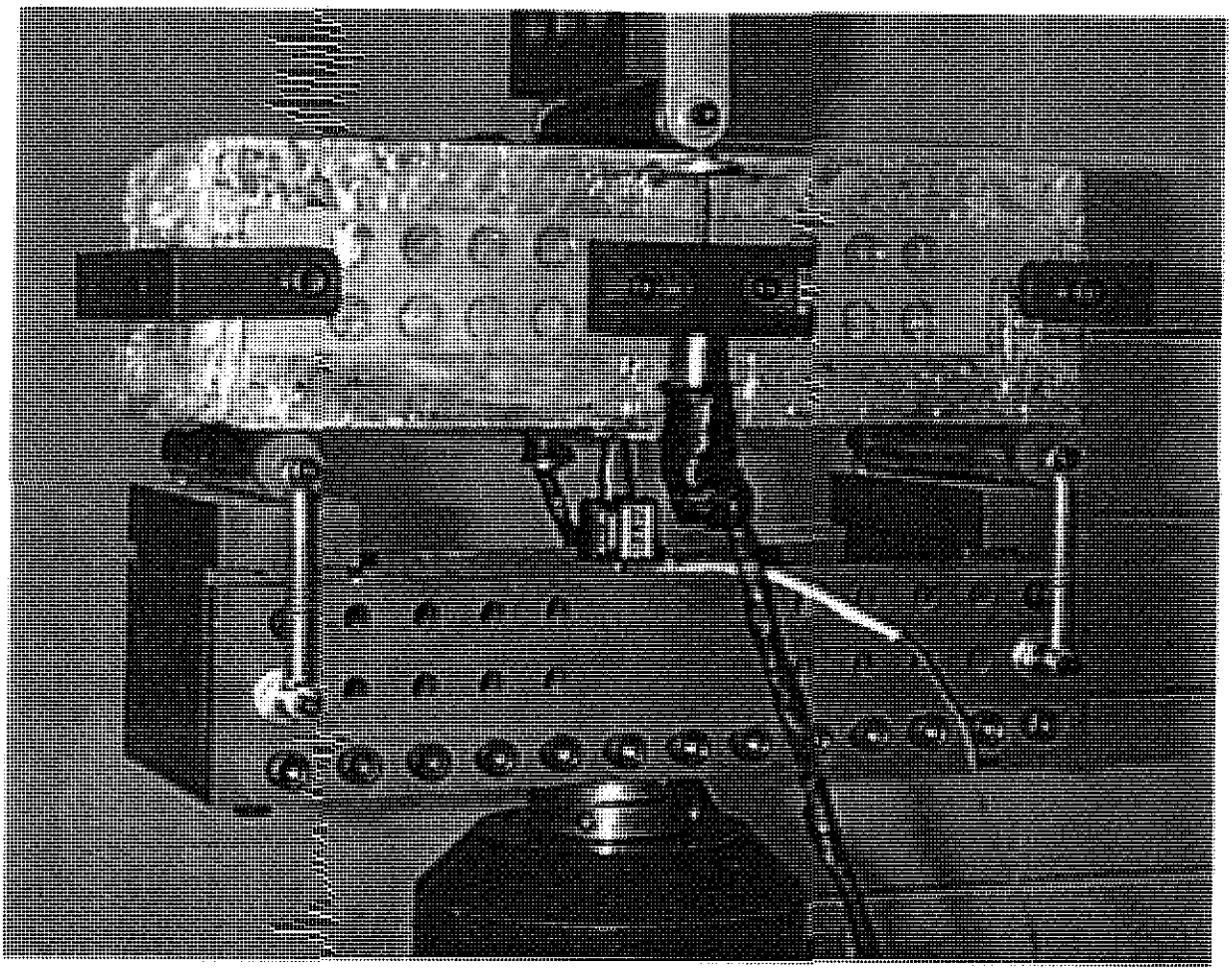

Figure 2.1 Fracture energy test setup using a MTS closed-loop electro-hydraulic testing system.

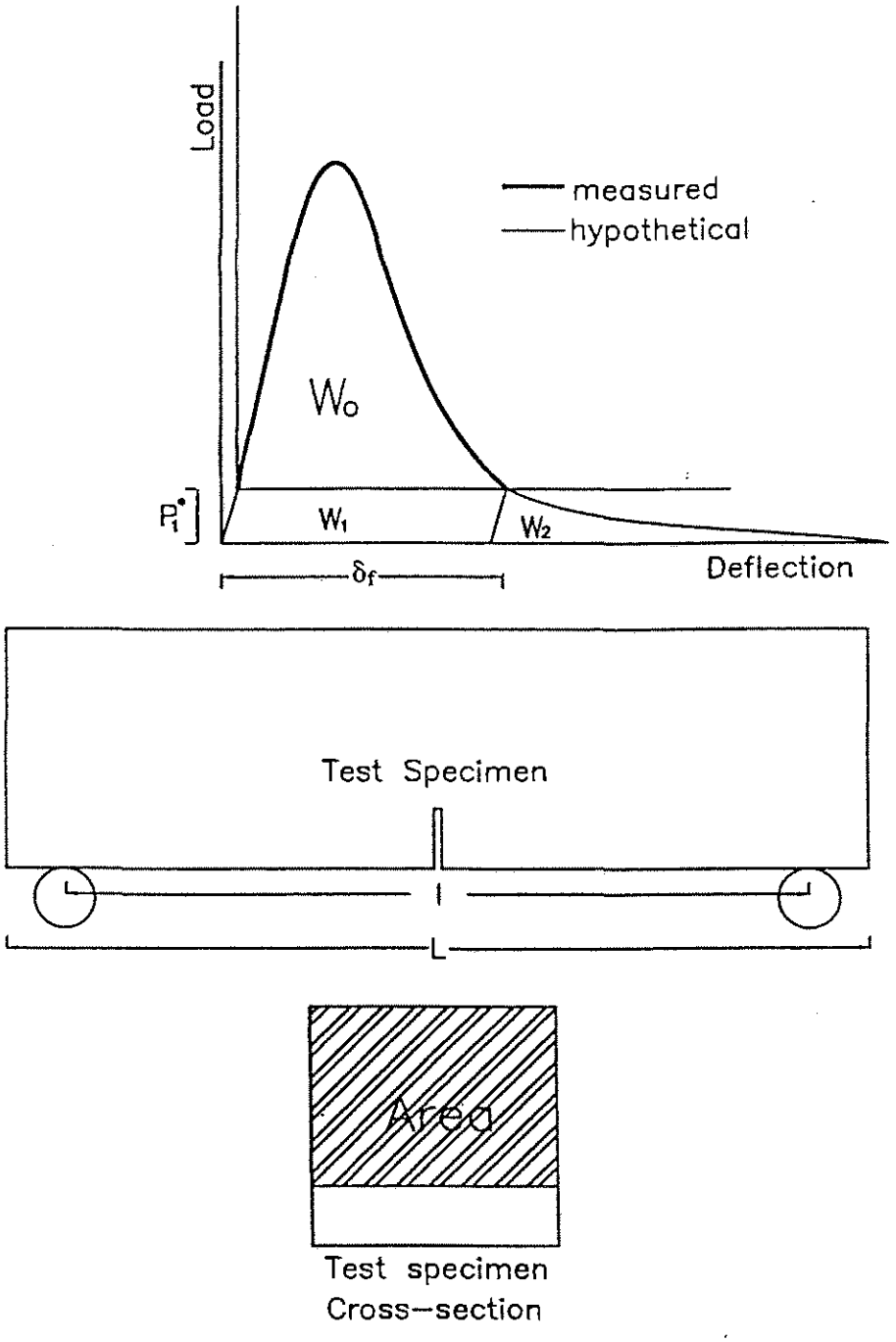

Figure 3.1 Schematic of fracture energy test specimen and load-deflection curve. (Kozul and Darwin 1997)

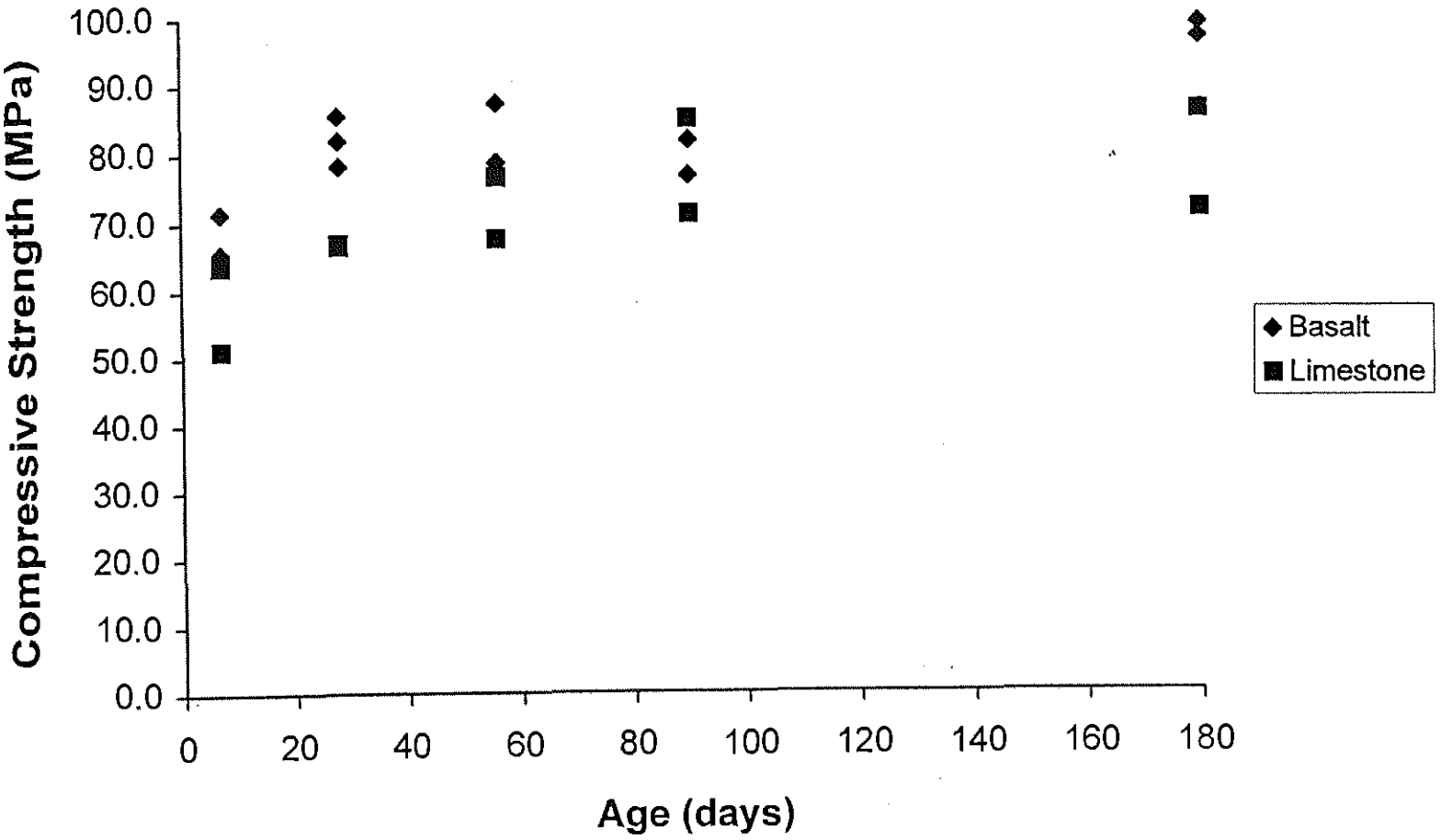

Figure 3.2 Compressive strength versus age for high-strength concrete.

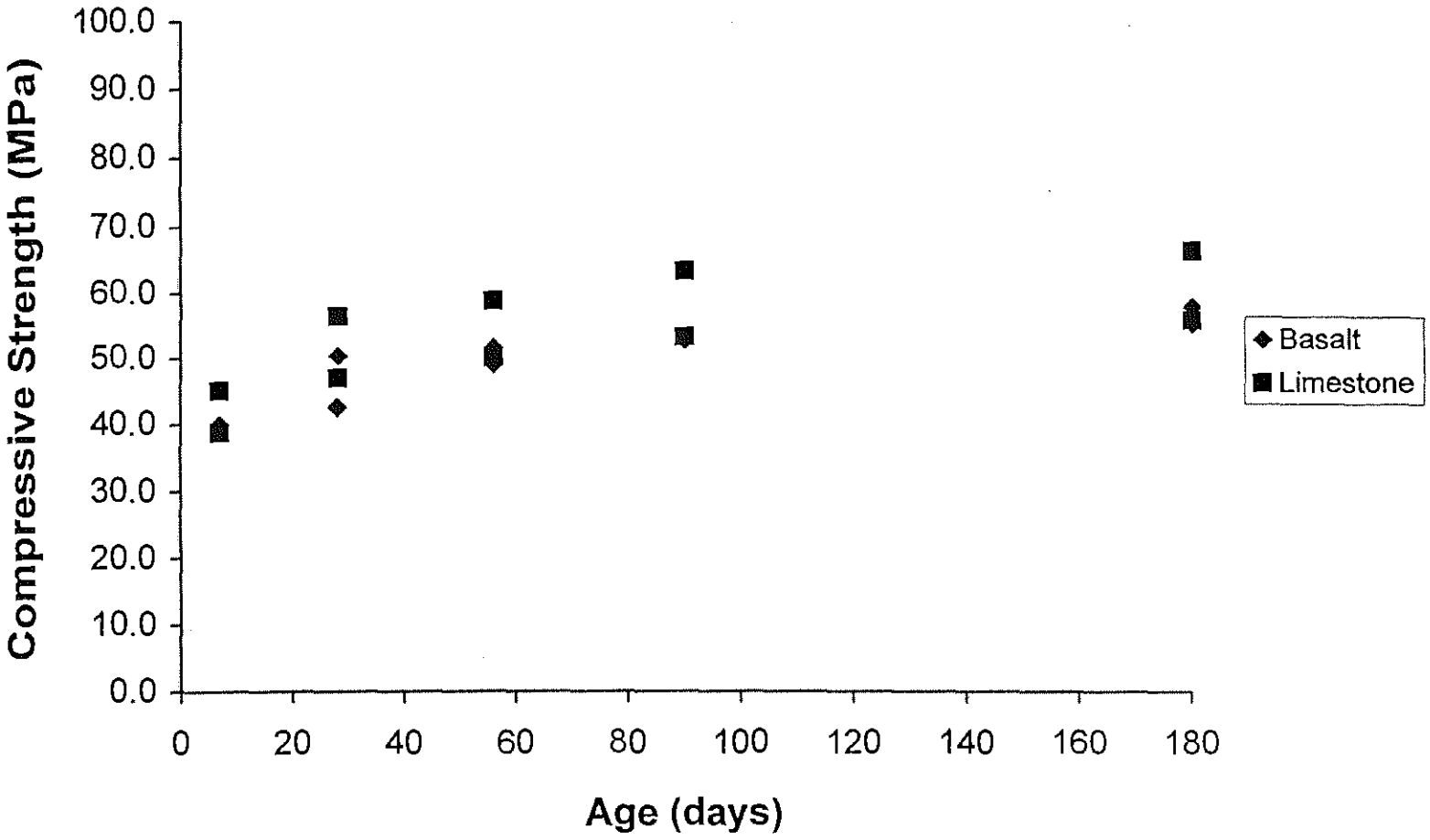

Figure 3.3 Compressive strength versus age for medium-strength concrete.

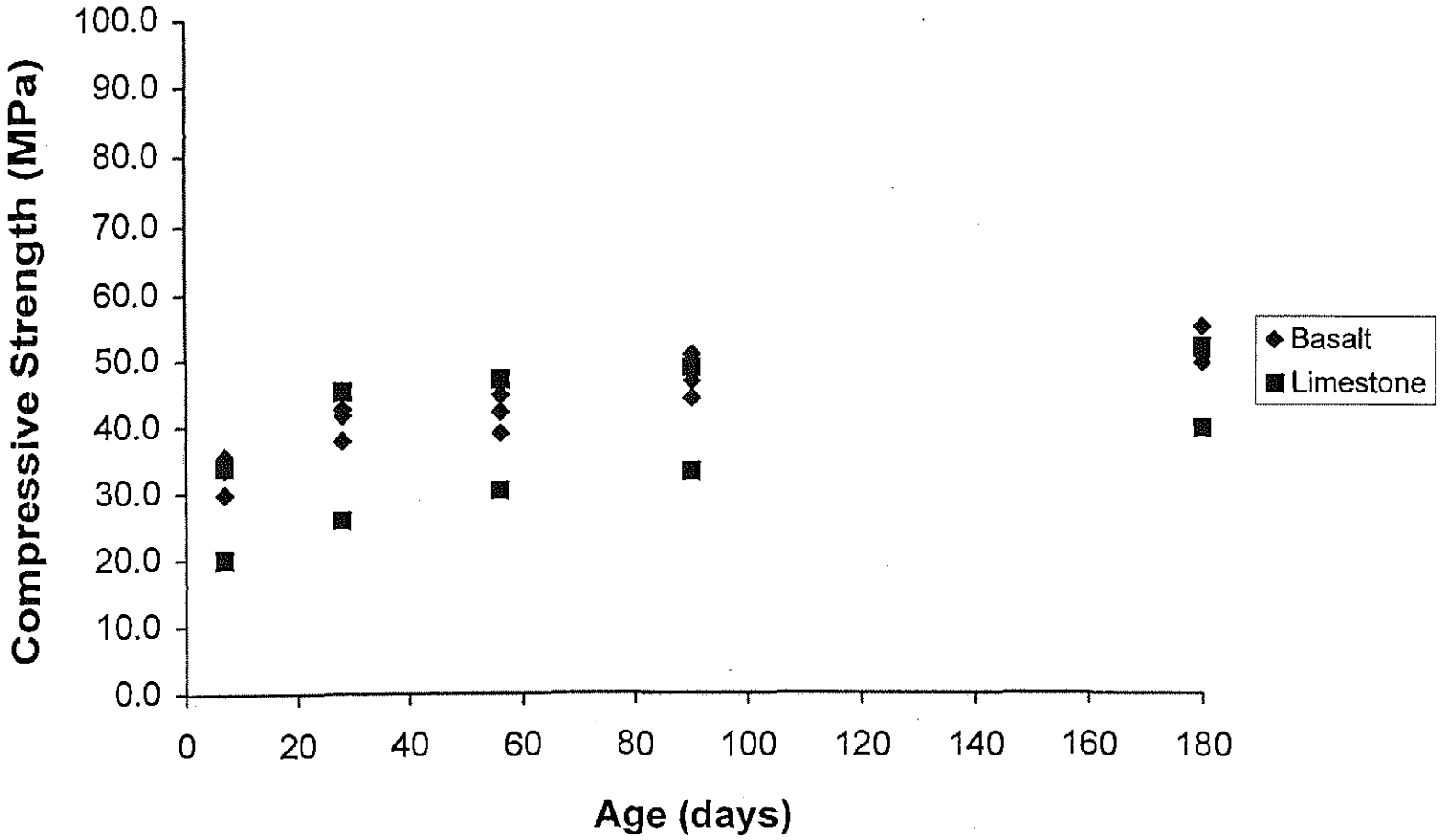

Figure 3.4 Compressive strength versus age for normal-strength concrete.

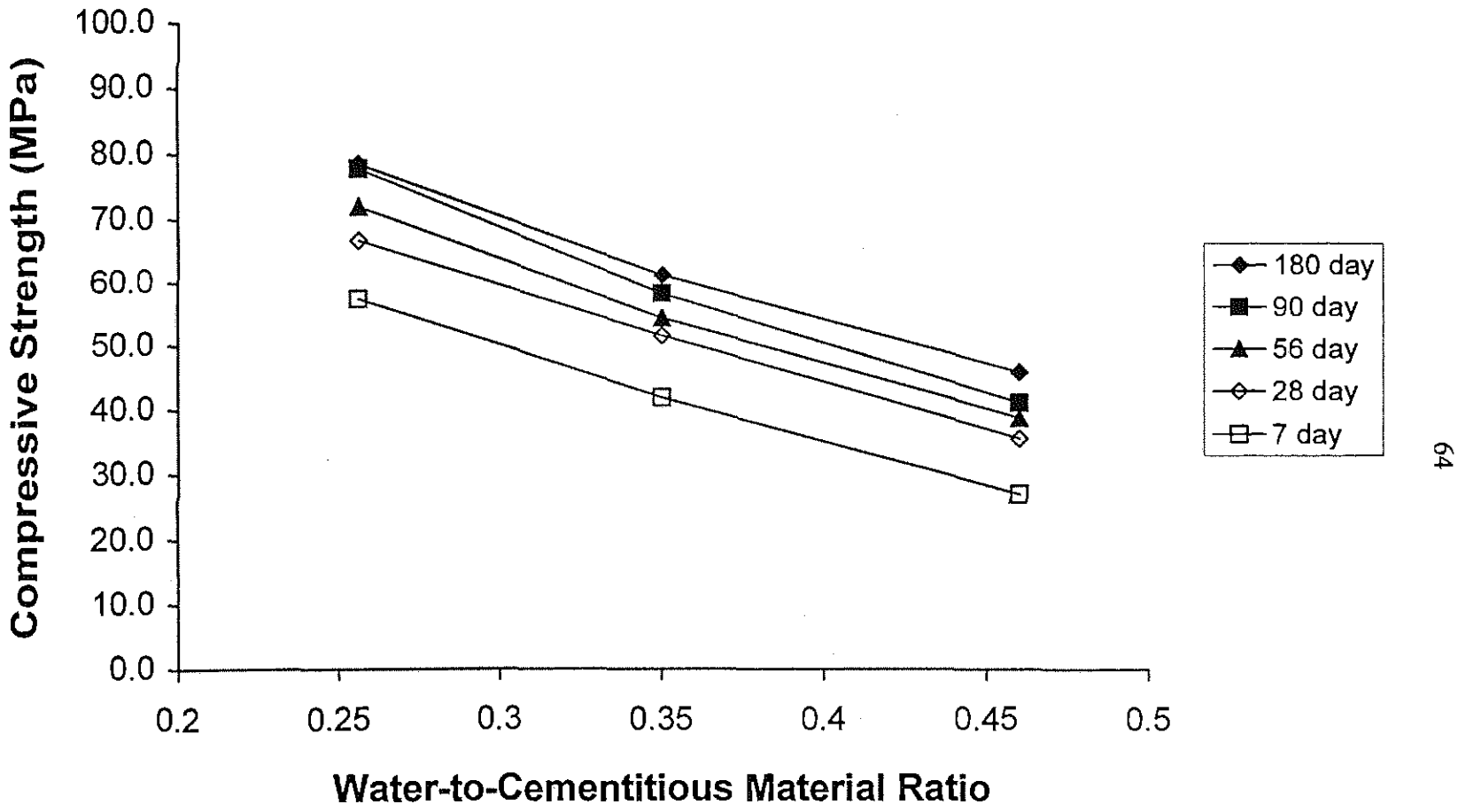

Figure 3.5 Average compressive strength versus average water-to-cementitious material ratio for limestone concretes.

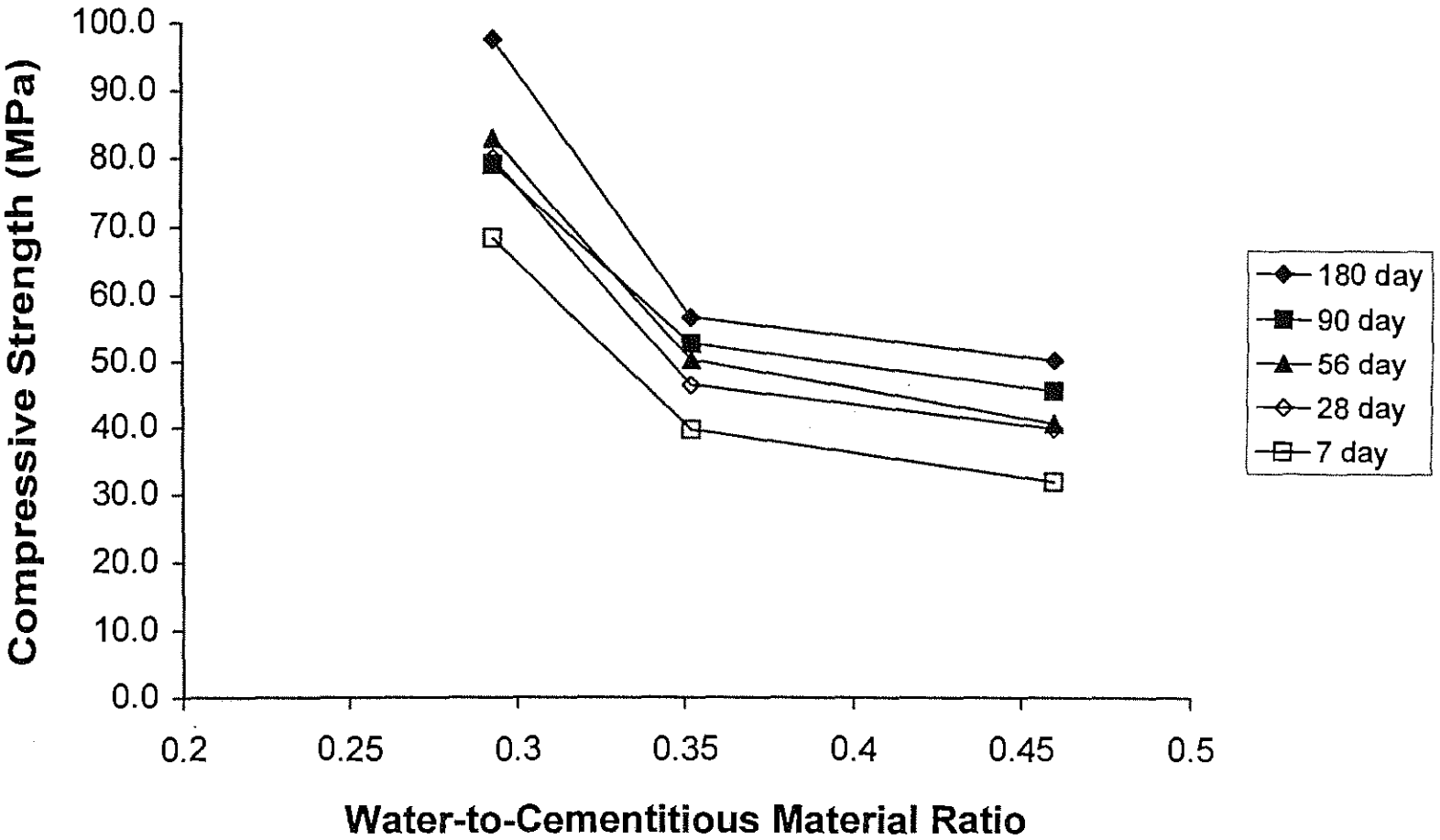

Figure 3.6 Average compressive strength versus average water-to-cementitious material ratio for basalt concretes.

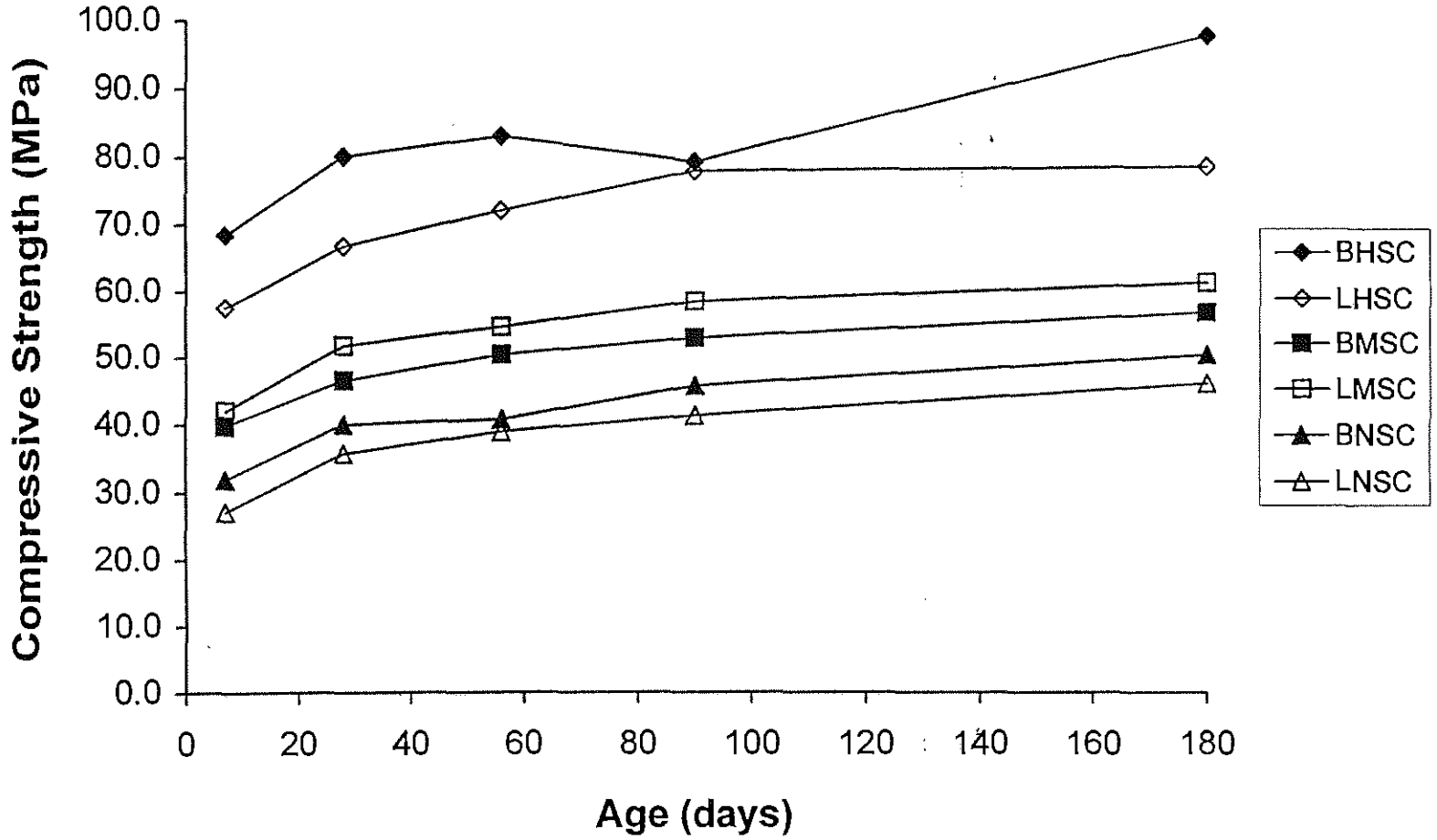

Figure 3.7 Average compressive strength versus age.

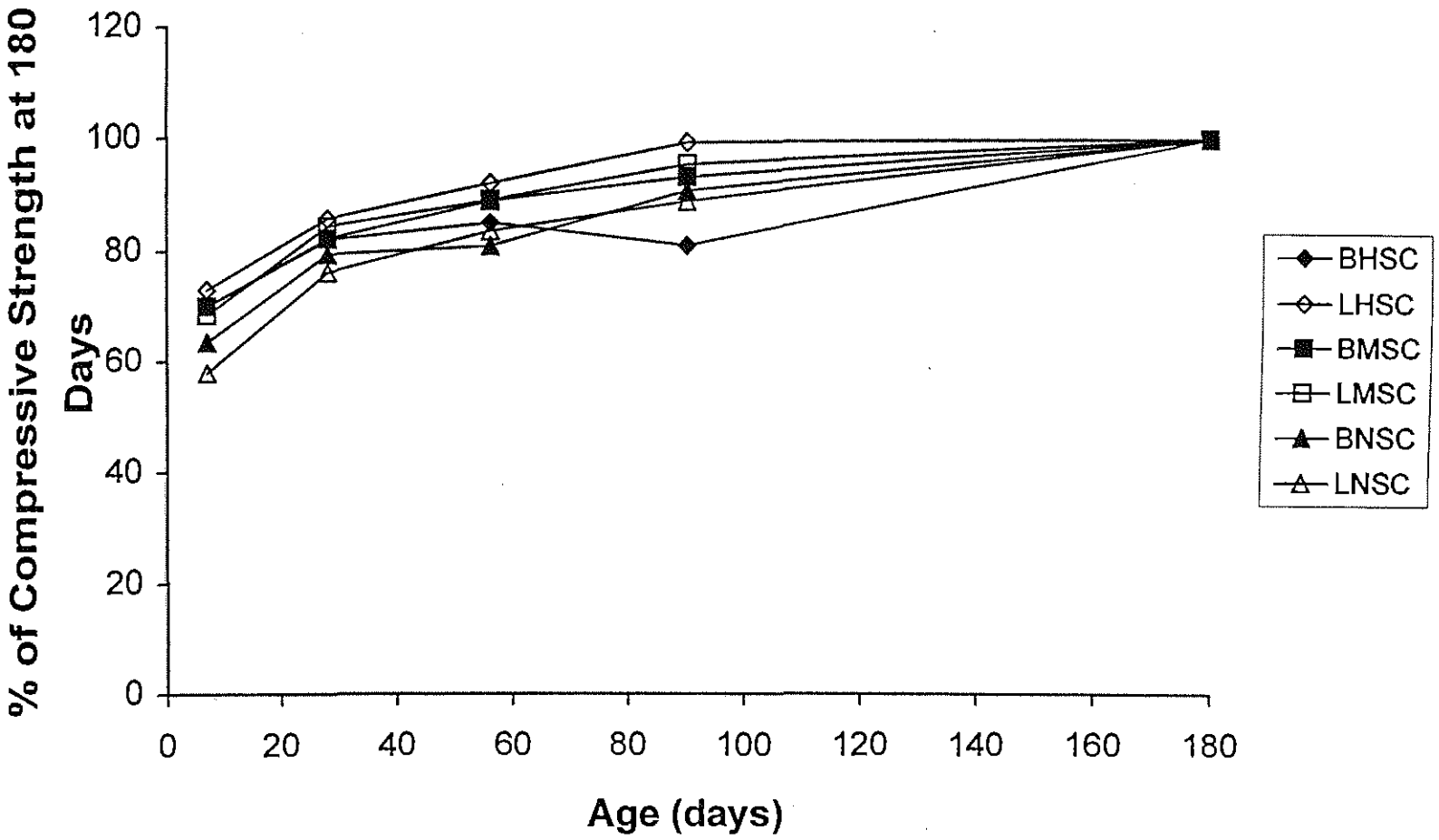

Figure 3.8 Average percentage of compressive strength at 180 days versus age.

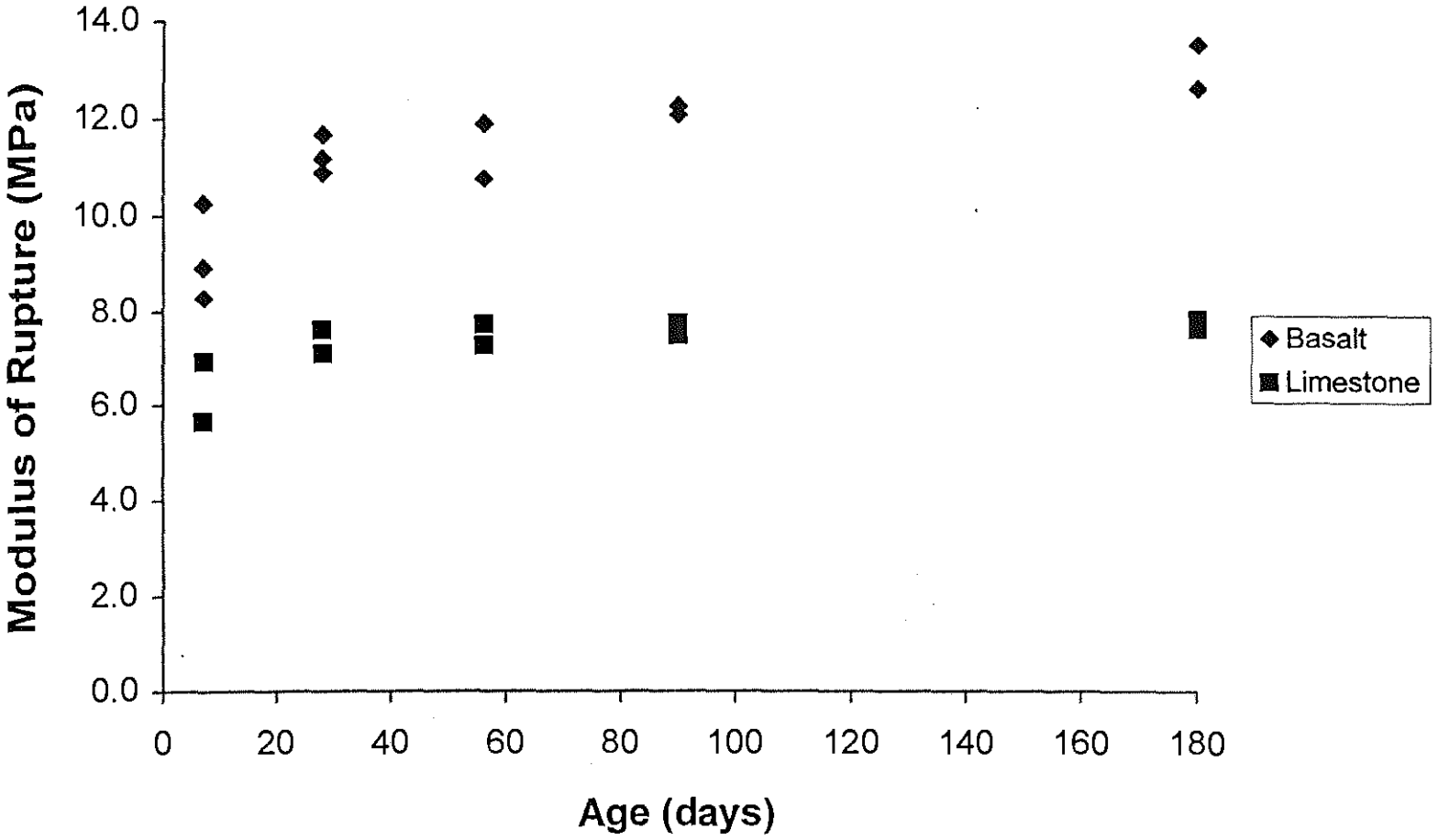

Figure 3.9 Modulus of rupture versus age for high-strength concrete.

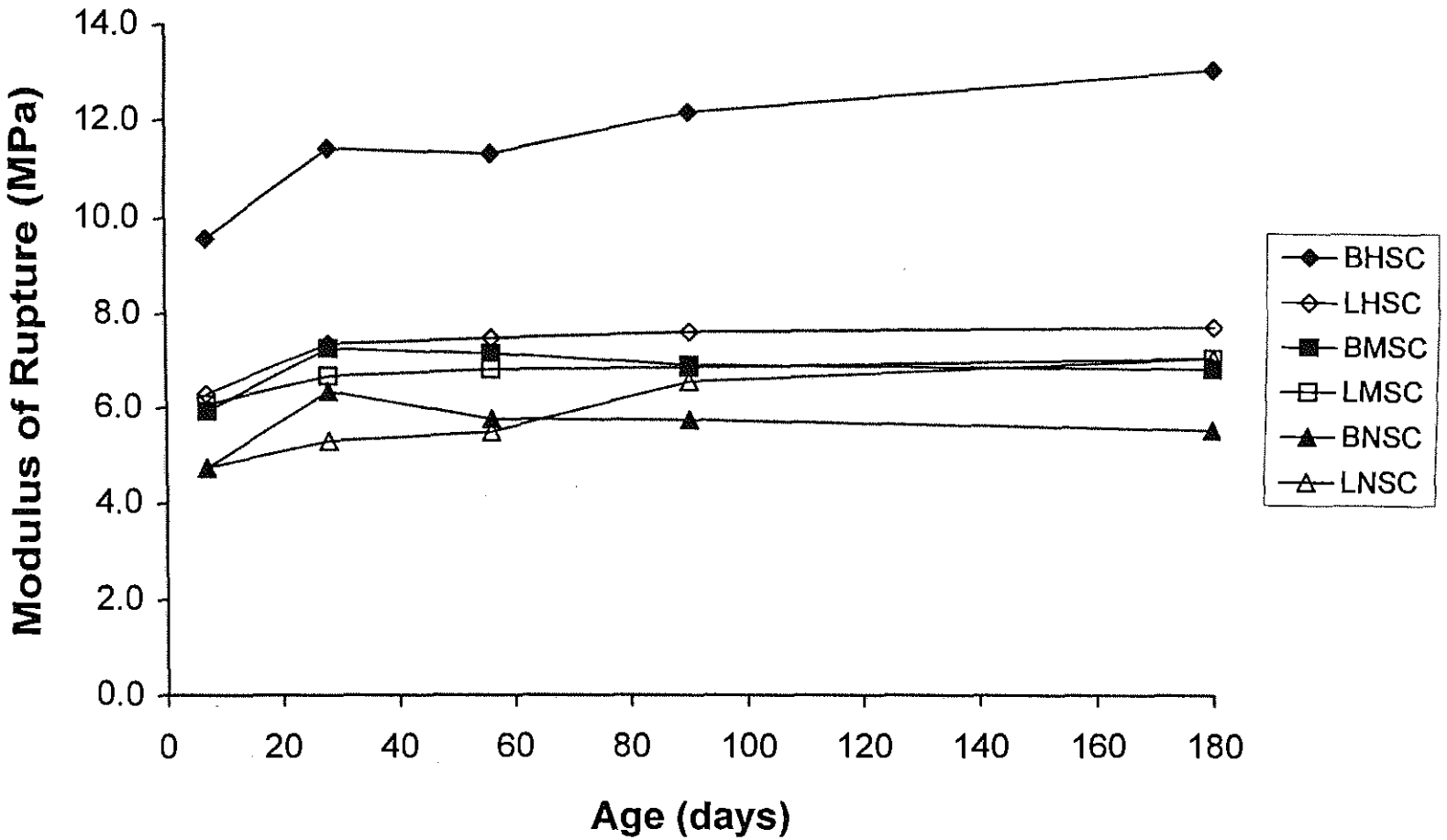

Figure 3.14 Average modulus of rupture versus age.

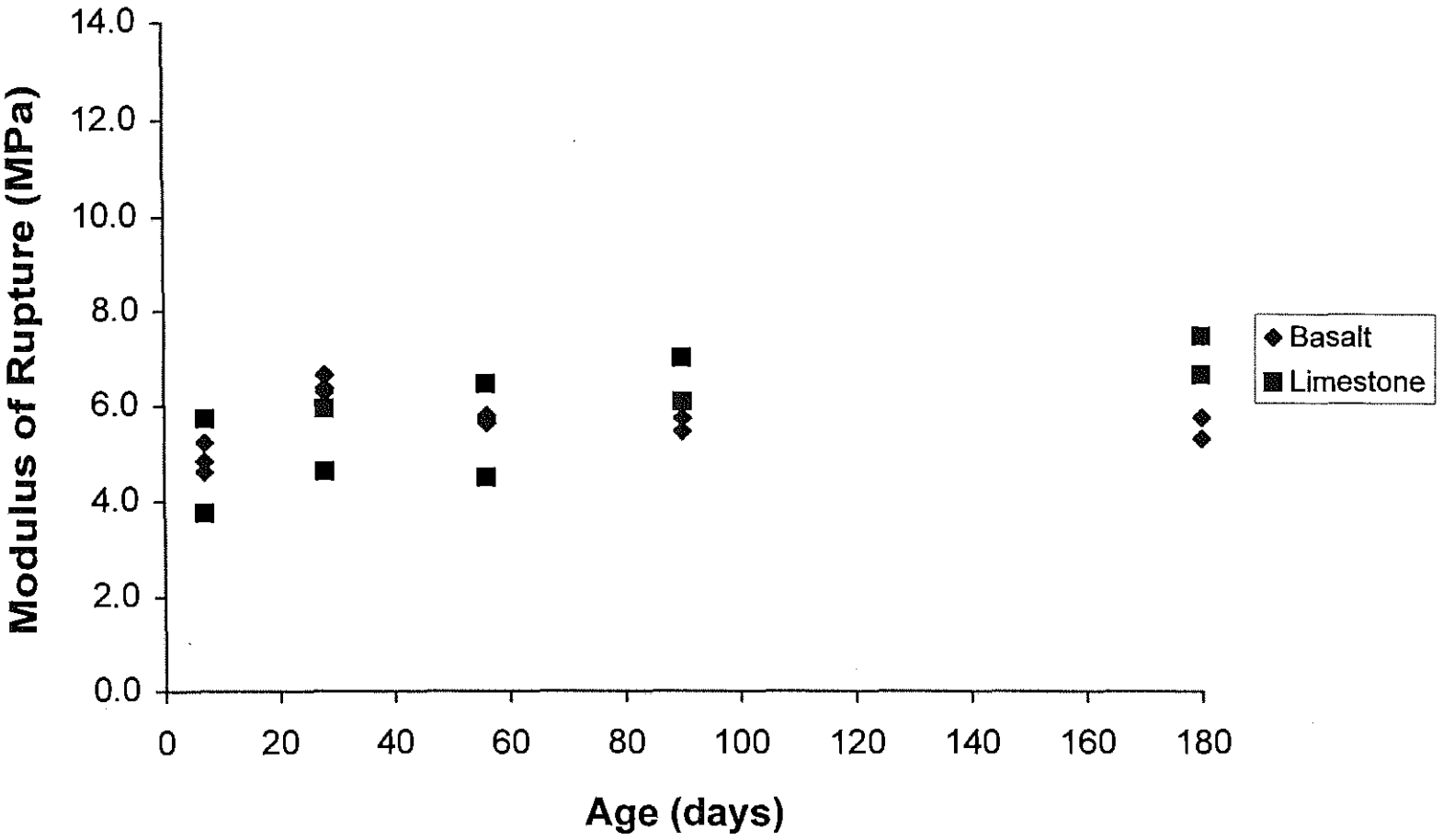

Figure 3.11 Modulus of rupture versus age for normal-strength concrete.

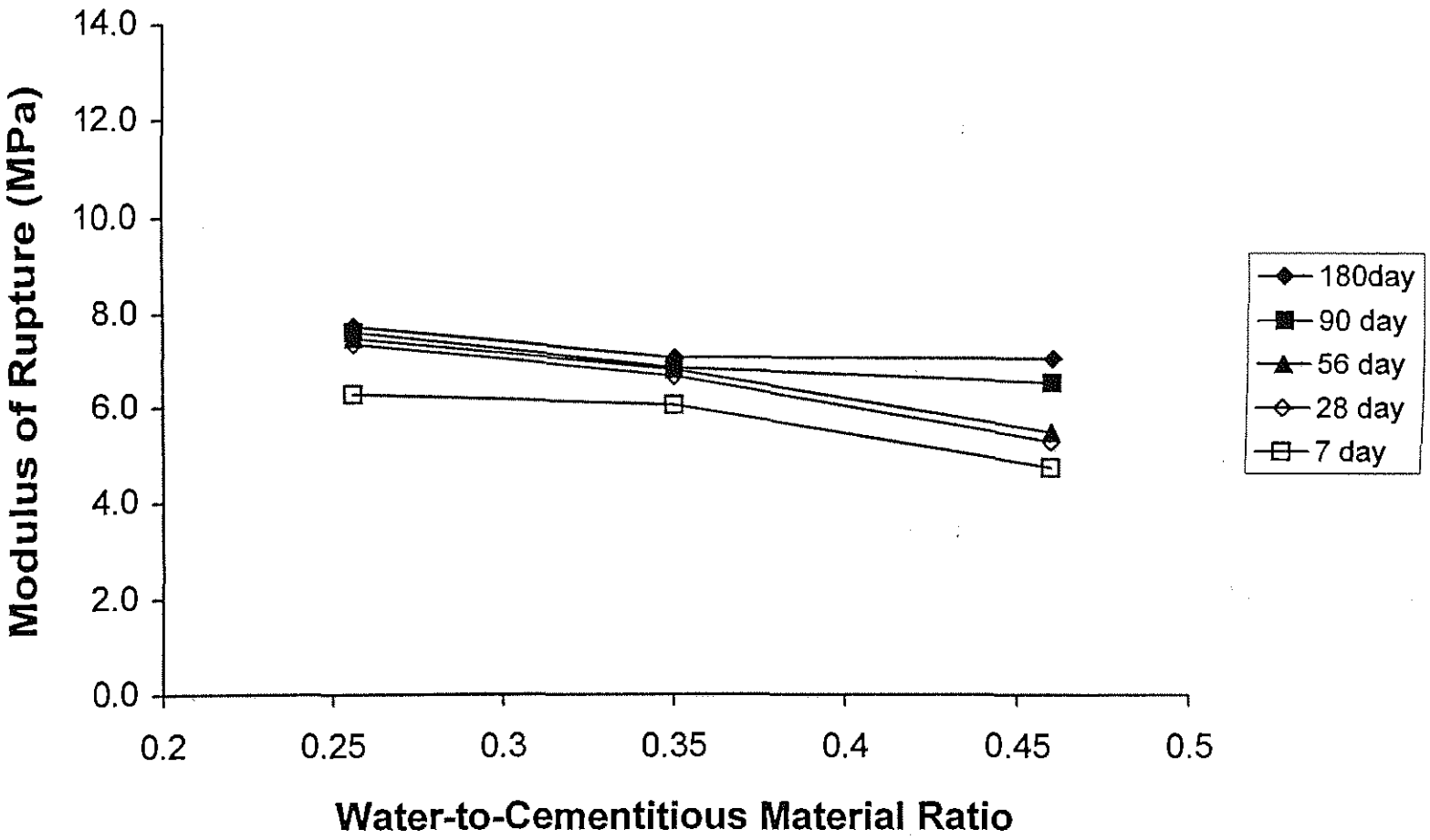

Figure 3.12 Average modulus of rupture versus average water-to-cementitious material ratio for limestone concretes.

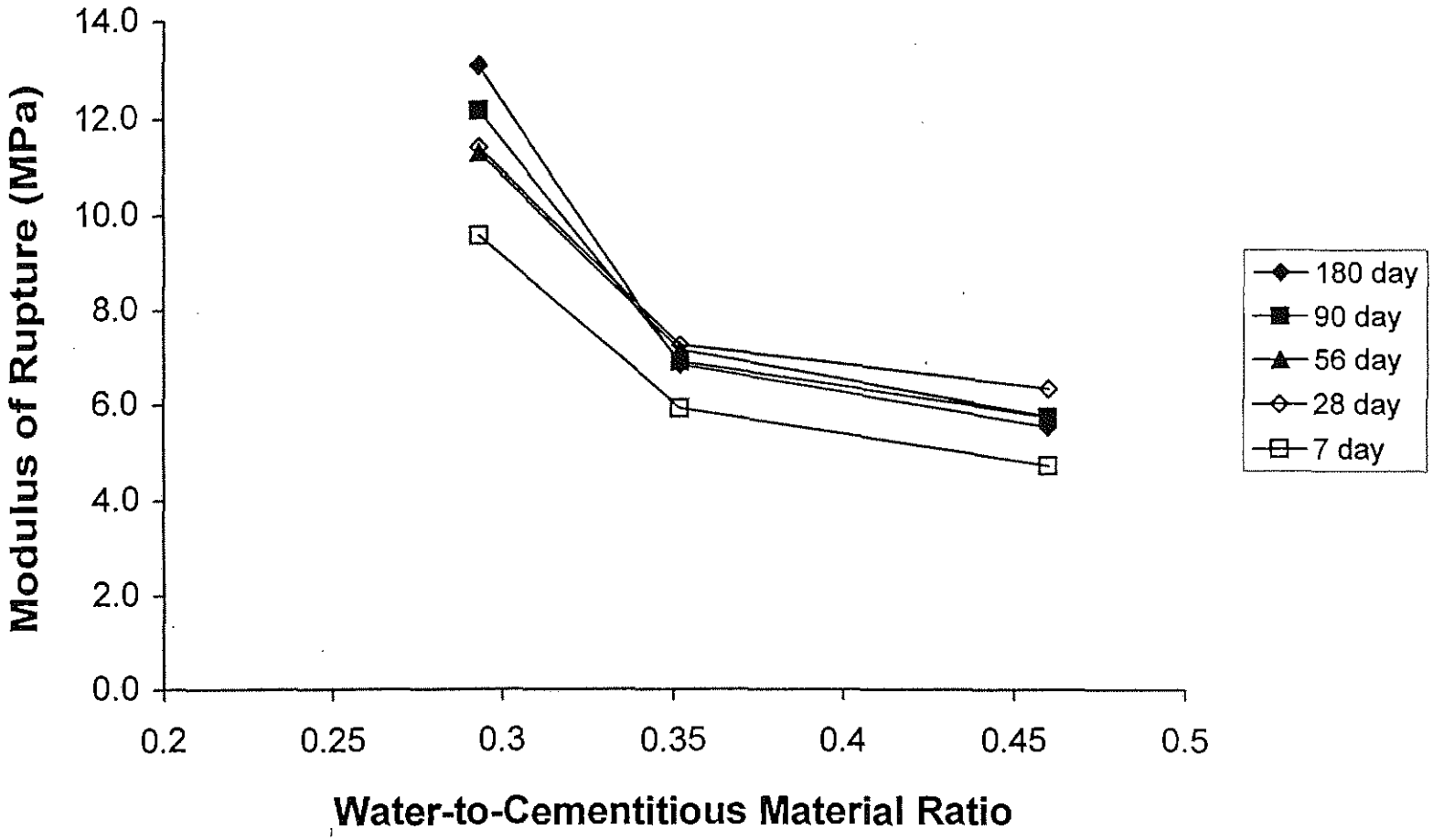

Figure 3.13 Average modulus of rupture versus average water-to-cementitious material ratio for basalt concretes.

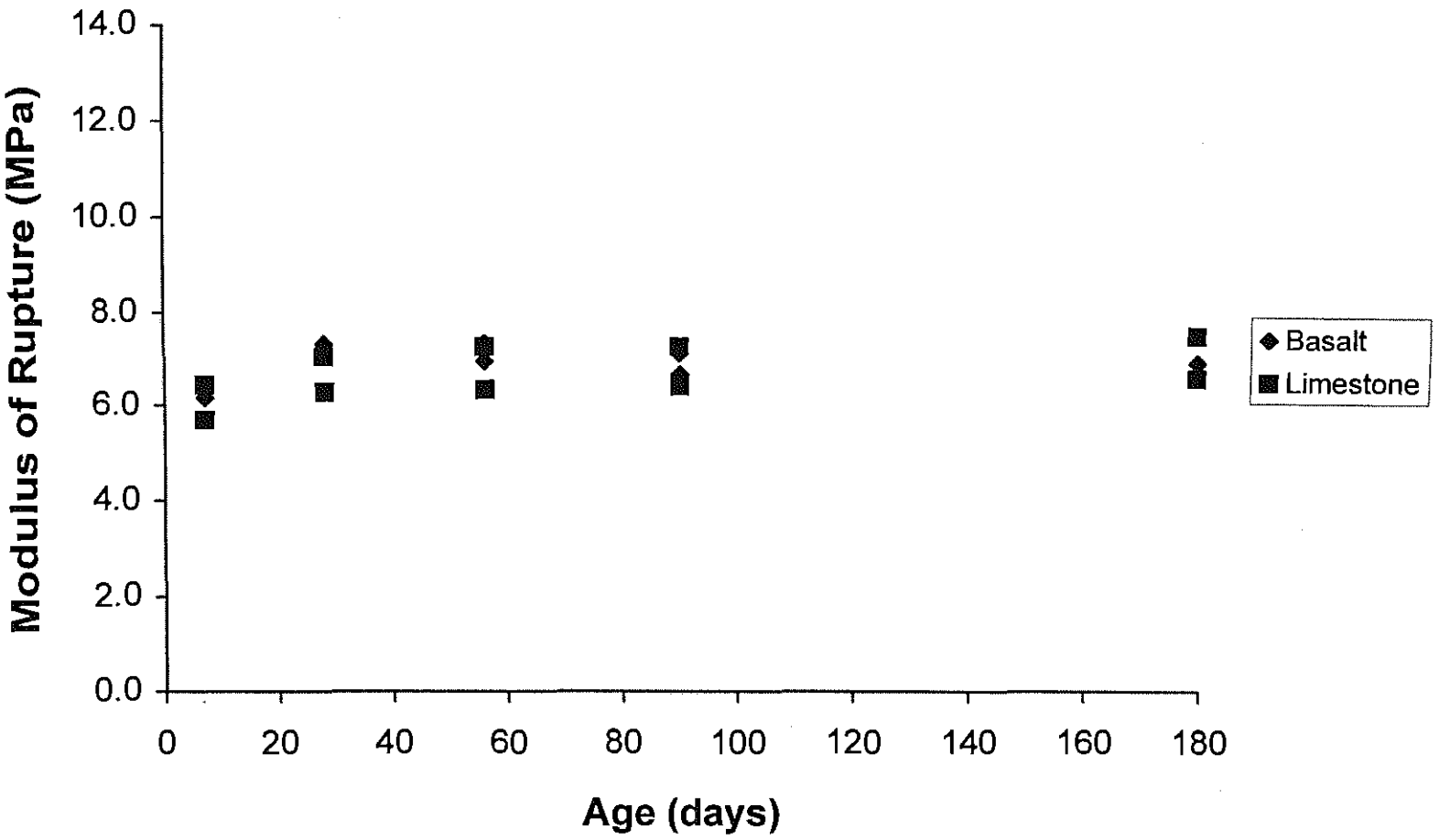

Figure 3.10 Modulus of rupture versus age for medium-strength concrete.

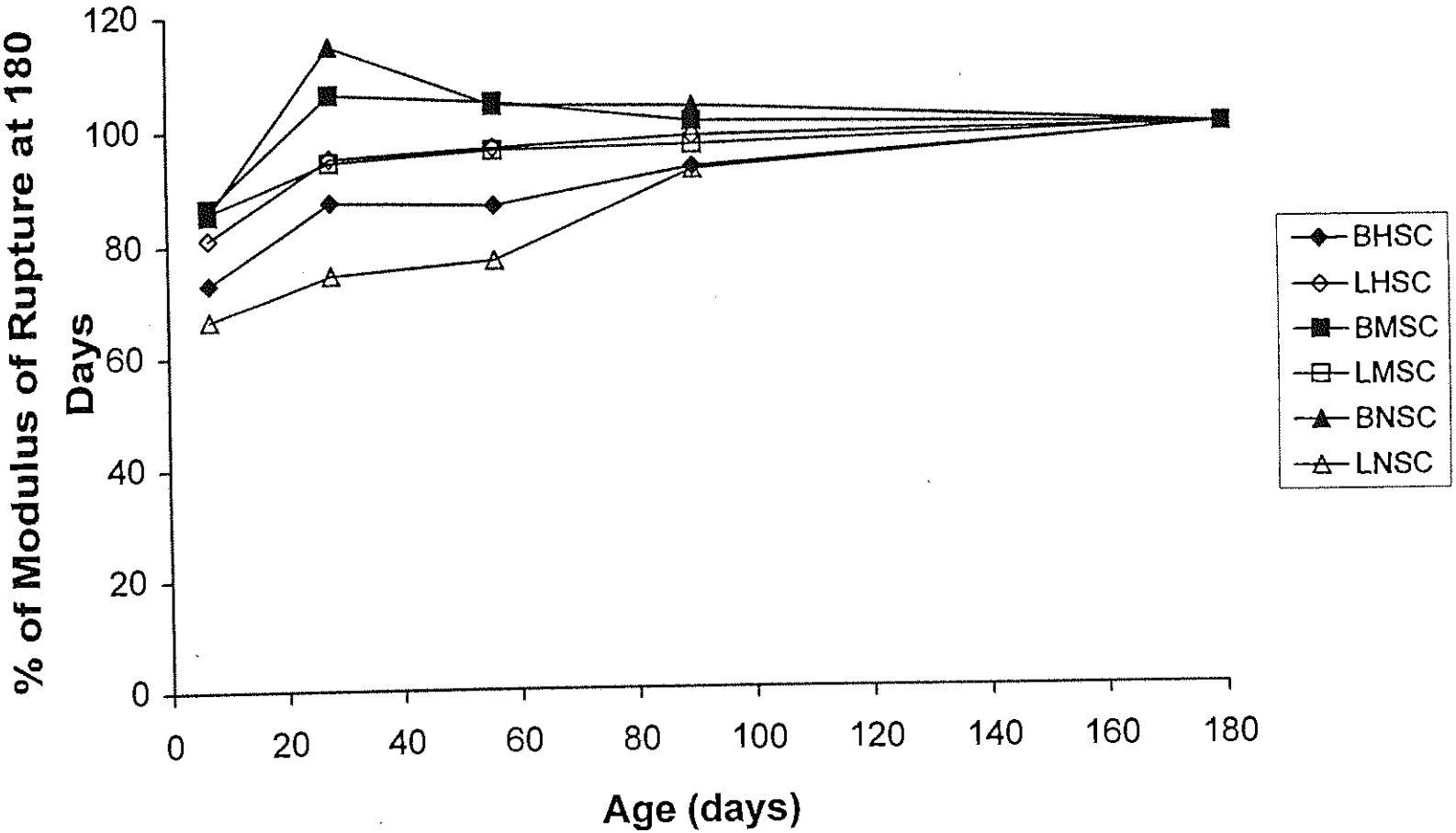

Figure 3.15 Average percentage of modulus of rupture at 180 days versus age.

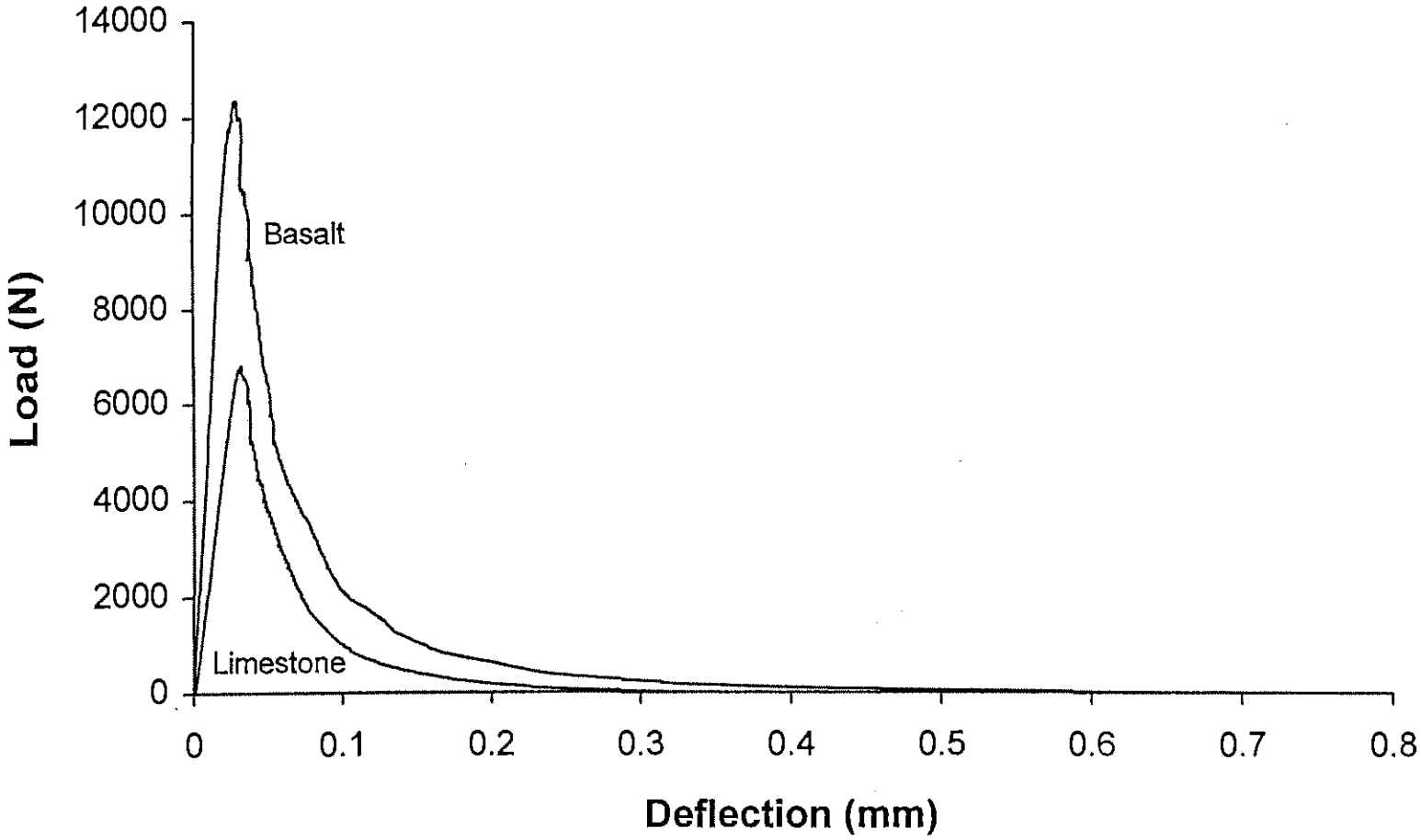

Figure 3.16 Fracture specimen load-deflection curves for 28-day basalt and limestone high-strength concretes. (HB1-28E and HL1-28E)

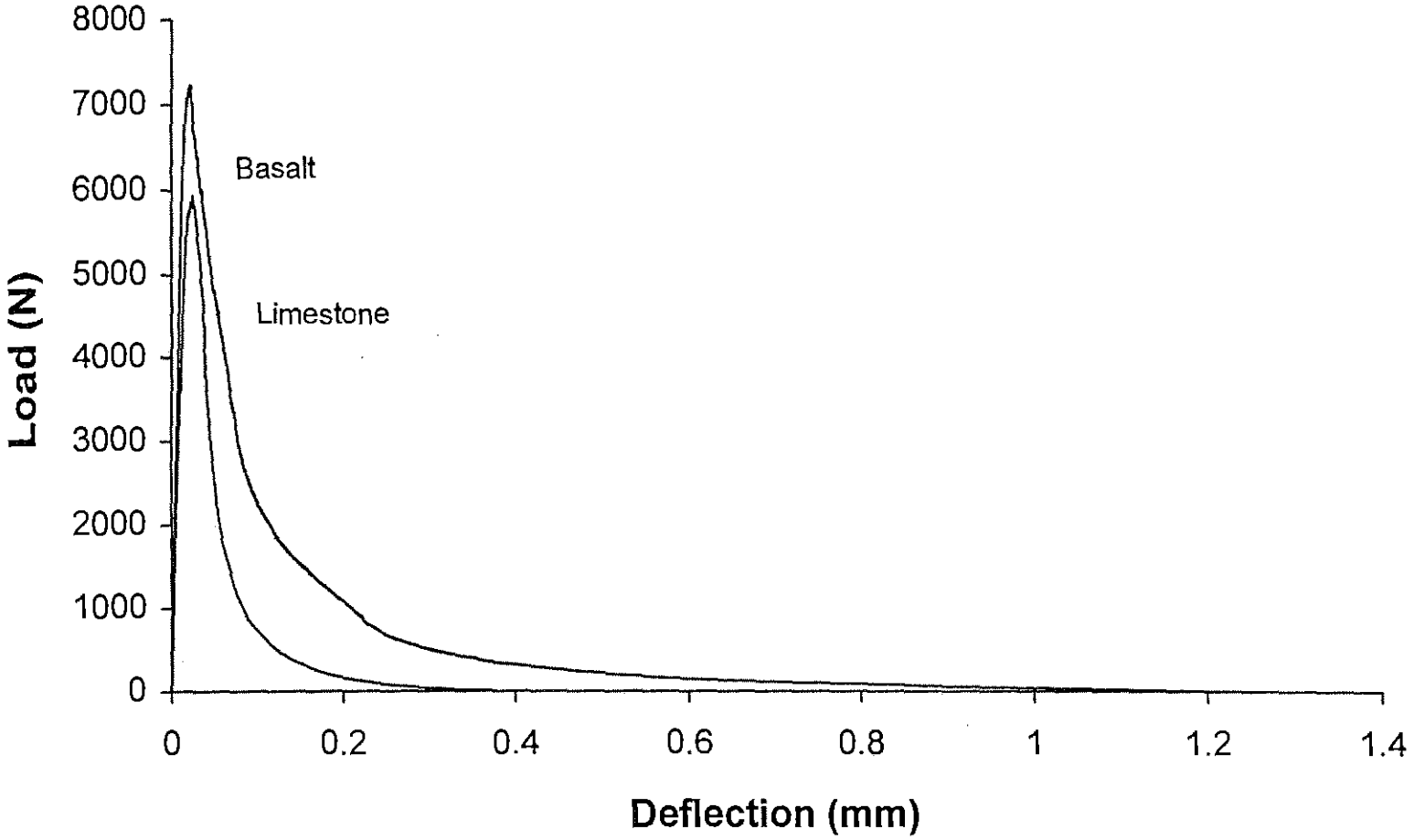

Figure 3.17 Fracture specimen load-deflection curves for 28-day basalt and limestone medium-strength concrete. (MB2-28E and ML1-28E)

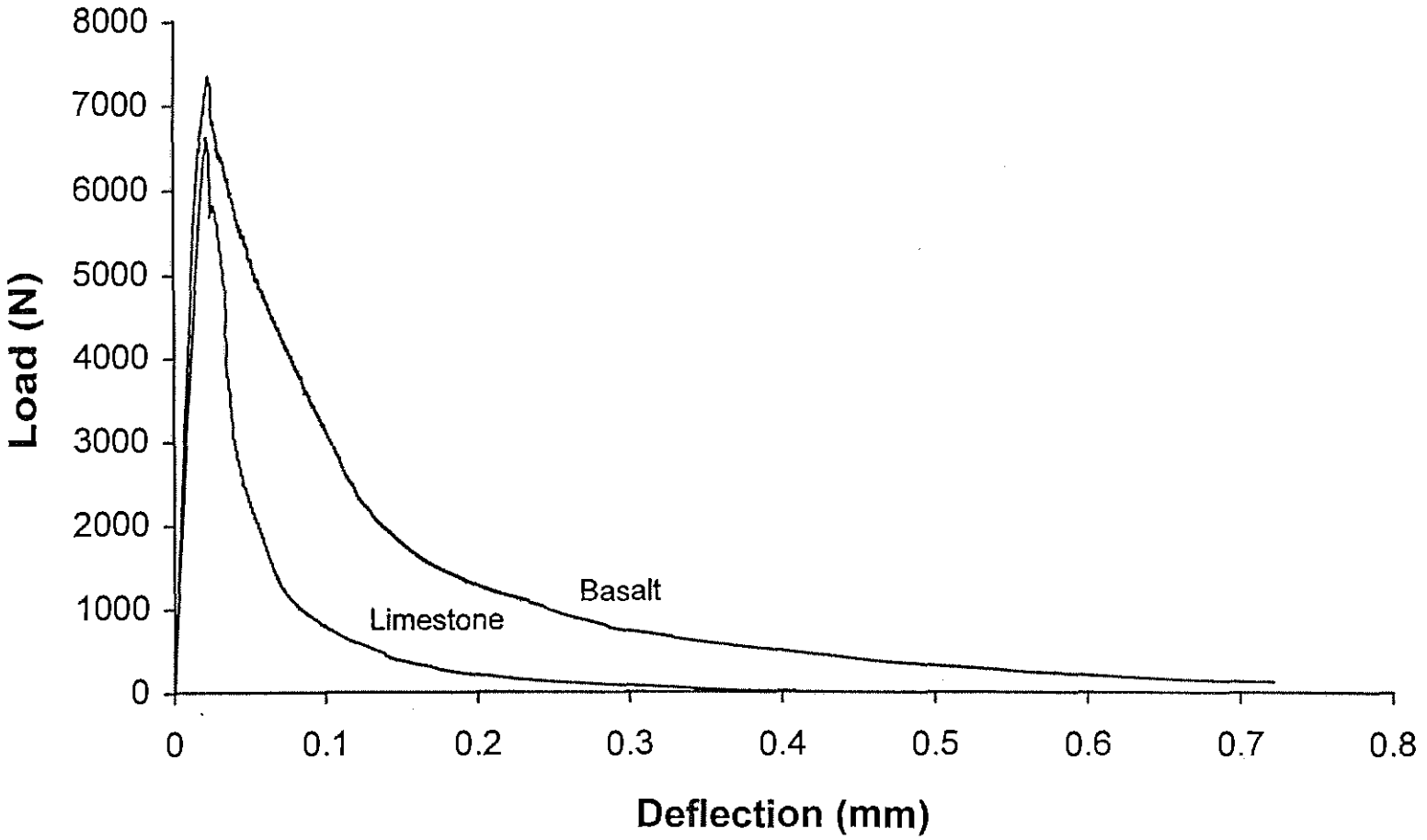

Figure 3.18 Fracture specimen load-deflection curves for 28-day basalt and limestone normal-strength concrete. (NB2-28E and NL1-28E)

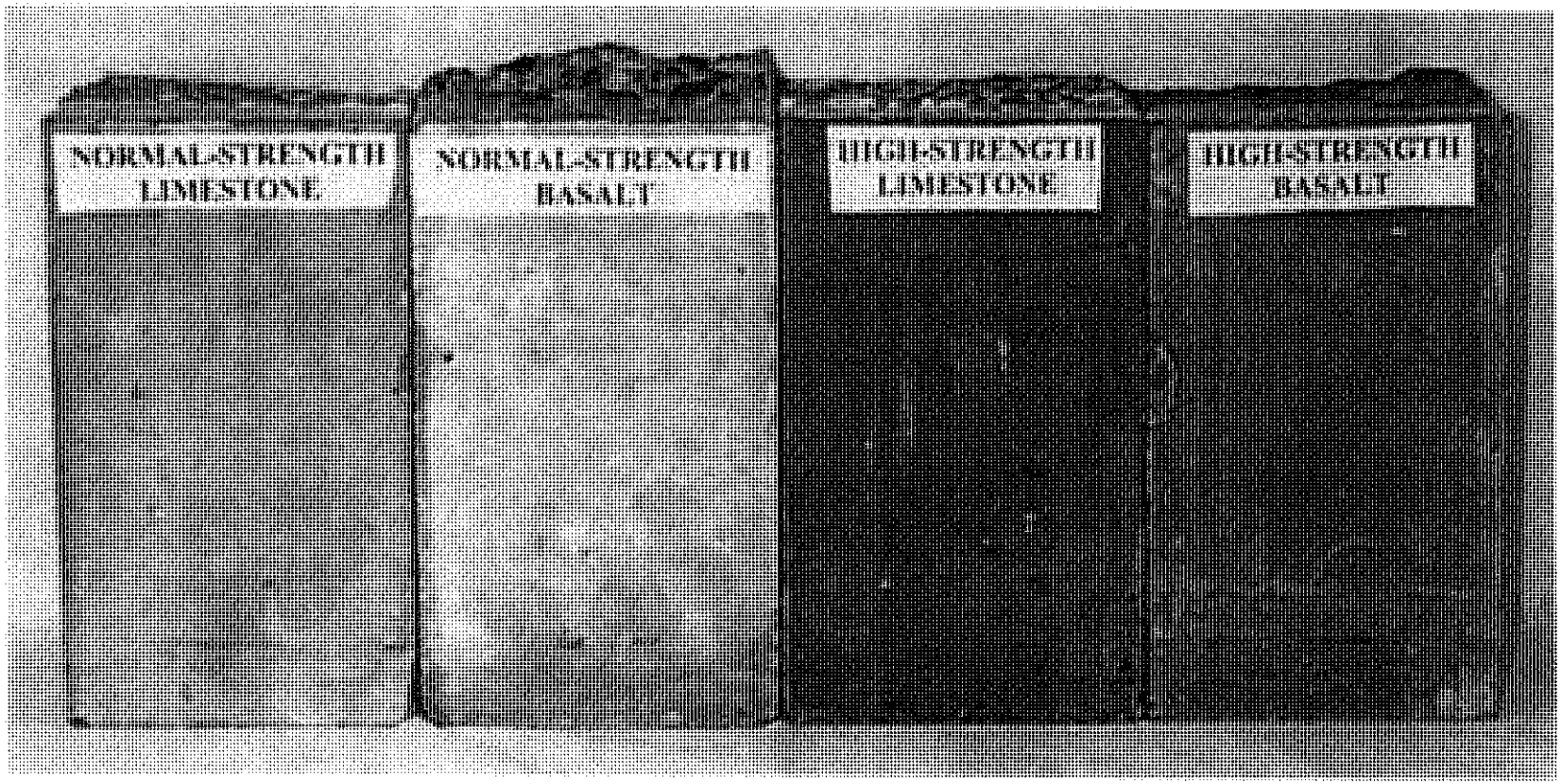

Figure 3.19 Profile surfaces of normal and high-strength concrete fracture specimens.

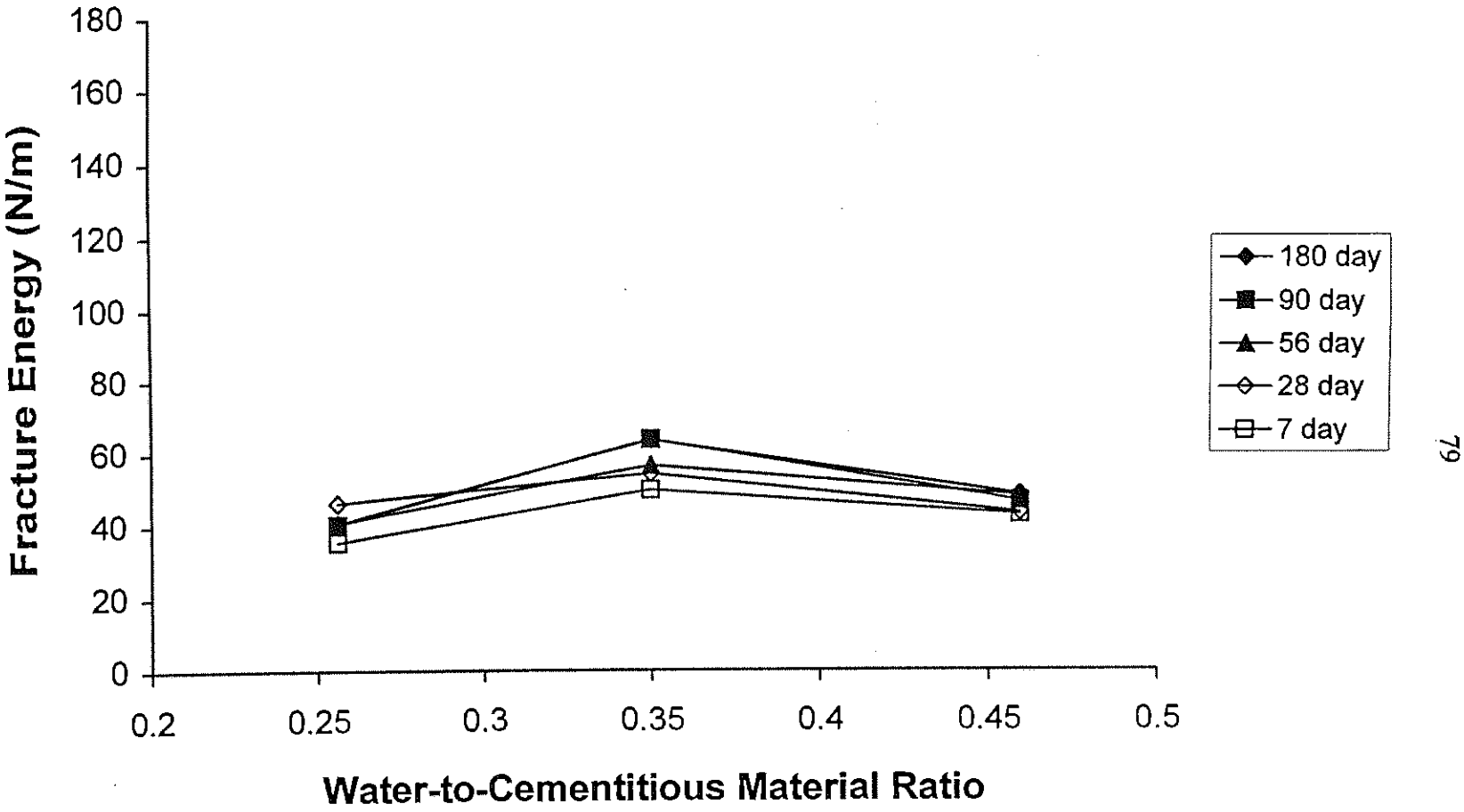

Figure 3.20 Average fracture energy versus average water-to-cementitious material ratio for limestone concretes.

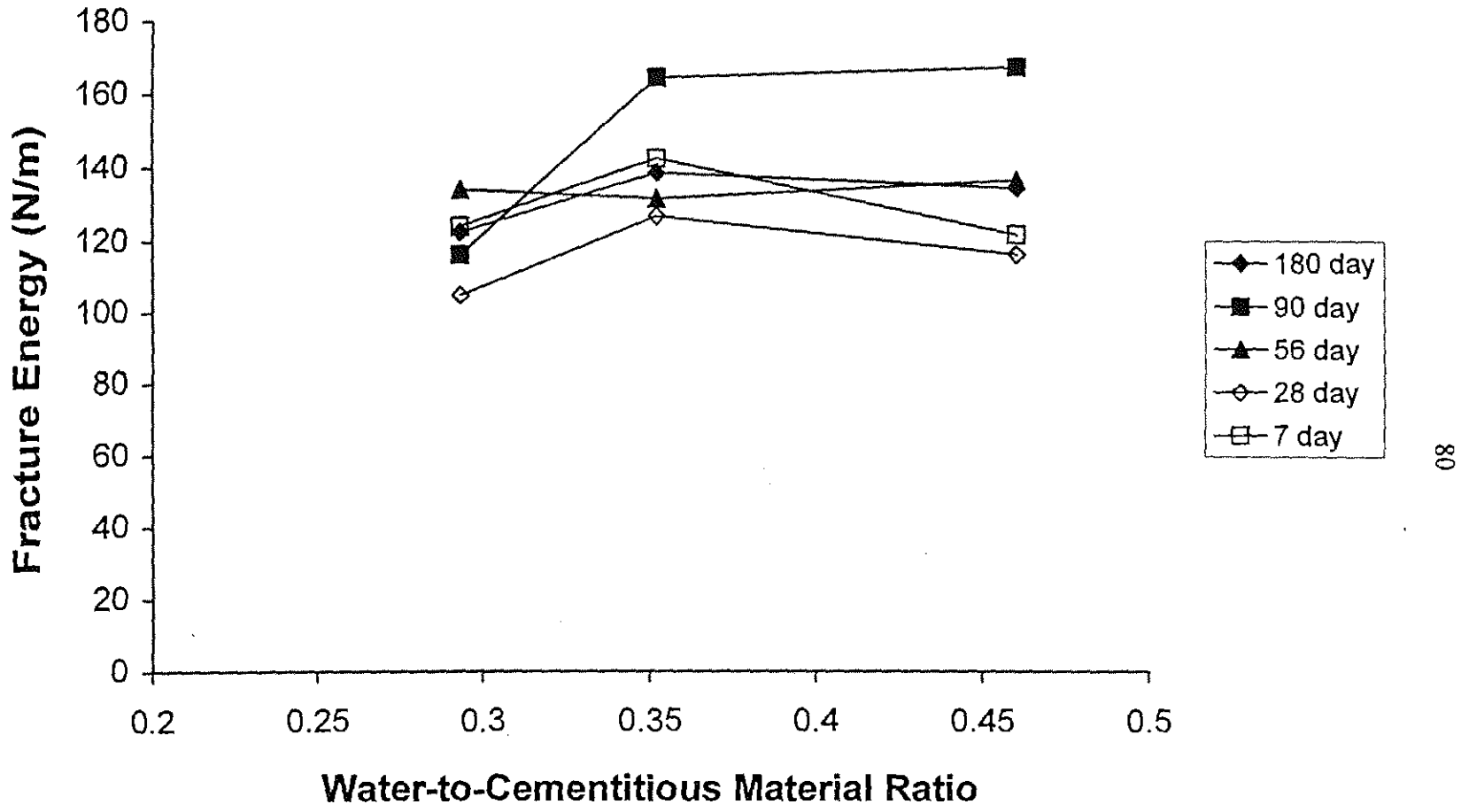

Figure 3.21 Average fracture energy versus average water-to-cementititous material ratio for basalt concretes.

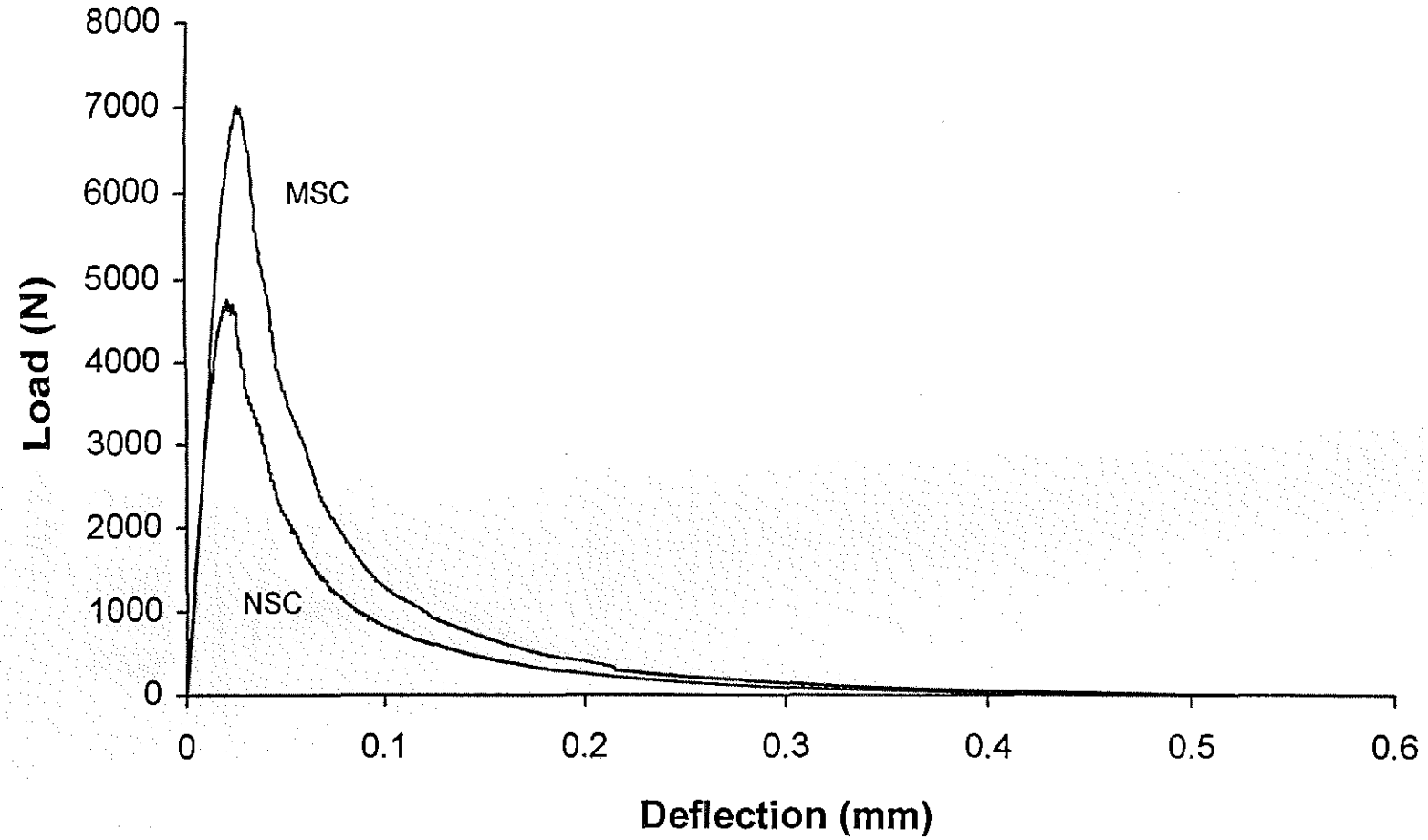

Figure 3.22 Fracture specimen load-deflection curves for 28-day limestone normal and medium-strength concrete. (NL1-28E and ML2-28E)

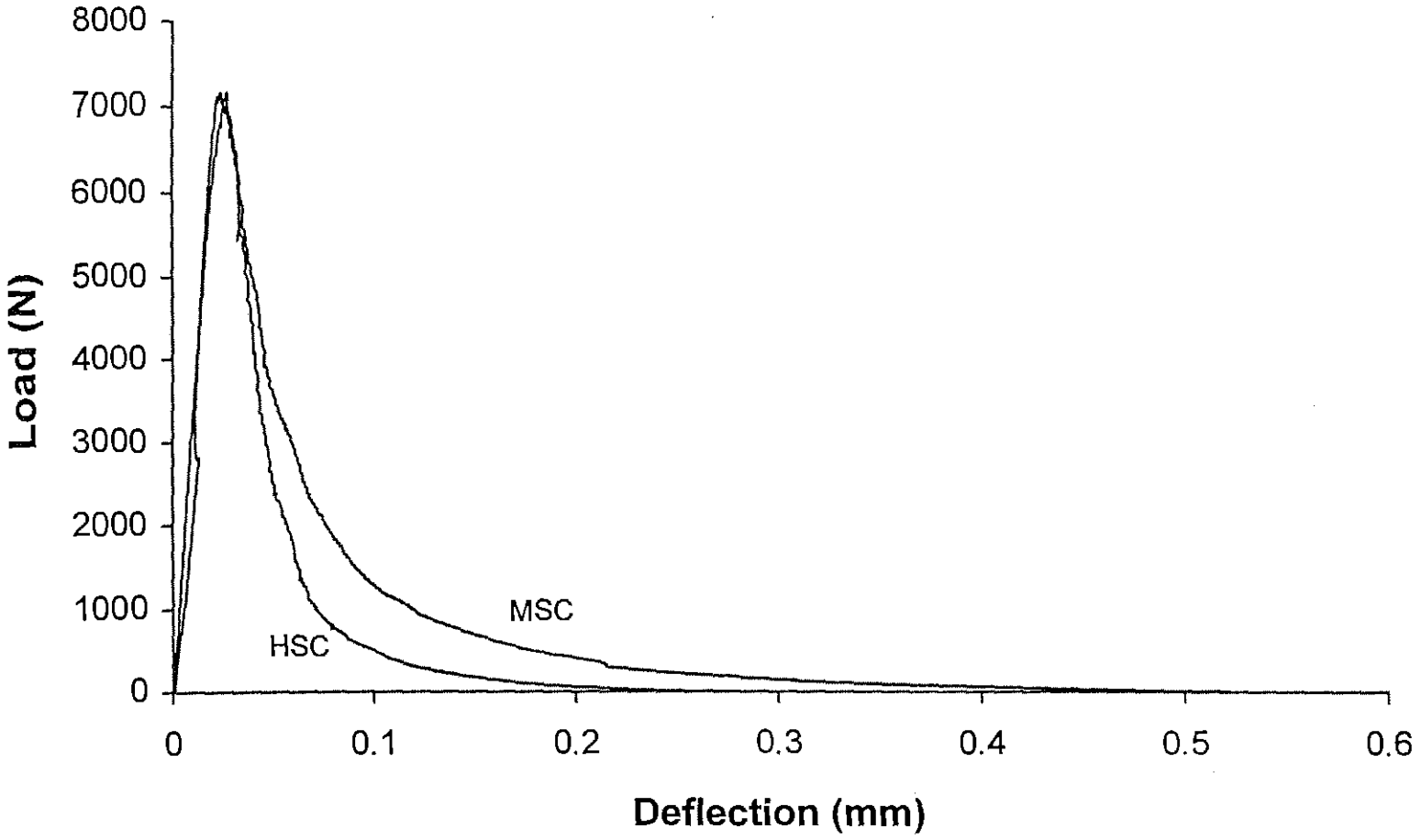

Figure 3.23 Fracture specimen load-deflection curves for 28-day limestone medium and high-strength concrete. (ML2-28E and HL2-28E)

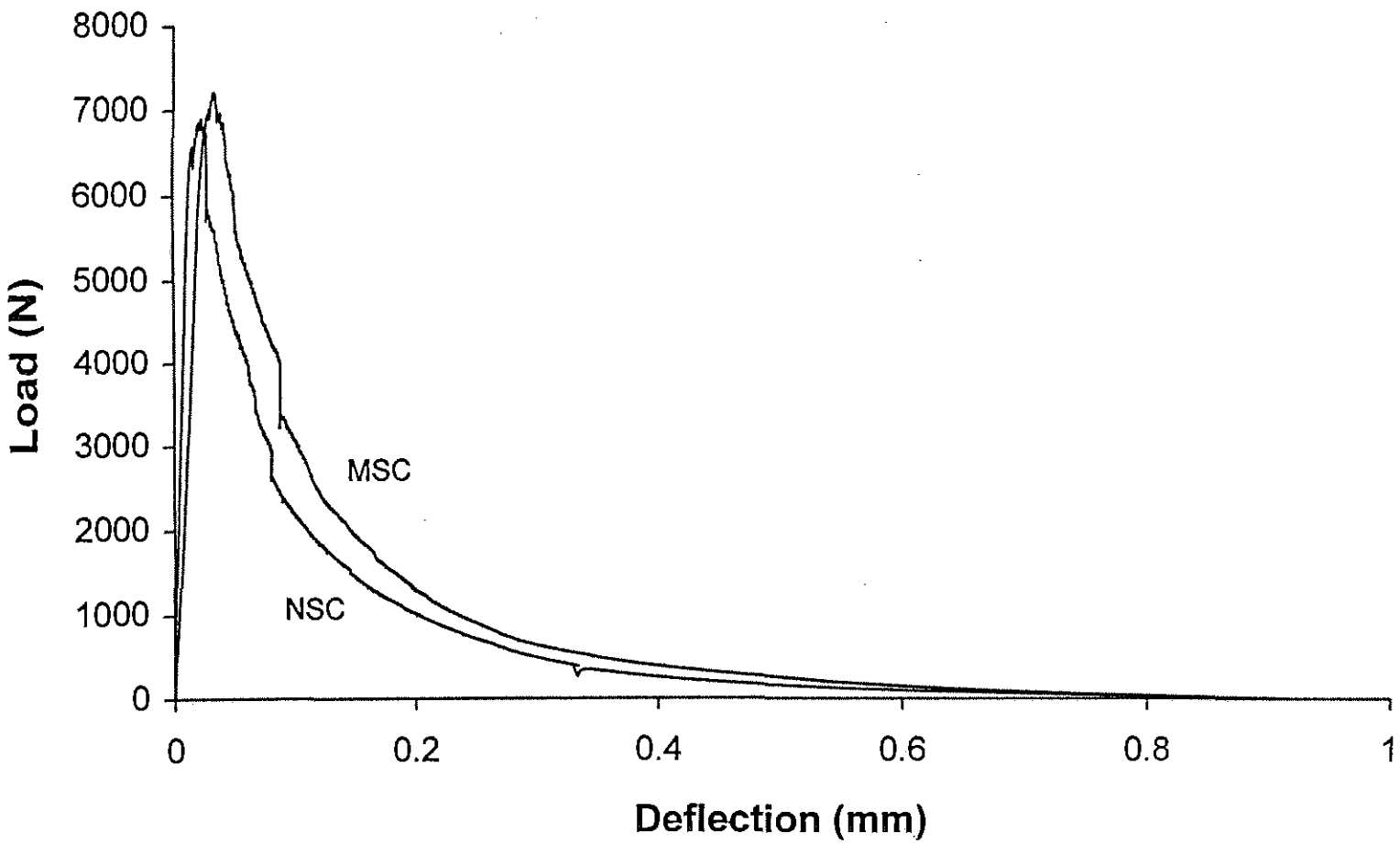

Figure 3.24 Fracture specimen load-deflection curves for 28-day basalt normal and medium-strength concrete. (NB1-28E and MB1-28E)

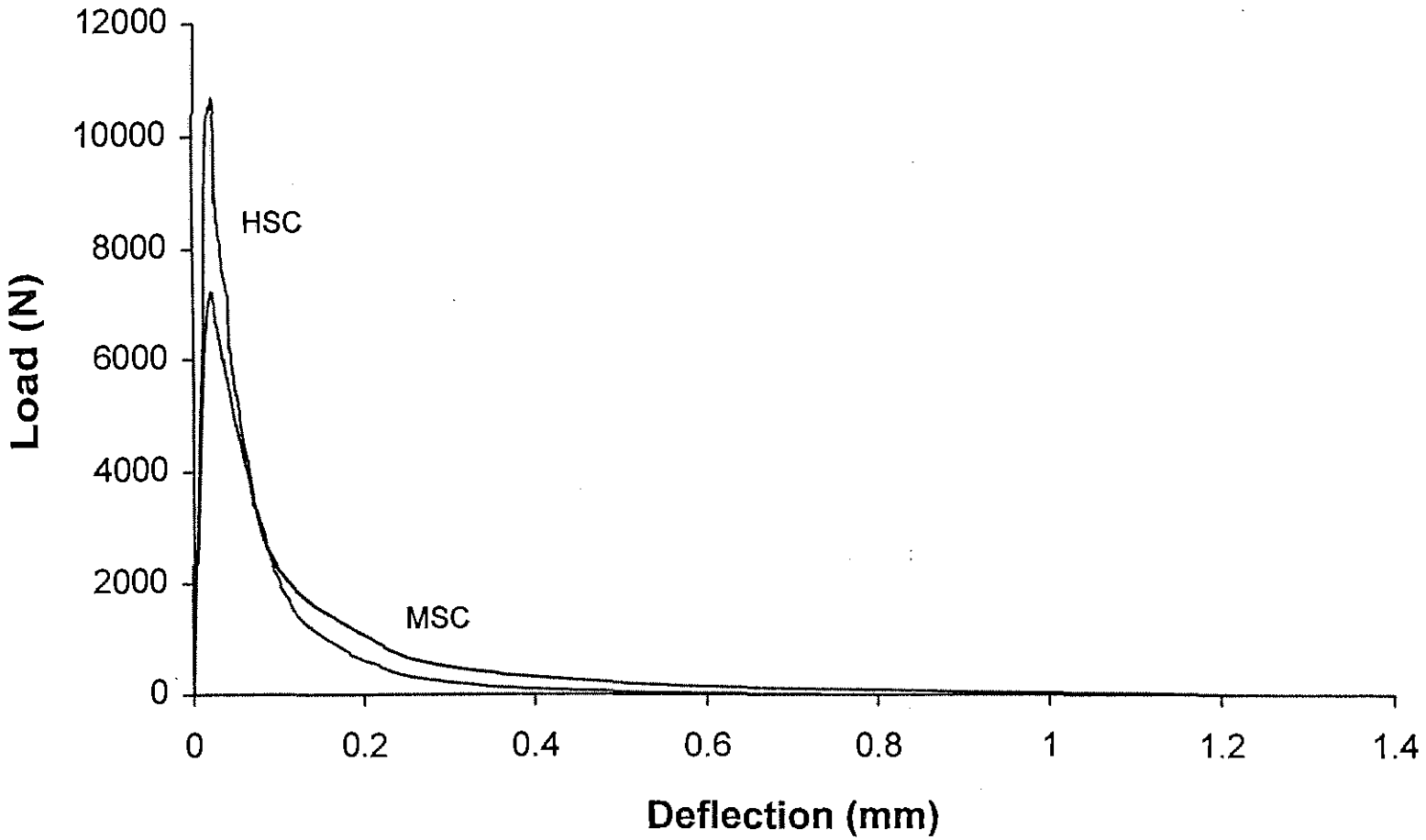

Figure 3.25 Fracture specimen load-deflection curves for 28-day basalt medium and high-strength concrete. (MB2-28E and HB2-28E)

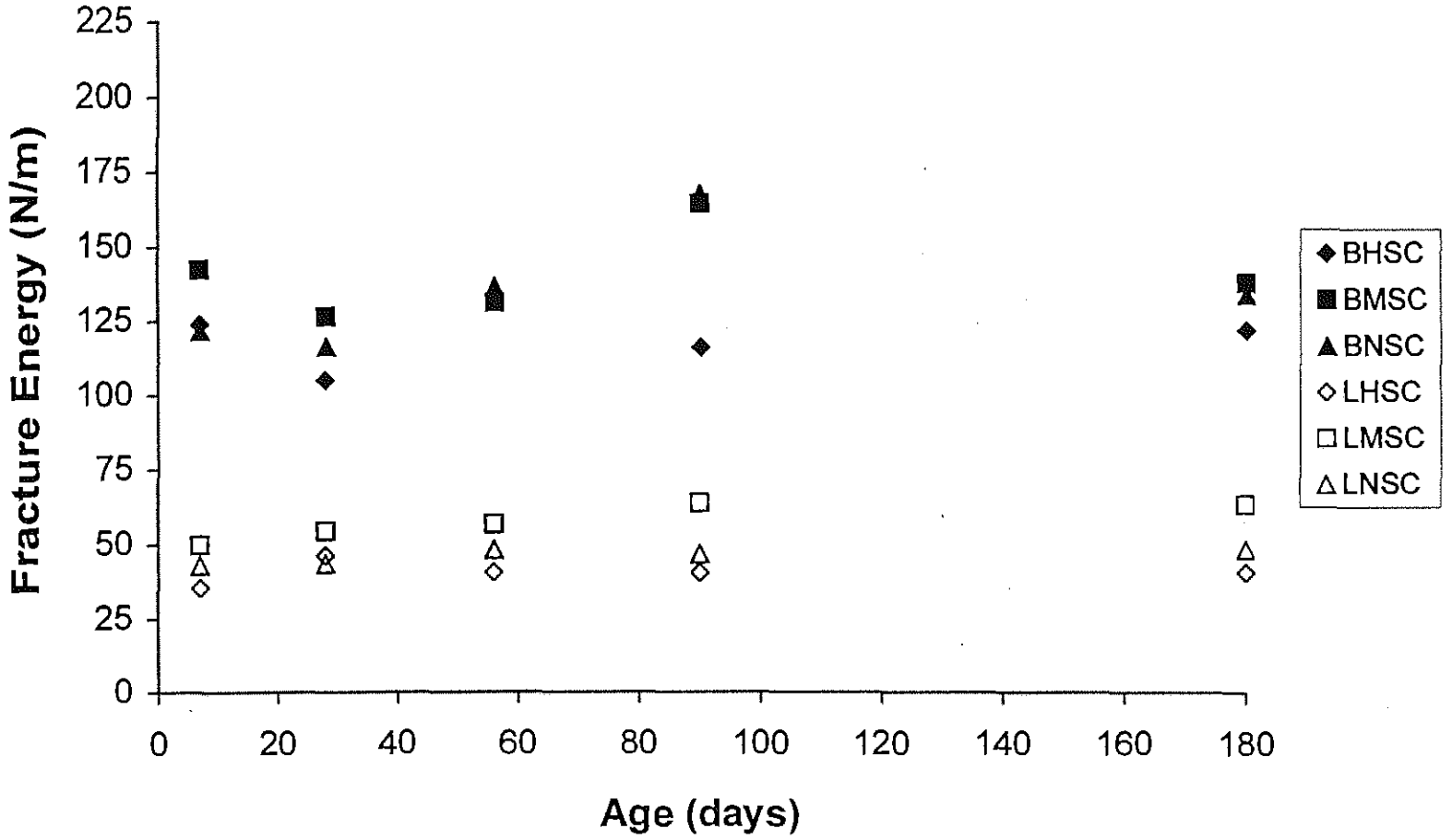

Figure 3.26 Average fracture energy versus age.

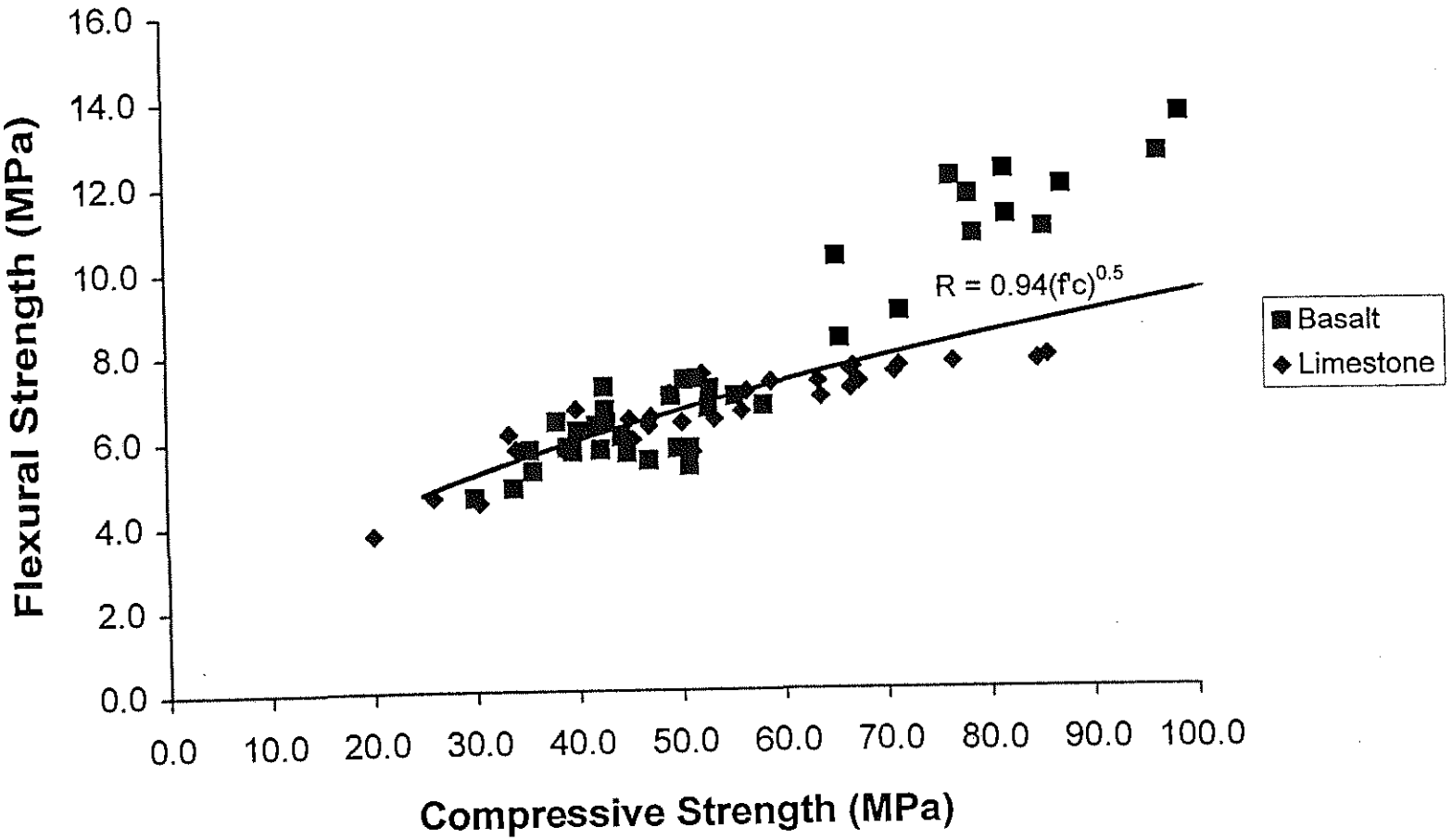

Figure 3.27 Flexural strength versus compressive strength for normal, medium, and high-strength concretes.

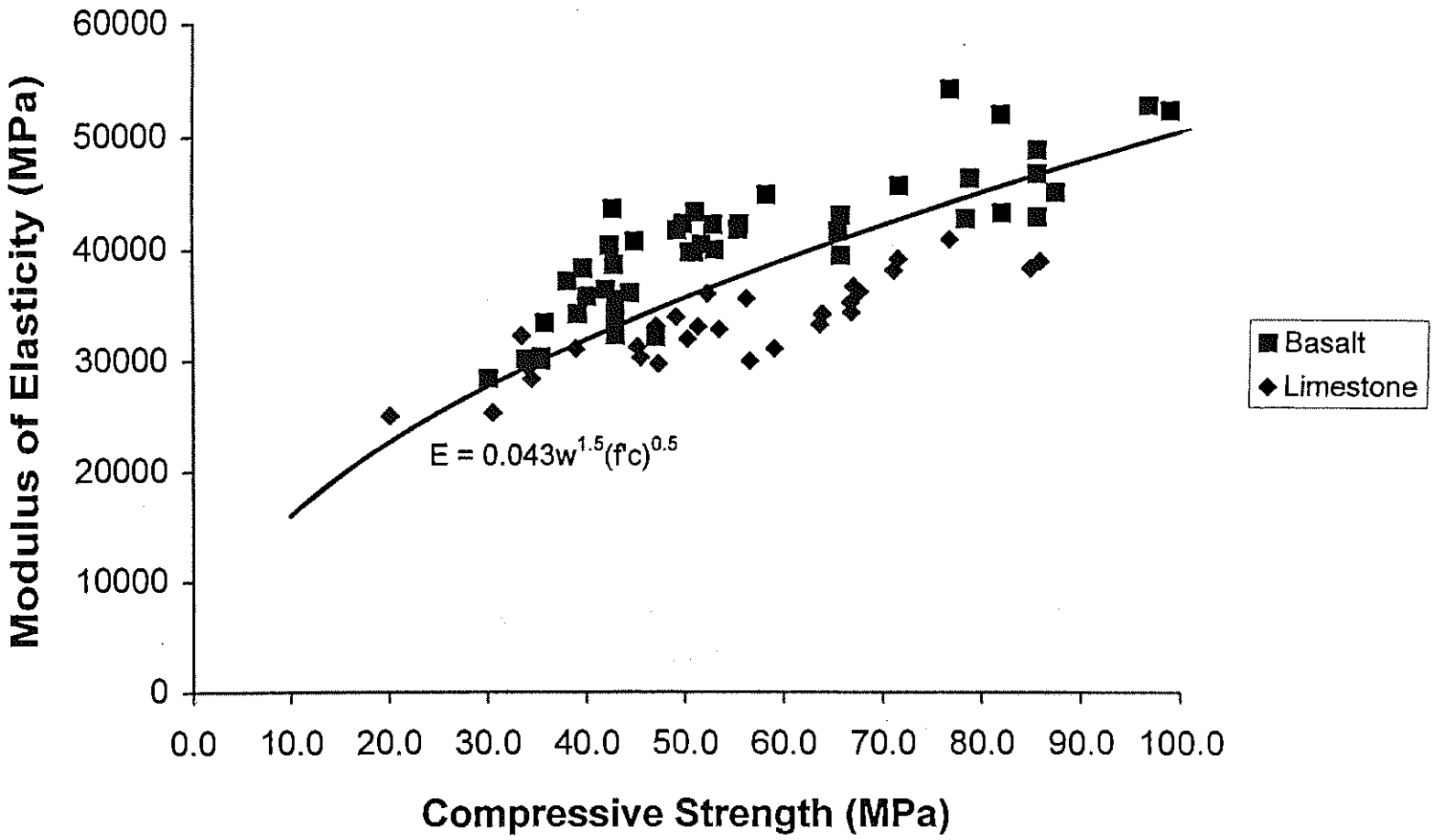

Figure 3.28 Modulus of elasticity versus compressive strength for normal, medium, and high-strength concrete.

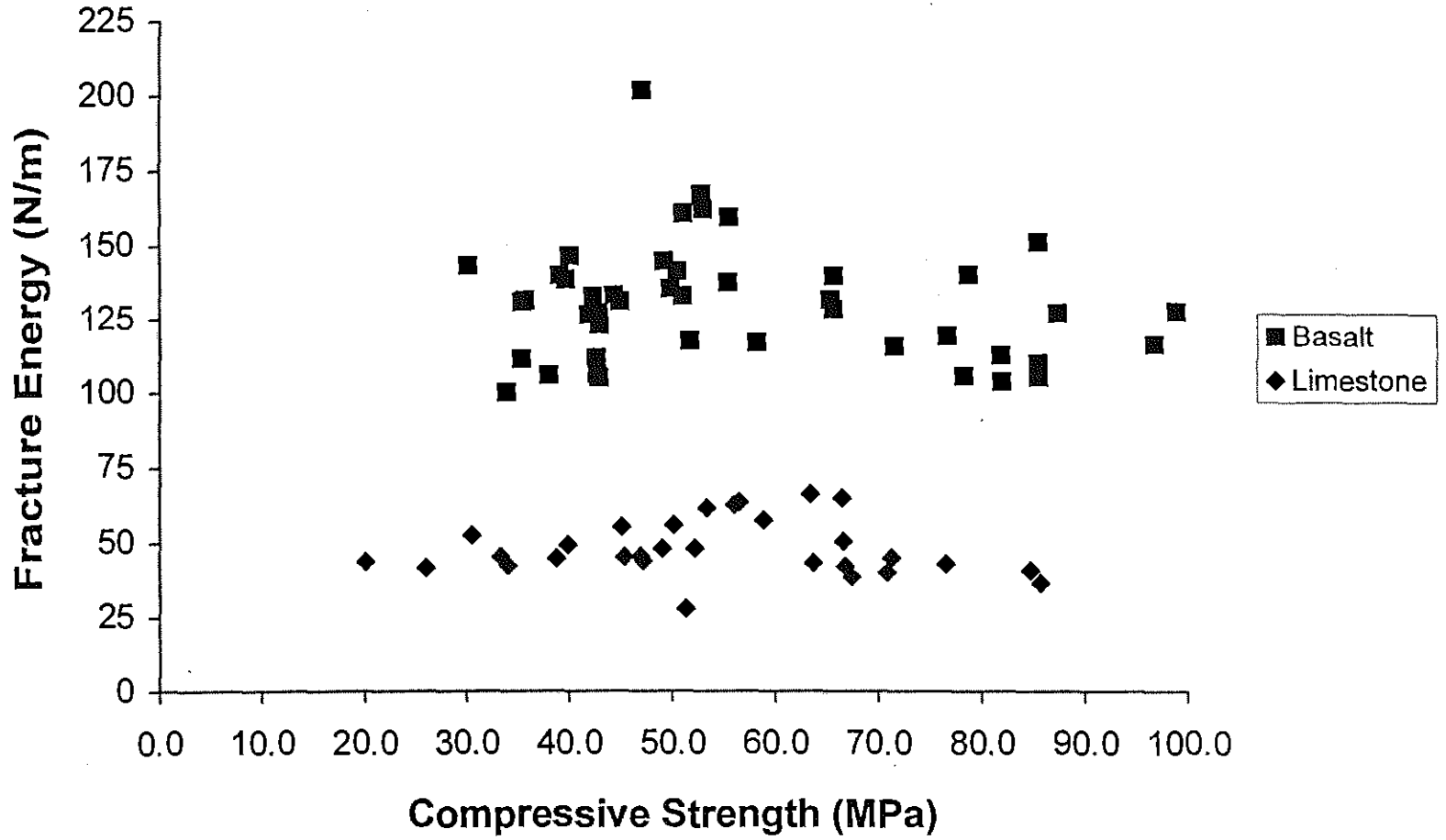

Figure 3.29 Fracture energy versus compressive strength for normal, medium, and high-strength concrete.

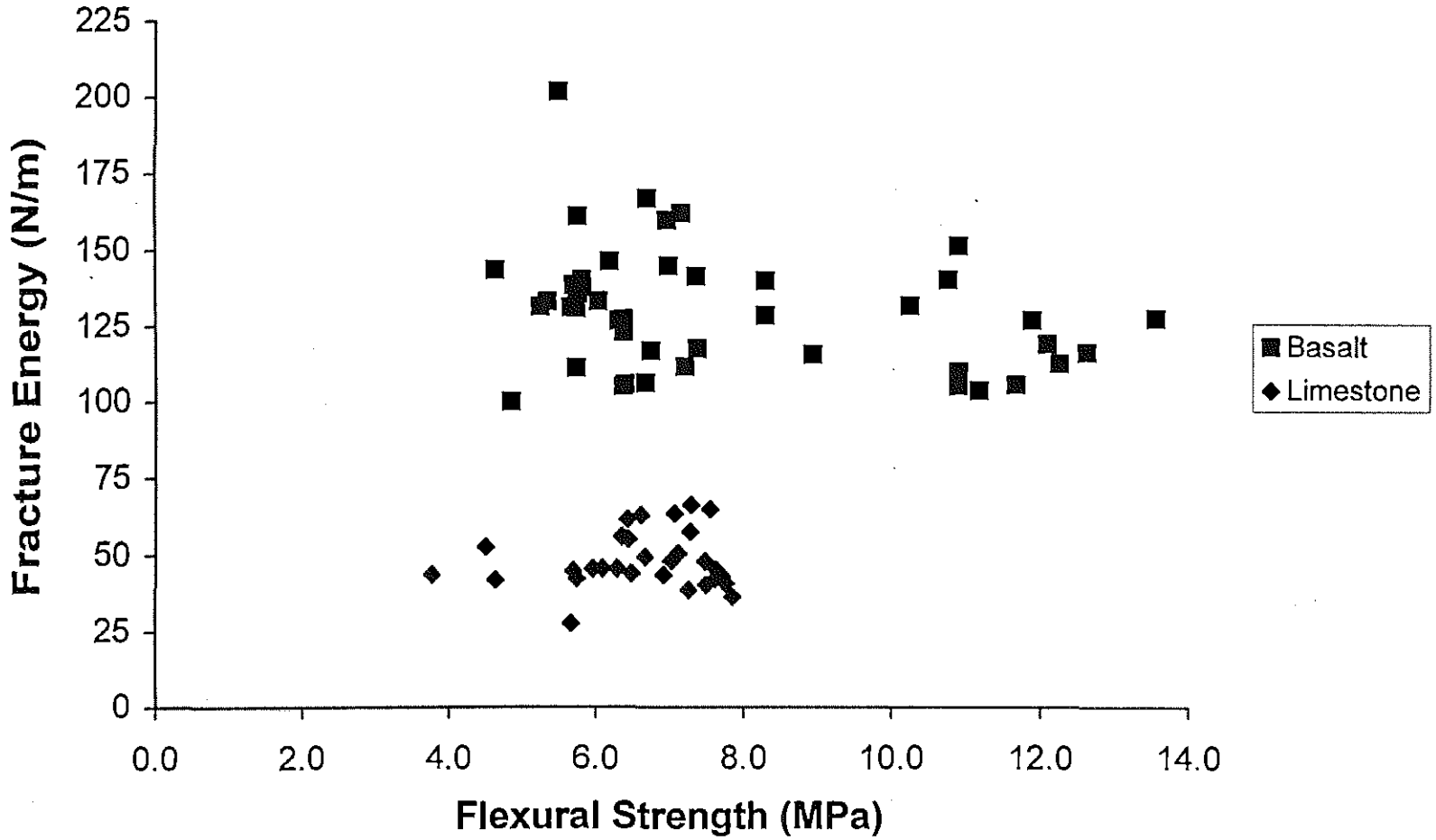

Figure 3.30 Fracture energy versus flexural strength for normal, medium, and high-strength concrete.

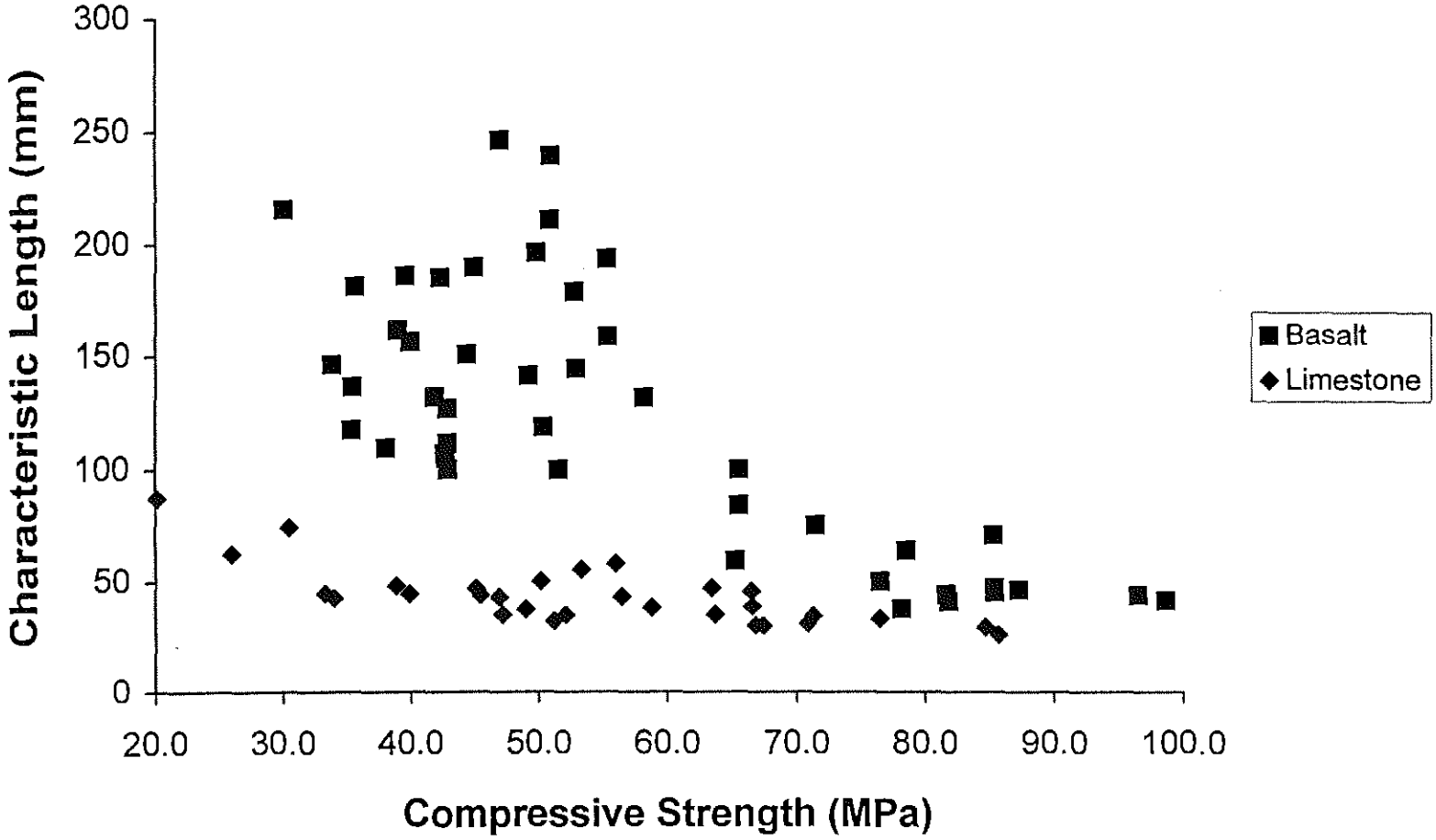

Figure 3.31 Characteristic length versus compressive strength for normal, medium, and high-strength concrete.

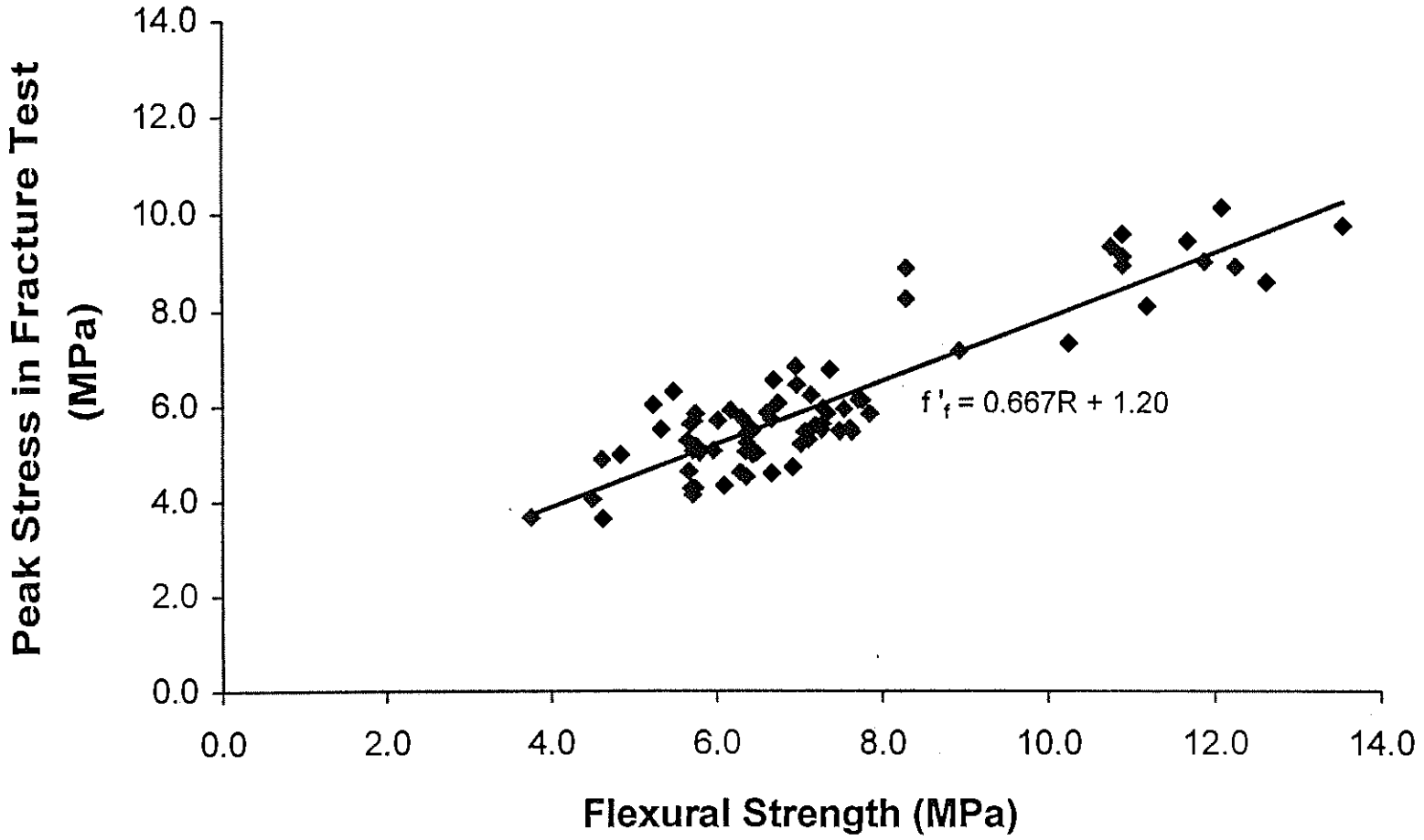

Figure 3.32 Peak stress in fracture test versus flexural strength for normal, medium, and high-strength concretes.

TABLE A.1

FRACTURE DATA (SI UNITS)

Specimen**	Peak Load (N)	Defl*(mm)	CMOD*(mm)	Wo (N-m)	Area (mm^2)	m1 (kg)
NB1-7E	6561	0.99	2.23	0.70	7849	8.84
NB2-7E	6223	1.81	4.86	0.99	7665	8.84
NB1-7E2	7940	1.35	2.83	0.95	7808	8.89
NB3-7E1	6712	1.32	2.68	0.93	7866	8.94
NB3-7E2	5618	1.17	2.11	0.79	7960	8.86
NB1-28E	6899	0.91	1.93	0.72	7577	8.85
NB2-28E	7344	0.72	1.67	0.86	7696	8.89
NB1-28E2	7464	1.05	2.41	0.75	7746	8.87
NB3-28E1	7148	1.49	3.90	0.89	7846	8.88
NB3-28E2	6877	1.01	2.24	0.87	7836	8.87
NB3-28E3	5382	0.83	1.82	0.70	7453	8.84
NB1-56E	7464	0.84	1.74	0.92	7816	8.87
NB2-56E	6494	1.24	2.67	0.97	7748	8.82
NB1-56E2	6721	0.99	2.34	0.93	7674	8.85
NB1-90E	7393	1.29	3.06	0.93	7770	8.91
NB2-90E	8376	2.02	4.87	1.43	7854	8.91
NB1-90E2	7379	1.73	3.94	1.12	7677	8.86
NB1-180E	6579	1.22	2.56	0.96	7697	8.91
NB2-180E	7032	1.09	2.24	0.94	7688	8.88
NB1-180E2	6725	1.37	3.15	0.98	7742	8.94
MB1-7E	7731	3.20	4.48	1.00	7794	9.03
MB2-7E	7726	0.89	2.95	0.97	7994	8.95
MB1-28E	7321	0.94	2.12	0.98	7617	8.98
MB2-28E	7237	1.24	3.12	0.79	7760	9.01
MB1-56E	8749	1.64	3.51	0.82	7768	9.03
MB2-56E	8318	0.89	1.72	1.02	7753	9.04
MB1-90E	8198	1.01	2.23	1.09	7824	9.02
MB2-90E	8678	1.75	3.96	1.19	7852	9.03
MB1-180E	8847	1.35	2.59	1.15	7756	9.00
MB2-180E	7846	0.84	1.58	0.82	7756	9.03
HB1-7E	9403	0.80	1.82	0.83	7810	9.10
HB2-7E	9723	0.76	1.60	0.93	7866	9.09
HB3-7E2	11738	0.88	1.79	0.93	7873	9.11
HB3-7E3	10795	0.98	2.11	1.00	7821	9.12
HB1-28E	12361	0.82	1.63	0.77	7816	9.11
HB2-28E	10595	0.72	1.42	0.75	7795	9.03
HB3-28E1	12388	0.58	1.17	0.76	7773	9.17
HB3-28E2	11712	0.79	1.58	0.79	7822	9.13
HB3-28E3	11925	0.74	1.46	1.06	7802	9.07

Specimen**	Peak Load (N)	Defl (mm)	CMOD (mm)	Wo (N-m)	Area (mm^2)	m1 (kg)
HB1-56E	11729	0.64	1.19	0.90	7776	9.11
HB2-56E	12241	0.70	1.42	1.02	7832	9.17
HB1-90E	13113	0.59	1.30	0.85	7757	9.09
HB2-90E	11476	0.72	1.24	0.82	7742	9.06
HB1-180E	11191	0.63	1.14	0.83	7787	9.09
HB2-180E	12530	0.66	1.22	0.92	7735	9.10
NL1-7E	4457	0.53	1.03	0.29	7466	8.56
NL2-7E	5556	0.34	0.66	0.30	7770	8.60
NL1-28E	4768	0.45	0.91	0.29	7816	8.57
NL2-28E	6614	0.41	0.88	0.32	7775	8.65
NL1-56E	5311	0.52	1.04	0.37	7807	8.59
NL2-56E	6494	0.34	0.73	0.31	7766	8.62
NL1-90E	5613	0.48	0.97	0.32	7761	8.57
NL2-90E	6792	0.40	0.84	0.33	7787	8.61
NL1-180E	5956	0.56	1.09	0.35	7761	8.60
NL2-180E	7063	0.44	0.86	0.34	7735	8.63
ML1-7E	5507	0.38	0.77	0.31	7725	8.61
ML2-7E	6427	0.38	0.71	0.39	7755	8.72
ML1-28E	5938	0.38	0.76	0.32	7717	8.64
ML2-28E	7019	0.53	0.95	0.45	7724	8.75
ML1-56E	6583	0.43	0.88	0.40	7783	8.64
ML2-56E	7290	0.38	0.73	0.40	7735	8.72
ML1-90E	7095	0.40	0.79	0.43	7748	8.67
ML2-90E	7726	0.37	0.71	0.47	7768	8.74
ML1-180E	7602	0.43	0.81	0.45	7761	8.66
ML2-180E	7664	0.41	0.76	0.46	7723	8.71
HL1-7E	6045	0.28	0.53	0.26	7768	8.59
HL2-7E	6049	0.43	0.60	0.30	7717	8.69
HL1-28E	6810	0.36	0.63	0.37	7738	8.60
HL2-28E	7157	0.28	0.54	0.29	7746	8.67
HL1-56E	7090	0.25	0.48	0.26	7710	8.53
HL2-56E	7615	0.25	0.46	0.29	7594	8.65
HL1-90E	6823	0.25	0.51	0.27	7600	8.57
HL2-90E	7860	0.30	0.56	0.28	7716	8.61
HL1-180E	6948	0.28	0.58	0.31	7677	8.58
HL2-180E	7566	0.23	0.53	0.26	7748	8.66

** H = high-strength concrete
M = medium-strength concrete
N = normal-strength concrete
E = fracture energy specimen

B = basalt
L = limestone
# = batch number, test age

* at failure

TABLE A.2

FRACTURE DATA (Customary Units)

Specimen**	Peak Load (lb)	Defl*(in)	CMOD*(in)	Wo (lb-in)	Area (in^2)	m1 (slugs)
NB1-7E	1475	0.039	0.088	6.24	12.17	0.606
NB2-7E	1399	0.071	0.191	8.72	11.88	0.606
NB1-7E2	1785	0.053	0.111	8.42	12.10	0.609
NB3-7E1	1509	0.052	0.105	8.24	12.19	0.612
NB3-7E2	1263	0.046	0.083	7.01	12.34	0.607
NB1-28E	1551	0.036	0.076	6.35	11.74	0.606
NB2-28E	1651	0.028	0.066	7.62	11.93	0.609
NB1-28E2	1678	0.041	0.095	6.60	12.01	0.607
NB3-28E1	1607	0.059	0.154	7.92	12.16	0.608
NB3-28E2	1546	0.040	0.088	7.68	12.15	0.607
NB3-28E3	1210	0.033	0.072	6.20	11.55	0.606
NB1-56E	1678	0.033	0.068	8.17	12.11	0.608
NB2-56E	1460	0.049	0.105	8.60	12.01	0.604
NB1-56E2	1511	0.039	0.092	8.22	11.90	0.606
NB1-90E	1662	0.051	0.121	8.25	12.04	0.610
NB2-90E	1883	0.080	0.192	12.68	12.17	0.611
NB1-90E2	1659	0.068	0.155	9.92	11.90	0.607
NB1-180E	1479	0.048	0.101	8.49	11.93	0.610
NB2-180E	1581	0.043	0.088	8.28	11.92	0.608
NB1-180E2	1512	0.054	0.124	8.63	12.00	0.612
MB1-7E	1738	0.126	0.176	8.87	12.08	0.619
MB2-7E	1737	0.035	0.116	8.58	12.39	0.613
MB1-28E	1646	0.037	0.084	8.64	11.81	0.615
MB2-28E	1627	0.049	0.123	6.98	12.03	0.617
MB1-56E	1967	0.065	0.138	7.25	12.04	0.619
MB2-56E	1870	0.035	0.068	9.04	12.02	0.619
MB1-90E	1843	0.040	0.088	9.69	12.13	0.618
MB2-90E	1951	0.069	0.156	10.54	12.17	0.618
MB1-180E	1989	0.053	0.102	10.15	12.02	0.617
MB2-180E	1764	0.033	0.062	7.25	12.02	0.618
HB1-7E	2114	0.031	0.072	7.36	12.11	0.623
HB2-7E	2186	0.030	0.063	8.23	12.19	0.623
HB3-7E2	2639	0.035	0.071	8.22	12.20	0.624
HB3-7E3	2427	0.038	0.083	8.83	12.12	0.625
HB1-28E	2779	0.032	0.064	6.78	12.11	0.624
HB2-28E	2382	0.028	0.056	6.63	12.08	0.619
HB3-28E1	2785	0.023	0.046	6.72	12.05	0.628
HB3-28E2	2633	0.031	0.062	7.02	12.12	0.625
HB3-28E3	2681	0.029	0.058	9.34	12.09	0.621

Specimen**	Peak Load (lb)	Defl*(in)	CMOD*(in)	Wo (lb-in)	Area (in^2)	m1 (slugs)
HB1-56E	2637	0.025	0.047	7.93	12.05	0.624
HB2-56E	2752	0.028	0.056	8.99	12.14	0.628
HB1-90E	2948	0.023	0.051	7.55	12.02	0.622
HB2-90E	2580	0.028	0.049	7.29	12.00	0.621
HB1-180E	2516	0.025	0.045	7.34	12.07	0.623
HB2-180E	2817	0.026	0.048	8.13	11.99	0.624
NL1-7E	1002	0.021	0.040	2.60	11.57	0.586
NL2-7E	1249	0.013	0.026	2.62	12.04	0.589
NL1-28E	1072	0.018	0.036	2.61	12.11	0.587
NL2-28E	1487	0.016	0.035	2.84	12.05	0.592
NL1-56E	1194	0.021	0.041	3.28	12.10	0.588
NL2-56E	1460	0.013	0.029	2.73	12.04	0.590
NL1-90E	1262	0.019	0.038	2.84	12.03	0.587
NL2-90E	1527	0.016	0.033	2.95	12.07	0.590
NL1-180E	1339	0.022	0.043	3.09	12.03	0.589
NL2-180E	1588	0.017	0.034	2.99	11.99	0.591
ML1-7E	1238	0.015	0.030	2.78	11.97	0.590
ML2-7E	1445	0.015	0.028	3.41	12.02	0.597
ML1-28E	1335	0.015	0.030	2.81	11.96	0.592
ML2-28E	1578	0.021	0.038	3.99	11.97	0.599
ML1-56E	1480	0.017	0.035	3.50	12.06	0.592
ML2-56E	1639	0.015	0.029	3.57	11.99	0.598
ML1-90E	1595	0.016	0.031	3.85	12.01	0.594
ML2-90E	1737	0.014	0.028	4.18	12.04	0.599
ML1-180E	1709	0.017	0.032	3.94	12.03	0.593
ML2-180E	1723	0.016	0.03	4.07	11.97	0.597
HL1-7E	1359	0.011	0.021	2.34	12.04	0.588
HL2-7E	1360	0.017	0.023	2.68	11.96	0.595
HL1-28E	1531	0.014	0.025	3.25	11.99	0.589
HL2-28E	1609	0.011	0.021	2.58	12.01	0.594
HL1-56E	1594	0.010	0.019	2.32	11.95	0.584
HL2-56E	1712	0.010	0.018	2.56	11.77	0.592
HL1-90E	1534	0.010	0.02	2.38	11.78	0.587
HL2-90E	1767	0.012	0.022	2.48	11.96	0.589
HL1-180E	1562	0.011	0.023	2.75	11.9	0.588
HL2-180E	1701	0.009	0.021	2.29	12.01	0.593

** H = high-strength concrete
M = medium-strength concrete
N = normal-strength concrete
E = fracture energy specimen

B = basalt
L = limestone
# = batch number, test age

* at failure